Republic of Iraq

Ministry of Higher Education and Scientific Research

University of Babylon

College of Materials Engineering

Department of Polymer and Petrochemical Industries

Fabrication and Characterization of polymer blends NanoComposites

A Dissertation Submitted to the Council College of Materials Engineering / University of Babylon in Partial Fulfillment of the Requirements for the Degree of Doctorate of Philosophy in Materials Engineering / Polymer

By

Zainab Abdul Raheem Abdul Hasan Nasar

(B.Sc. in Non-Metallic Materials Engineering, 2011)
(M. Sc. In Polymers Engineering, 2014)

Supervised by:

Prof. Dr. Zoalfokkar Kareem Alobad

Prof. Dr. Mohammed A. Akraa

2022 AD

1444 AH

بِسْمِ ٱللَّهِ ٱلرَّحْمَٰنِ ٱلرَّحِيمِ

(قَالُواْ سُبْحَانَكَ لاَ عِلْمَ لَنَا إِلاَّ مَا عَلَّمْتَنَا
إِنَّكَ أَنتَ الْعَلِيمُ الْحَكِيمُ).

صدق الله العلي العظيم

سورة البقرة

الآية(٣٢)

Supervisors Certification

We certify that this thesis entitled" **Fabrication and Characterization of polymer blends NanoComposites** " had been carried out under our supervision for the student (**Zainab Abdul Raheem Abdul Hasan Nasar**) at the University of Babylon/Collage of Material's Engineering/Department of Polymer Engineering and Petrochemical Industries in partial fulfillment of the requirements for the degree of Doctorate of Philosophy in Materials Engineering / Polymer Engineering.

Signature:

Prof. Dr. Zoalfokkar Kareem Mezaal

Supervisor

Date: / /2022

Signature:

Prof. Dr. Mohammed A. Akraa

Supervisor

Date: / /2022

Examination Committee Certification

We certify that we have read this thesis entitled "**Fabrication and Characterization of polymer blends NanoComposites**" and as an Examination Committee examined the student (**Zainab Abdul Raheem Abdul Hasan Nasar**) on its contents and that, in our opinion, it meets the standard of a thesis and is adequate for the award of the Doctor Degree of Philosophy in Materials Engineering/ Polymer Engineering.

Signature:

Prof. Dr. Mohammed. H. Almaamori

Babylon University/ College of Materials Engineering

Date: / /2022

(Chairman)

Signature:
Prof. Dr. Ahmed Fadhil Hamzah
University of Babylon/ College of Materials Engineering
Polymer and Petrochemical Industries Department
Date: / /2022
(Member)

Signature:
Prof. Dr. Jawad Kadhim Oleiwi
University of Technology/ College of Engineering
Materials Engineering Department
Date: / /2022
(Member)

Signature:
Assist. Prof. Dr. Qahtan Adnan Hamad
University of Technology/ College of Engineering
Materials Engineering Department
Date: / /2022
(Member)

Signature:
Assist. Prof. Dr. Asra Ali Hussien
University of Babylon/ College of Materials Engineering
Polymer and Petrochemical Industries Department
Date: / /2022
(Member)

Signature:
Prof. Dr. Zoalfokkar Kareem Mezaal
University of Babylon /College of Materials Engineering
Polymer and Petrochemical Industries Department
Date: / /2022
(Member)

Signature:
Prof. Dr. Mohammed A. Akraa
University of Babylon /College of Education for Pure Sciences/ Physics Department
Date: / /2022
(Member)

Approval of Polymer and Petrochemical Industries
(Head of the Department)

Signature:
Prof. Dr. Zoalfokkar Kareem Mezaal
Date: / /2022

Approval of Materials Engineering College
(Dean of the College)

Signature:
Prof. Dr. Imad Ali Disher
Date: / /2022

Dedications

To

My Father and Mother

My Sister

My Brothers

and

My friends

Acknowledgments

First and foremost, I am indebted to the all-powerful almighty "God", for giving me the strength and ability to understand, learn and complete this research.

It gives me great pleasure and profound privilege to place on record my deep sense of gratitude and indebtedness to my supervisors, **Prof. Dr. Zoalfokkar Kareem Mezaal Al-obad** and **Prof. Dr. Mohammed A. Akraa** Whose constructive comments, unflagging optimism, and scholarly guidance throughout the present work have driven me towards the success of this endeavor. Without their supervision and guidance, this work would not have been completed.

I wish to thank all the staff of the laboratories of the Collage of Materials engineering, especially in the Polymers laboratories (Ban Jwad, Ali Yhea and Fadaa Ather, Yaser Ammar) for their support during this work.

Finally, I would like to thank everyone help me in any way to achieve the present work.

Zainab alsaadi

2022

Abstract

Epoxy material is used in many industrial applications, but because of its brittleness, it limits its use, and due to its poor tribological properties, like wear resistance, which makes the use of epoxy as wear-resistant coatings less, such as coatings for oil and gas pipelines.

In the first part of this study, five different toughening agents were used to enhance the toughness of pure epoxy resin. The different toughening agent's triblock copolymer (TBCP), polyether polyol (PU base), liquid silicon rubber (LSR), liquid PVC adhesive, and polysulphide polymer (PSR) used with hardener (izoforon diamine). A series of epoxy blends were obtained with variations of load content of 3, 6, 9, and 12% wt. and studied the tensile properties, fracture toughness strength, impact strength, hardness, and pull off adhesion. The structural and physical characteristics were studied by Scanning Electron Microscopy (SEM), Fourier Transform Infrared Spectroscopy (FTIR), and Differential Scanning Calorimetry (DSC)

Based on the results of tests, the best toughening agent/ EP blend was (epoxy+3%TBCP) and have been selected to prepare the second part of epoxy nanocomposites were reinforced with different percent of tungsten carbide nanoparticles (WC) with load content (1, 2 and 3) w.t% respectively, once with epoxy matrix only and once more with (epoxy+3%TBCP)matrix.

The results showed that the FTIR results proved that there is no chemical reaction, and there is only physical interaction between the toughening agents and the epoxy matrix. The results clarified that by increasing the weight percentage of TBCP, tensile strength and elastic modulus properties were enhanced and the best percent was at 3% TBCP. The rate of

improvement at this percent has reached [100%, and 57%], It was shown that the TBCP confers better fracture properties and impact strength to the epoxy resin at low content loading without losing the other mechanical properties.

Further, epoxy systems were modified using PU polyol, PVC, and PSR. The resulting blends were extensively characterized qualitatively and quantitatively to reveal the effect of each toughening agent on the epoxy properties. It was shown that all these agents confer better fracture properties to the epoxy resin at low content loading with some losing other tensile mechanical properties.

In the case of LSR modified epoxy matrix, by increasing the weight percentage of LSR, tensile strength and pull-off adhesion strength were enhanced and the best percent was at 6% LSR. The rate of improvement at this percent has reached[12%, and 25%].

The results clarified that by increasing the weight percentage of WC nanoparticles for WC/EP nanocomposite, mechanical properties were enhanced and the best percent was at 2% WC. The rate of improvement at this percent has reached for tensile strength and modulus [55%, 46%], fracture toughness [350%],pull off strength [25%] and wear resistance [63%]. For WC/3%TBCP/EP nanocomposite, mechanical properties were enhanced and the best percent was at 2% WC. The rate of improvement at this percent has reached for elastic modulus [46%],fracture toughness[250%], pull off strength [38%] and wear resistance [63%].

List of Contents

Abbreviations

Abbreviations	Definition
ASTM	American Society for Testing and Materials
BCP	Block copolymer
(CTBN)	Carboxyl-terminated acrylonitrile-butadiene
(CTPB)	Carboxyl-terminated polybutadiene
DSC	Differential scanning calorimetry
DGEBA	Diglycidyl ether of bisphenol A
DMA	Dynamic mechanical analysis
DDM	4,4'-diaminodiphenylmethane
eSBS47	Epoxidation of styrene-block-butadiene-block-styrene triblock copolymer
EP	Epoxy
FESEM	Field Emission Scanning Electron Microscopy
FTIR	Fourier transform infrared spectroscopy
(HTPB)	Hydroxyl-terminated polybutadiene
IPN	Inter-penetrating network
LEFM	linear elastic fracture mechanics
PVC	liquid polyvinyl chloride adhesive
LSR	liquid silicon rubber
MWCNTs	Multi-walled carbon nano- tubes
PCL	Poly(caprolactone)
PU	Polyurethan polyol
PEO	Polyethylene glycol
PPO	Polypropylene glycol
EO-PPO-EO	Polyethylene glycol-block-polypropylene glycol-block-polyethylene glycol
PSF	Polysulfone
PSR	Polysulphide polymer
SEM	Scanning electron microscopy
SENB	Single edge notch bending fracture toughness
SWCNT	Single-walled carbon nanotubes
ISO	The International Organization for Standardization
TEM	Transmission electron microscopy
TBCP	Triblock copolymer
XRD	X-ray diffractometer

List of Symbols

Symbols	Meaning	Unit
A	The cross-sectional area	Mm
a_{cU}	Impact strength	KJ/m2
b	Width	Mm
E	Modulus of elasticity	GPa
h	Thickness	mm
K_{IC}	Critical stress intensity factor	MPa
Mn	Number average molecular weight	g/mol
P	Force	N
S	The rate of sliding	mm/min
S.D	Sliding distance	mm
t	Time	min
T_g	Glass transition temperature	°C
TiO_2	Titanium dioxide	-
W.R	Sliding wear	g/mm
W_B	The energy at break	J
WC	Tungsten carbide nanoparticles	-
ΔW	Change in weight	g
ε	Strain	mm
σ	Stress	MPa

List of Figures

List of Tables

Chapter One

Introduction

Chapter One
(Introduction)

1.1Introduction

A polymer is a giant chemical compound made up of repeating units of the same or different monomers, with or without material loss [1]. When compared to thermoplastic, thermoset is a stronger polymer because its crosslinking is spread out in all three directions [2]. Epoxies are thermosetting polymers cured using a broad variety of curing agents, usually known as hardeners[3]. Epoxy is used in many applications due to its amorphous thermoset with prime hardness and mechanical strength[4].

Unfortunately, cured epoxy systems have one major drawback: significant brittleness, demonstrating low fracture toughness and poor resistance to crack initiation and propagation. This severely limits their applicability in applications needing high fracture strength [5]–[8]. There have been a lot of efforts made to enhance their physical properties by applying a variety of different chemicals that are toughening or strengthening agents [9].

There are a few different ways that the toughness of epoxy resins may be improved, e.g., plasticization of the polymer, induction of an inter-penetrating network (IPN), and the insertion of a second, well-dispersed phase of one of two things: soft rubbery particles or rigid inorganic particles [10].

Polymer blending can be a cost-effective method for developing a material with specific properties according to customer requirements [11]. In the case of polymer blends, all components are polymeric, which means the matrix and the minor component are deformable above the glass transition

temperature for amorphous or above the melting temperature for semicrystalline polymers [12]

Organic compounds having metal adhesion features find widespread using it as metal anticorrosive agents in a variety of industries, such as aeronautics, automobiles, architecture, ships, and oil tanks, to name a few [13]. In most cases, they are coated onto the surface of the metal in the form of a thin coating, which prevents corrosive chemicals from penetrating the metal surface[14]. Among organic compounds, those based on the epoxy resin are some of the most common due to their useful qualities and adaptability [15], [16]. Epoxy was selected as the coating of interest because of its versatility; it may be used to protect metal and concrete buildings, electrical components, structural adhesives, and many other things[17].

Metals protected by an epoxy coating are vulnerable to surface wear and abrasion due of the complex cross-linked structure of neat epoxy, its ability to protect metal against corrosion is quite low[18].

Polymer composites are commonly used in engineering besides structural components where these are exposed to wear[19]. It is very successful to enhance the performance of polymer composites, particularly their friction and wear characteristics, by including well-dispersed inorganic particles into a polymer matrix. This improvement has been proven to be highly effective [20]. Different researchers have endeavored to promote the toughness of the epoxy system by using different toughening modifier agents. Other researchers have tried to improve the tribological properties of the pure epoxy matrix by adding different types of micron- and nanometer-sized fillers to make composite coatings.

1.2 Aim of This Study

This work aims to prepare and characterize an epoxy coating layer with good toughness depending on polymer blending and enhancement wear resistance with tungsten carbide nanoparticle reinforcement for industrial application.

1.3 Objectives

The following study tasks were defined in order to accomplish the objectives, which are as follows:

- For the synthesis of epoxy, mixtures are blended with five toughening agent (triblock polymer(TBCP), PU polyol, silicon rubber(LSR), liquid polyvinyl chloride (PVC), and polysulfide polymer (PSR)).
- To find the best type of toughening agent that give better mechanical properties.
- To find the best percentage of toughening agent
- The thermal and mechanical characteristics of the epoxy polymer are going to be investigated.
- Epoxy matric, WC/EP, and TBCP/WC/EP nanocomposites containing (3% wt)TBCP will be analyzed to see how the WC content affects the morphological, thermal, and mechanical characteristics.
- To study the influence of adding WC nanoparticle on wear rate of epoxy nanocomposite.

1.4 Dissertation Outline

The dissertation has a total of five chapters, which are put in the following order:

In Chapter 1, an overview of the study's context and objectives is provided. The outline for this thesis is also included here.

Chapter 2, gives an overview of thermoset polymer, epoxy, various toughened agents, TBCP, polyol, WC nanoparticle, and nano-reinforcing polymer composites. including a literature study of matrix toughening agents using epoxy matrices. The effect of rigid particle addition on friction and wear rate of epoxy composites has also been studied and included in the review of the literature.

Chapter 3, experimental part of the materials and methods used in the tests performed for this study, from the toughening agent/epoxy combination used to create the modified epoxy through the epoxy nanocomposite manufacturing stages. The physical and mechanical test techniques and equipment that are used to characterize blends and nanocomposites are also described in this chapter.

In chapter 4, the results and discussion of the effect of using different matrix toughening agents on the thermal, morphology, pull-off adhesion, and mechanical properties of epoxy blends are included. In this chapter, the effects of adding WC nanoparticles to two systems of epoxy, WC/epoxy, and WC/TBCP/epoxy, on the thermal, morphological, mechanical, tribological, and pull-off adhesion properties are also shown and discussed.

In Chapter 5, we draw some conclusions about this evidence collection and provide some recommendations for further research.

Chapter Two

Theoretical Part and Literature Review

Chapter Two

Theoretical Part and Literature Review

2.1 Thermoset Polymer

By forming covalently cross-linked permanent networks when exposed to heat, thermosetting polymers transform irreversibly into an infusible and insoluble substance. Cross-linking is sometimes accomplished by irradiation[21,22].

Resins that have been highly cross-linked tend to be very hard and brittle[23]. Thermosets, unlike crystalline polymers, have a glass transition temperature(T_g) rather than a melting point[24]. Epoxy resins, phenolics, alkyds, allyl resins, vinyl esters, and unsaturated polyesters are all useful examples of thermosetting resins. In thermosetting polymers, the chains are covalently bonded together in a cross-linked or network structure. They can't be reworked once the cross-linking procedure makes them solid. Engineers use thermosets in fields that call for strong resistance to temperature, such as coatings, adhesives, electronic and electrical substances, etc. because thermosets cannot be remelted[21].

2.2 Epoxy

As a kind of good-performance thermoset, epoxy polymer systems are widely employed like a matrix material in industries including vehicles, electronics, and aerospace. To get this kind of versatility, you need to choose an epoxy resin/hardener system that works well and then process it according to a good curing schedule[25]. Because of their great adherence to a wide different of substrates, high heat and chemical resistance, and high

mechanical characteristics, epoxy polymers are often utilized as thermosetting substances[26]. These materials are manufactured by the chemical change of multifunctional epoxy monomers, which results in the formation of a polymer network that is produced in an irreversible manner[27]. Coatings, adhesives, electrical insulation, construction, and composites are just a few of the many applications for epoxy resins. Although coatings account for more than half of all epoxies' applications, epoxy composite materials are a growing field in their own right[28]. New materials are being employed in a broad variety of sporting equipment and have even become a deciding element in high-level competition. Its widespread adoption can be attributed to the significant performance improvements it brings to sports equipment thanks to the various new materials' excellent characteristics, such as high specific strength, specific modulus, lightweight, wear resistance, and so on. several cutting-edge materials, including carbon fiber and epoxy resin composites, nylon fiber composites, and unsaturated polyester composites[29].

2.2.1 Basic Fundamentals of Epoxy Thermosets

The presence of an oxirane group or epoxy episode, a group consisting of three participants with an atom of oxygen connected to two carbon atoms as illustrated in figure2.1, is what gives these compounds their names, epoxy or epoxide[27,30].

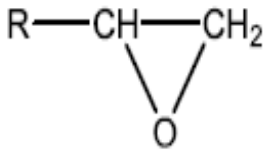

Figure2.1. The structure of an epoxy or an oxirane ring [27].

The epoxy ring is a versatile terminal group that may be linked to many different aliphatic or aromatic chemical compounds. It can also reside inside the body of a molecule. Epoxy groups are more reactive than other ethers, making them desirable for polymerization processing. This is because of the extremely strained ring structure[31].

The term "epoxy resin" is used to describe any substance that typically contains several epoxy groups inside a single molecule. In most cases, bisphenol-A and epichlorohydrin are reacted to produce the prevalent glycidyl epoxy resin. Epoxy resin's overall structure is seen in figure 2.2. Epoxy polymers may transition from a liquid state to solid matter as the number of repetition units "n" increases [32].

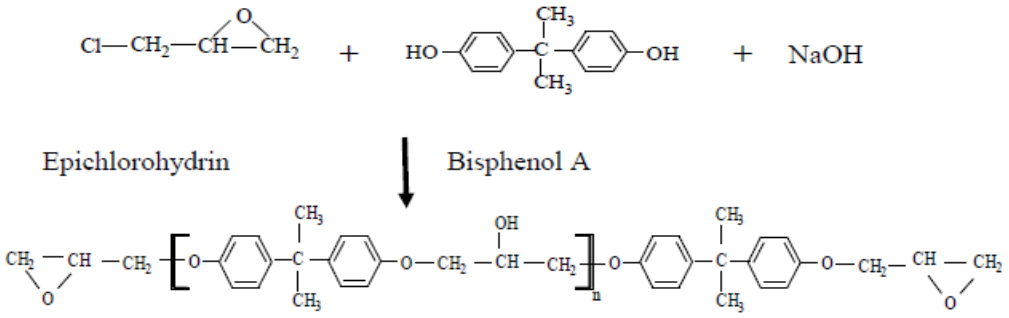

Figure2.2 Chemical structure of epoxy resin[32].

All epoxy resins have the same fundamental structure, consisting of an alpha or aromatic polymer chain that has at least two epoxide rings, one at each end. Epoxy groups are glycidyl groups, which are cyclic ethers[33].The Diglycidyl ether of bisphenol A (DGEBA) is shown schematically in figure 2.3 [12] to highlight its "idealized" structure.

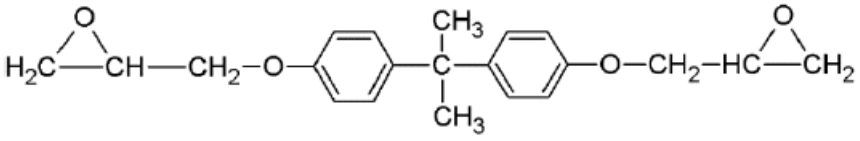

Figure2.3 Schematic of epoxy resin, DGEBA [33].

Some of the aspects in which epoxy is different from other polymers are as follows:

- good mechanical characteristics,
- resistance to chemicals, moisture, and corrosion,
- Thermally efficient,
- Superior adhesion,
- excellent dielectric resistance;
- little shrinkage after curing,
- Its low viscoelasticity,
- excellent dimensional stability,
- high degree of machinability[34].

2.2.2 Structure of Networks

If molecules are to cross-link in three dimensions (3D), their functionality (f), or the number of reactive moieties per mole of reactant, must be greater than two. An intermediate or final product molecule with a functionality of 2 is always produced when two 2-functionality precursor molecules react. A linear structure is produced by the reaction, as shown in figure2.4. When molecules with more than two functionalities react, however, they form branches, which eventually form a network structure[35].

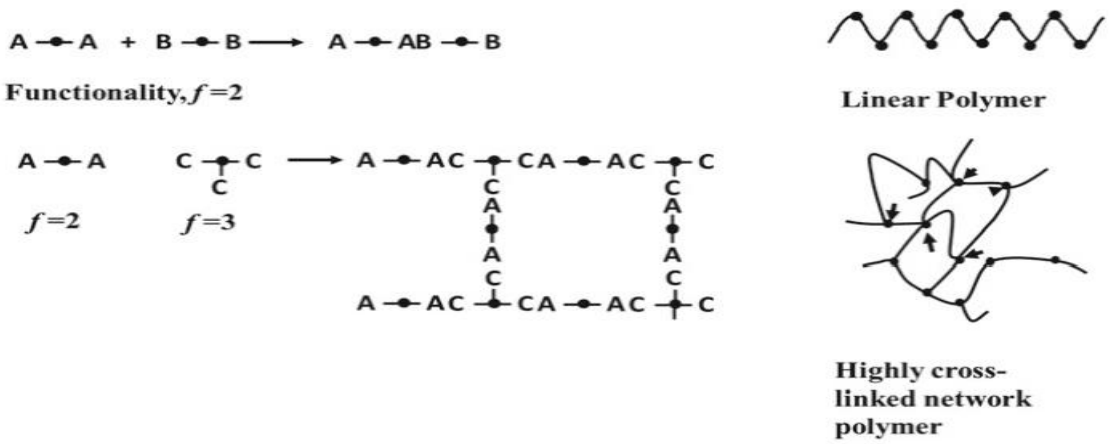

Figure2.4 Schematic representation of linear polymerization and network formation for molecules with functionality of >2[35].

The structure and characteristics of the cured resin are very sensitive to the resin-to-hardener ratio. In a similar manner, the material's performance is impacted by the curing agent and resin used. Thus, epoxy materials may be characterized as highly versatile thermosets. The level of cure may be quantified by measuring the degree of cross-linking. At high levels of cross-linking, the most desirable features are realized. The final cross-link density obtained is heavily dependent on the curing temperature. The chemical resistance of the cured matrix improves as a consequence of heating, which enhances molecular mobility and cross-link density. Figure 2.5 is a schematic showing how the network is formed[21].

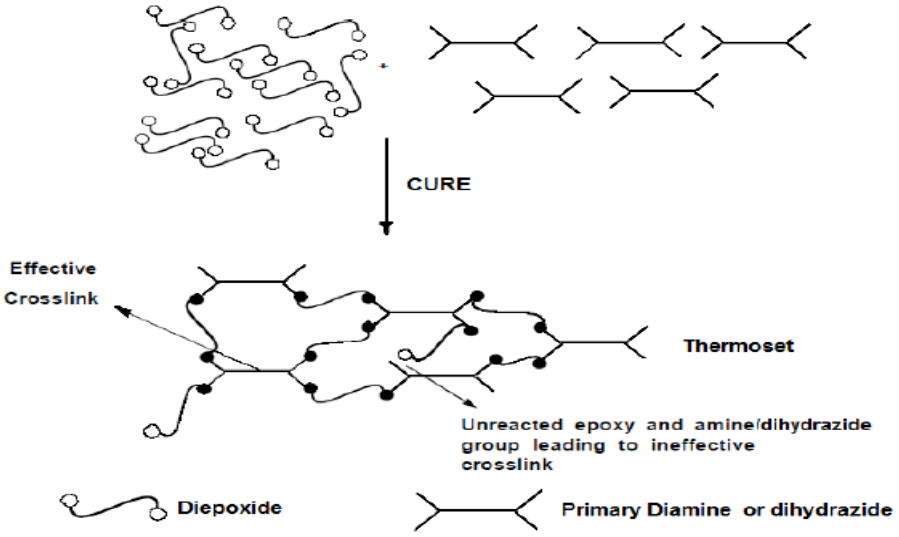

Figure2.5. Building up of networks of resin and hardener [21].

2.2.3 Epoxy Resin Curing

There is a sequence of cross-linking reactions that may transform epoxy resins from their flexible thermoplastic state into brittle, hard thermoset solids[36]. Cross-linkers are used to cure epoxy resins, which transforms them into a solid, infusible, and insoluble three-dimensional thermoset network. Using the correct cross-linkers, also known as hardeners or curing agents, in combination with the suitable epoxy resins yields the best possible performance attributes. The skills of the field process, the pot life, the cure environmental, and the desired physical features all play a role in deciding which curing agent is best. Curing agents not only impact the formulation's viscosity and reactivity but also the kinds of chemical attractions created and the level in terms of the cross-linking that will go place. As a result, these factors influence the cured thermosets' resistance to chemicals, electricity, mechanical stress, and temperature.

The epoxy and hydroxy functional groups in epoxy resins are responsible for the material's chemical reactivity. When epoxy groups react, the oxirane ring opens up and linear C-O bonds are formed. This property is responsible for epoxies' excellent dimensional stability after curing and their minimal shrinkage. Heat is necessary for a successful cure and the elimination of volatiles when polycondensation cures through hydroxyl groups, which typically results in the creation of volatile by products like water or alcohol[37].

2.2.3.1 Curing agents

Catalytic or coreactive compounds are used as curing agents. In contrast to the coreactive curing agent, which serves as a comonomer during the polymerization process, the catalytic curing agent operates as an initiator for epoxy resin homopolymerization or as an accelerator for other curing agents. The primary and secondary amines, phenols, thiols, and carboxylic acids are the most significant classes of coreactive curing agents (and their anhydride derivatives) are those with active hydrogen atoms. Catalytic cures are triggered by Lewis acids like boron trihalides and Lewis bases like tertiary amines[37]. In epoxy technology, curatives are most frequently called curing agents. Specific types of curing agents are frequently referred to as hardener, activator, or catalyst[36]. Differential scanning calorimetry (DSC) is often used to evaluate the epoxy resin-hardener system's reactivity by determining the amount of heat produced, the presence of unaltered morphology, and the T_g attained after curing. The curing kinetics may be studied using DSC, allowing as a method for determining when something will be fully cured, and that consists of crucial relevance in the technological context. IR spectroscopy gives direct information about how the reaction is happening

and adds to the data collected by DSC by keeping track of the removal of epoxy groups as the cure progresses[21].

2.4 Applications of Epoxy Resin

Epoxy resins are multipurpose construction materials and coating agents due to their excellent qualities, which include resistance to humidity and chemicals, good adherence to different substrates, and outstanding mechanical features.

Epoxy resins may be used in three major areas:

• Coatings

• Adhesives

• Construction and structural materials [38]

2.4.1 Coatings

Easy processing, high safety, great solvent and chemical resistance, toughness, minimal shrinkage on cure, mechanical and corrosion resistance, and excellent adherence to various surfaces are just some of the reasons why epoxy resins are so often employed as heavy-duty anticorrosion coatings[39]. In order to avoid corrosion, particularly when storing acidic foods like tomatoes, metal cans and containers are often coated with epoxy resin. Epoxy resins are utilized for a variety of good-performance and aesthetic flooring fields, including terrazzo, chip, and colored aggregate[40,41].

2.4.2 Adhesives

Epoxy adhesive has several technological applications. In a wide variety of situations, epoxy adhesives may be tailored to establish a strong bond on a variety of substrates. Adhesives may have their qualities modified to suit specific needs by using a wide variety of nanoparticles, each of which has its own set of characteristics. However, it is important to look into the kind of nanoparticles used, the form of the nanoparticles, and the functioning of the nanoparticles when working with nano-reinforced epoxy adhesives [42].

Epoxy resin-based adhesives are capable of forming a strong connection between two materials, regardless of whether those materials are the same or different, and can adhere to metals, glass, ceramics, wood, fibers, and many kinds of plastics[38]. The category of adhesives known as "structural adhesives" includes epoxy adhesives rather frequently among its elements. These good-performance adhesives are utilized in the manufacturing of a wide variety of products, including airplanes, vehicles, bicycles, boats, golf clubs, skis, snowboards, and other sports equipment, as well as other applications that call for high-strength bonding. When adhesives are going to be used in cryogenic engineering, it's important to make sure they have the best shear strength at both cryogenic and normal temperatures[43,44]. In order to achieve maximum durability, commercial epoxy adhesives include phase-separated thermoplastics, rubber particles, or hard inorganic particles within the matrix[45]. Adhesives are often cured at high temperatures to initiate chemical attraction at the surface/adhesive contact and enhance their strength[46,47].

One major drawback of adhesives as a connecting method is their susceptibility to moisture and water vapor. Their glass transition temperature (T_g) and chemical degradation also restrict their service temperature ranges, making them less versatile than metal fasteners. Since all adhesives include polar groups, water's significant polar component of surface free energy explains why it is particularly destructive to chemical bonding. Damage to joints caused by dampness is a two-step process. Both adhesive water absorption and adhesive water adsorption occur at the contact[48].

2.4.3 Construction and Structural Materials

The use of epoxy resins in construction may be broken down into two categories: the first of which combines epoxy resins with other materials to make construction components. The other uses epoxy resins in electrical and electronic engineering. Epoxy resins are widely used in composites, where they serve as matrix materials. When many qualities are required but only one material can provide them, composites are the best option[38].

2.5 Polymer Blend

Blending two or more polymers together results in a new material with novel physical characteristics known as a polymer blend[49]. There are four primary categories of polymer blends that have been the subject of substantial research: thermoplastic-thermoplastic blends; thermoplastic-rubber blends; thermoplastic-thermosetting blends; and rubber-thermosetting blends. There has been a lot of interest in polymer blending because it can be used to quickly and cost-effectively create polymeric materials with a wide range of potential commercial uses. That is to say, the blends' characteristics may be adjusted to suit their intended use by carefully choosing the

polymers that go into the mixture[50]. As a result of the intense competition in today's markets, manufacturers of plastics are being forced to develop new, more cost-effective materials that provide improved property combinations in order to serve as a suitable substitute for conventional metals and polymers. Although the raw ingredients for plastic are more expensive in terms of weight, than the raw materials for metals, the cost of the finished product made from plastic is less expensive. In addition to this, polymers are resistant to corrosion, have a low weight combined with a high level of toughness (which is important for achieving a high level of fuel economy in automobiles and aerospace applications), and are utilized in the production of a wide variety of products. Some of these products are biomedical devices, plastic items for the home, parts for the inside and outside of cars, and aerospace applications[50,51].

Creating a brand novel polymer and getting it ready for commercial use might take a long time and a hefty investment. It is feasible to shorten the period till commercialization to as little as two or three years by using a polymer mixing process, which is also highly cost-effective to run[51]. The creation of polymer blends accounted for fifty percent of all plastics manufactured in 2010, marking a significant step toward the elimination of conventional polymers. The polymer industry is becoming increasingly sophisticated in today's modern times, as ultra-high-performance injection molding equipment and extruders are now available on the market. These machines and extruders make it possible to effectively detect or manipulate phase-separations and changes in viscosity during the processing stages[50,52].

The process of combining two or more polymers into a single material has emerged as one of the most effective methods for enhancing the cost-to-performance ratio of plastics used in commercial applications. For instance, blending may be used to increase impact resistance, lower the cost of a costly engineering thermoplastic, or improve the processability of a high-temperature or heat-sensitive thermoplastic. Blending can also be used to decrease the cost of an expensive engineering thermoplastic. Blends produced in commercial environments could be phase-separated, homogenous, or a combination of the two[53].

2.6 Unmodified Epoxy Fracture Behavior

The epoxies, in their unaltered forms, break easily and brittlely, tensile stress is the most prevalent and causes fracture, and the issues of stress concentration noticeable flaws (cracks) appear. Traditionally, linear elastic fracture mechanics(LEFM) has been used to investigate the fracturing behavior of these epoxies [54], This is due to the fact that these materials are very brittle and only undergo localized plastic deformation when broken. Thus, the strength of epoxies is often quantified by calculating the critical strain-energy release rate, fracture energy (the amount of energy per unit area required to initiate a crack), or critical stress intensity factor (K_{IC}). When doing so, make sure the plane strain situation is minimal[55].

2.7 Epoxy Resin Toughening

Epoxy's major flaw is that its strongly cross-linked network makes it very brittle[56]. In addition, the inherent brittleness of epoxy resins prevents their use in a number of cutting-edge applications that need for great toughness, such as adhesives and fiber-reinforced polymers used in aerospace

applications. This severely restricts the applications in which epoxy resins may be used[57]. Because of all of these considerations, the highly cross-linked microstructure of the epoxy renders it very brittle, and as a result, the epoxy has poor resistance to the initiation and propagation of cracks[58–60]. Epoxy has a fracture energy that is, respectively, two and three orders of magnitude lower than that of engineered thermoplastics and metals. This suggests that epoxy has to be made tougher in order to have a larger range of applications. The fracture toughness of epoxy was the focus of significant research and development over the last several years[60]. There are many ways to make epoxy polymers tougher, such as through plasticization, the formation of an inter-penetrating network (IPN), and the addition of a second, well-dispersed minority phase made up of either soft rubbery particles or hard inorganic particles[10].

The addition of a second phase made up of materials including thermoplastics, block copolymers, and stiff or soft particles is a common technique employed for this purpose[58,61,62]. If inorganic or organic particles are employed, the resulting epoxy polymer is called "particulate-filled epoxy," whereas if soft rubbery particles are utilized, the glass transition temperature (T_g) is substantially lower than that under service circumstances. The process of adding a rubbery second phase is commonly referred to as the "rubber-toughening" method[58,60].

2.8 Techniques for Producing a Tough Epoxy Polymer

2.8.1 Block copolymer (BCP)

A novel method that uses amphiphilic di- and tri-block copolymers (BCP) as a toughening agent has significantly improved epoxy fracture toughness.

The BCP may be thought of as a micellar structure, formed when the compatible block dissolves into the matrix and the incompatible block microphase separates from it during mixing. Because BCP's micelle particles are so small and it only takes a small amount, BCP-toughened epoxies keep their matrix T_g and modulus while still having low viscosities that make them easy to work with[63,64]

2.8.2 Polyol

Compounds with more than two hydroxyl groups are known as polyols or polyhydric alcohols. Polyols allow the network chain's backbone to be flexible[65]. Polyether polyol and polyester polyol are the two most common types of polyols [66]. Polyether polyols account for more than 90% of all industrial polyol usage; polyester polyols for 9%; and other speciality polyols for less than 1%[65].

As can be seen in figure 2.6, polyether polyols are produced by reacting epoxides (oxiranes) with active hydrogen-containing starting compounds[67]**.**

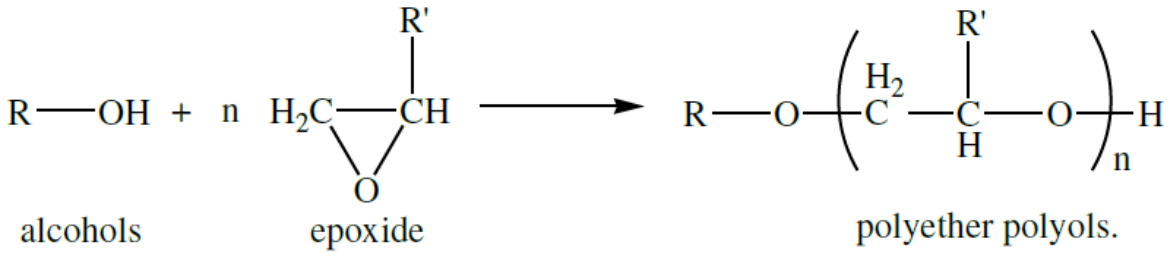

Figure 2.6: Synthesis of polyether polyol [67].

where R and R' were additional portions of the structure for alcohols and epoxides. As can be seen in figure 2.7[67], polyester polyols are synthesized by the polycondensation of various carboxylic acids and hydroxyl molecules.

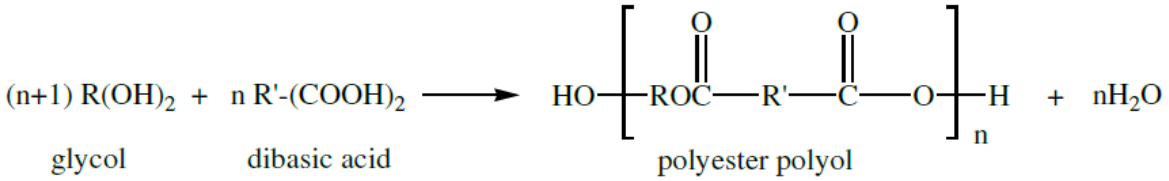

Figure2.7: Synthesis of polyester polyol[67].

For both glycol and dibasic acid, R and R' indicated for their respective complement structures.

2.8.3 Toughening of liquid rubber

Rubber phase insertion into the brittle epoxy matrix, either by reactive liquid rubber or rubber particles, is one of the effective approaches to toughening epoxy resins (EPs)[68]. Epoxy resins that have undergone rubbery modification have been shown to be the most effective strategy. In order to accomplish this goal, either functionally terminated liquid rubber or prefabricated rubber particles are used. To toughen the thermoset matrix, low molecular weight liquid rubbers are preferable because they prevent an excessive rise in viscosity and, as a result, boost the system's capacity to be processed easily and quickly. The amount of molecules that make up one gram of rubber grows throughout the cure polymerization process, and the phase separation of the rubber results in the production of a two-phase morphology. It has been shown that this is because the randomness of how the rubber is set up has become less. It is generally known at this point that rubber domains toughen the epoxy matrix to achieve good mechanical and

electrical characteristics by acting as stress concentrators. Epoxy resins may be modified with synthetic rubbers that have reactive functionalities like methyl, hydroxyl, carboxyl, anhydride, amine, or thiol groups. Carbon fiber reinforced epoxy matrix composite has been improved by Barcia et al. by using hydroxyl-terminated polybutadiene (HTPB). Epoxy resin matrices' mechanical characteristics have been tuned by adding hydroxyl-terminated, internally epoxidized polybutadiene. Another intriguing research demonstrates that epoxidized polybutadiene rubber has been discovered to be a useful modifier for epoxy systems. As an efficient toughening agent for epoxy matrix, carboxyl-terminated polybutadiene (CTPB) has also been examined. Carboxyl-terminated acrylonitrile-butadiene copolymer (CTBN) is a popular liquid rubber used to modify epoxy resin[69].

Functional groups in liquid rubber react with epoxy or hardener to significantly improve interfacial adhesion[70]. The epoxy resin toughening agent carboxyl-terminated butadiene acrylonitrile liquid rubber (CTBN) has seen extensive application[71,72]. Thomas et al.[73], looked into the effects of CTBN loadings on the mechanical and thermal properties of cured epoxy blends. They found that cured epoxy blends with 15 wt.% of CTBN and an average domain size of 0.5–1.0 μm had the best balance of properties, and the addition of CTBN lowered the glass transition temperature (T_g) of the epoxy matrix[74].

2.8.4 Chemically-Induced Toughening (Network Polymer Interpenetrating) (IPN)

An alternative approach to toughening the brittle epoxy polymers is the use of an interpenetrating polymer network (IPN), as shown in figure 2.8.

Interpenetrating polymer networks are a subtype of networks that are formed when two different types of polymers unite to create a single network[55]. In order to generate IPNs, the second polymer must be combined with epoxy. It doesn't matter whether these IPNs are generated simultaneously or sequentially by separate processes; what matters is that they properly bind with one another in order to improve the mechanical characteristics. This is due to the fact that remaining entangled in chains leads to a rise in bond formation. Thermosets like unsaturated polyesters have been mentioned by several of the researchers[55,75],cyanate esters and elastomers like polyurethane are used in the production of IPNs.

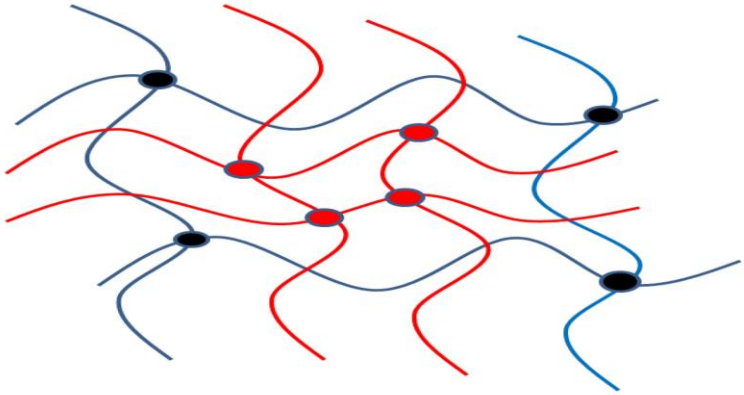

Figure 2.8: Interpenetrating Polymer Network (IPN)[55].

Fracture toughness levels have increased after the chemical modification. This technique lowers the glass transition temperature and other mechanical properties like tensile modulus and tensile strength. Because of this, they are not used very often[55].

2.8.5 The incorporation of thermoplastics into the structure

Toughening modifiers for thermosetting polymers, and epoxies in particular, can benefit from the use of thermoplastics because they do not appreciably

lower the glass transition of the cured network. Polysulfone (PSF)-modified epoxies are among the most extensively investigated thermoplastics due to the extensive research done on their mechanical characteristics, fracture performance, phase separation, and morphology. When Hedrick et al. toughened epoxies using phenolic hydroxyl and amine-terminated PSF oligomers, they saw a 100% improvement in fracture toughness without a corresponding decrease in thermal characteristics[76].

2.9 Nanocomposite

Composite materials containing at least one component with a nanoscale dimension are considered nanocomposites[34]. One nanometer equals 10^{-9} m [77]. The matrix, which can be made of metal, ceramic, or polymer, for example, is often the main ingredient that gives the composite its durability[78]. Because of their superior properties compared to those of conventional and microcomposites, these composites were developed. Nanocomposites have two or more phases that are separated by an interface and have different chemical and physical characteristics. as seen in a simplified form in figure 2.9[79].

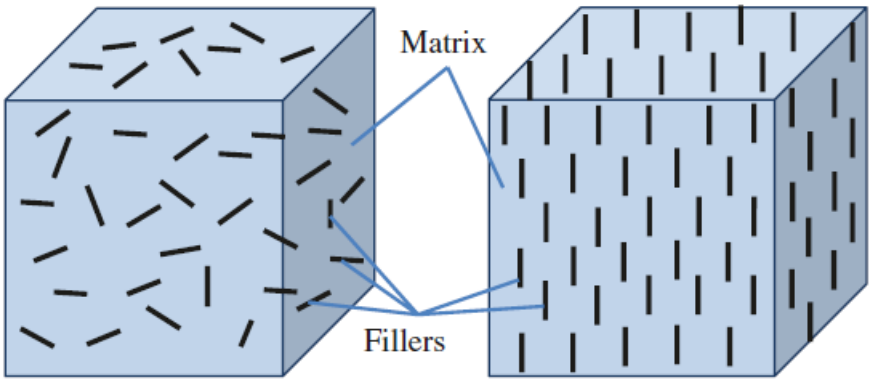

Figure2.9: The phases of a composite[78].

Nanocomposites may be incorporated into intricate aircraft geometry while also lowering production waste. Lightweight and low-maintenance fuselages and structures may be created with this. It was thought that the nanocomposite system would be a good candidate for use as a tribological material in spacecraft. Due to high phase temperatures, aerospace structures need to be made from strong and stiff materials that can keep their mechanical qualities[80]. There are several benefits to using polymer composites, particularly epoxy composites, over metals. They are less likely to corrode, have a higher ratio of strength to weight, can be put together with fewer parts, use less fuel because they are lighter, and are easier to fix, maintain, and service, among other things[56].

2.10 Nano Fillers

The typical particle size of nanofillers is between 1 and 100 nanometers. Reduced filler dimensions result in a larger surface area (per volume of filler) accessible for interaction with the matrix, leading to significant gains in reinforcing efficiency. At this point, it is well known that adding a nanofiller to a polymer matrix can make the matrix much stronger mechanically[81]. Dimensional categorization of nanostructured materials is an effort to classify these materials more thoroughly[82]. Depending on their macroscopic dimensions, nanostructure materials fall into one of four broad categories: zero-dimensional (i.e. nanoparticles), one-dimensional (i.e. nanorods or nanotubes), two-dimensional (typically realized as thin films or layers of thin films) [83], or three-dimensional (largely powders, fibrous, multilayer, and polycrystalline materials) as shown in figure2.10[78,82]

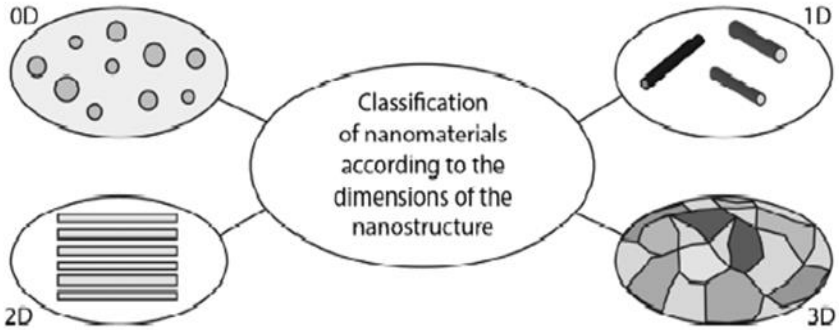

Figure 2.10: Classification of materials according to the dimensionality of the nanostructures [82]

Epoxy has limited impact strength and low wear resistance, limiting its use in tribological applications. Thus, epoxy is reinforced with appropriate reinforcement particles to improve its tribological features. Wear and mechanical qualities are enhanced by the use of hard oxides and carbides such as silicon oxide, alumina, and tungsten carbide. One of the best ways to spread out nano-particles is to use sonication. This makes sure that the reinforcement is distributed evenly. Void content in a WC/Epoxy nanocomposite sample decreases with increasing reinforcement weight percent, reaching a minimum at 2 wt% due to homogeneous WC particle dispersion, leading to improved erosion wear resistance and hardness in epoxy with 2 wt% WC compared to 1 wt% and 3 wt% WC[84]. The use of nanofillers with a small volume, between 1% and 5%, may increase the characteristics of composite materials that are equivalent to those of traditional microfillers with a volume ranging from 15% to 40%[85].

2.11 The Dispersion of Filler

Homogeneous dispersion of nanofillers in the base polymers lead to a large volume fraction between atoms which cause strong interfacial interaction between nanofillers and polymer matrices. As a result, the nanocomposite with a large number of interfaces provide enhanced performance to the polymers. Because hydrophilic nanoparticles and hydrophobic polymer matrices don't get along very well with the extremely energetic surface of nanofillers, nanoparticles tend to agglomerate, resulting in suboptimal interfacial interactions[86,87]. One crucial component affecting nanofilling dispersion is the filler's geometry[88]. Even if nanoparticles are successfully dispersed into a base polymer, poor particle distribution within the polymer will prevent the material from achieving its full potential. Nanofillers may be dispersed to control whether or not the particles are clumped together, or disseminated to ensure that the nanoparticles are evenly dispersed throughout the polymer matrix. In figure 2.11, see how nanoparticles are dispersed and distributed[87,89].

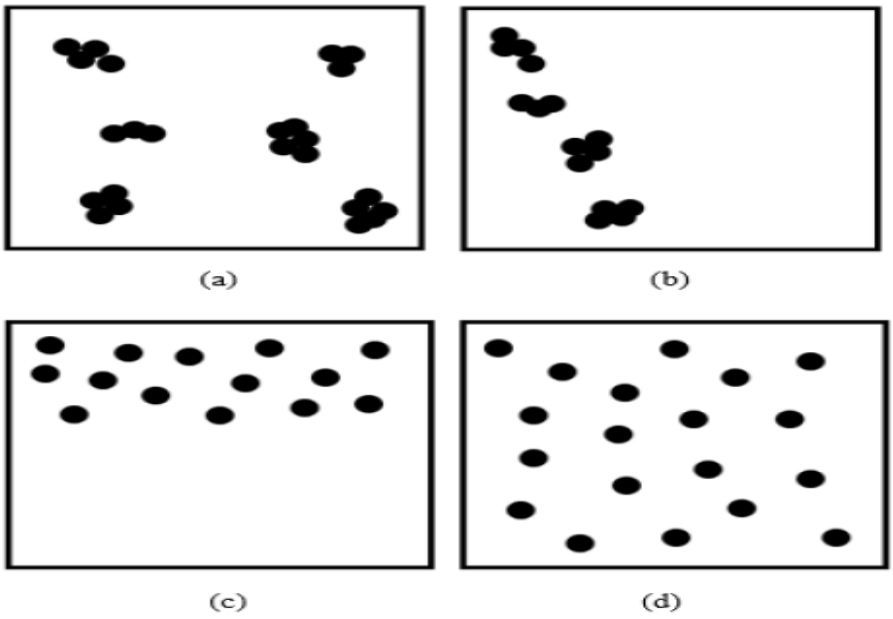

Figure 2.11:Explain the nanoparticles' dispersion and distribution state:(a) Badly dispersed, but evenly distributed. (b) Uneven distribution and poor dispersal. (c) Excellent dispersion but weak distribution (d) Optimal distribution and dispersal[87,90].

2.12 Tungsten Carbide (WC) Particles

Carbides are abrasives that come in powder form and are known for their extreme hardness, which makes them ideal for use as refractory materials. They are distinct crystalline configurations that may be assumed by compounds that include carbon and a metal or a semimetal element[91]. For its exceptional hardness, wear resistance, and thermal shock resistance, among other characteristics, tungsten carbide (WC) is a ceramic material of significant industrial interest. Because of these features, it is often used in the production of abrasives and other types of cutting tools [92].

Carburization of tungsten metal, which is produced by hydrogen reduction of tungsten oxide, is the first step in the production of tungsten carbide. Ball milling is used to combine tungsten powder with carbon black with the

desired particle size and dispersion. Particle size and dispersion may be managed by the use of carbon black. Carburization takes place at temperatures between 1,400 and 2,650 °C in the presence of hydrogen. When carbon black and hydrogen combine, they make gaseous hydrocarbons. When these gaseous hydrocarbons combine with tungsten, they make tungsten carbide:

$$W + CH_4 \rightarrow WC + 2H_2.$$

After being carburized, WC particles are typically milled to break them up into smaller pieces. It's possible for the final particle size to be anything from 0.5 μm to 30 μm[93]. The colloid chemical procedures involving tungsten and carbon compounds are the most appealing of the existing ways for fabricating high purity WC nanopowders with defined size parameters. The obvious benefits of this method lie in its potential to mix the components at the molecular level, in its ability to manage the dispersions of precursor and product particles, in its ability to reduce the temperature to 1000–1100 °C, and in its ability to shorten the period of the synthesis[92].

2. 13 Polymer Nanocomposites

Polymers are the best choice for making nanocomposites because they have properties that work well together, like elasticity, viscosity, and plasticity, that inorganic nanocrystals don't have[58]. These composites typically consist of a nanofiller (nanofibers, nanowhiskers, nanoplatelets, or nanoparticles) spread inside a polymeric matrix. The first industrially made nanocomposites were polymer nanoclay materials[93,94]. A polymer

nanostructure composite is a multiphase hybrid solid substance that incorporates one of the components as nanoscale fillers that possess least one dimension that is less than 100 nm dispersed inside a polymer matrix[95,96]. The addition of nanoparticles distributed in a polymer matrix has been shown to significantly improve mechanical, thermal, optical, and physicochemical characteristics compared to either the pure polymer or traditional composites (microscopic) with extremely low filler loading, generally 5 wt% or lower[95]. Matrix materials for composites are usually thermosets, but there has been a lot of interest in thermoplastic composites as well as carbon, ceramic, and metallic composites for high-temperature and other difficult applications[53]. Epoxy is the most commonly used thermoset in composite applications. Epoxy resins have a low cost and are simple to work with, but they are brittle and absorb a lot of moisture, which may weaken the bond between the filler and the matrix. The mechanical properties of composites are greatly influenced by the size, type, concentration, and dispersion of filler, as well as the degree to which the filler and matrices (also known as the continuous phase) adhere to one another at the interface, and the characteristics of the matrix itself[53]. Nanocomposite properties depend on the aspect ratio, the structure of the nanocomposite, and the affinity of the nanoreinforcement with the polymer matrix[97]. In composites, the resin matrix plays a significant role. To improve toughness while keeping other high-performance qualities, alterations to epoxy resin matrices are the most common approach[98].

In recent years, epoxy nanocomposites have garnered a great deal of attention as a result of the special physicochemical features they exhibit as a result of combining the nanoparticles with the epoxy. Aerospace structures

must also meet design criteria for their mechanical properties, such as being light, strong, tough, durable, resistant to wear and tear, able to withstand impacts, and not getting scratched[85,99].

2. 14 Methods for Preparing Polymer Nanocomposites

Cost, productivity, and end-product effectiveness must all be considered when settling on the optimal procedure for a certain polymer/nanoparticle combination. Most of the time, these are the ways that nanoparticles are spread out evenly in a polymer matrix like ultrasonic , high Shear Mixing, Solvent and combined approache [100] :

2.14.1 Ultrasonic (Sonication Method)

This technique employs ultrasonic equipment to uniformly distribute nano-fillers across a polymer matrix. Here, ultrasonic tools convey considerable impact energy while generating only a little shear in the ultrasonic space. The use of a sonicator has the potential benefit of causing nanoparticles that had clumped together to begin dispersing again. Greater specific surface area is the root cause of the propensity for agglomeration. As a result, excellent dispersion is challenging to achieve with single-walled carbon nanotubes (SWCNT). The studies have shown that mechanical agitation, followed by sonication, is an effective way to effectively disseminate nano-fillers inside a polymer matrix. A. Chatterjee and M.S. Islam, respectively[79,101], have manufactured and described TiO_2/epoxy nanocomposites. Everything they set out to do, they did successful the dispersal of nano-TiO_2 filler into a polymer matrix by using a Vibracell ultrasonic processor. Figure. 2.12 shows the Vibracell ultrasonic processor [79].

Figure 2.12: A vibracell ultrasonic processor[101]

2.15 Literature Review

Maider Larran˜aga et al., (2007) advised the epoxy-based blends with varying PEO/PPO molar ratios. Poly(ethylene oxide)-co-poly(ethylene oxide)-co-poly(ethylene oxide) (PEO-PPO-PEO) block copolymers were used. The mechanical characteristics of blends may be studied in relation to the morphologies formed and the interactions between components. The observed rise in flexural modulus may be connected to the reduction in free volume, as shown by mechanical, morphological, and dynamic mechanical investigations. The flexural modulus, strength, and fracture toughness may all improve in altered systems that are still miscible. Both macrophase and microphase-separated systems with low concentrations of block copolymers had an increase in fracture toughness, but not in flexural modulus or strength[102].

Arundhati et al., (2010) looked into how to make epoxy resin (DGEBA) stronger by mixing it with polysulfide and an aromatic anhydride hardener.

The addition percentages were 10, 20, 30, 40, and 50 phr. A study of the cured system's morphology showed that there was a two-phase zone where particles of liquid rubber were spread out into an epoxy matrix. When about 20 phr of elastomer was mixed in, the properties of the material got tougher. When the amount of elastomer was increased, even more, the phase changed. With a higher polysulfide concentration, mechanical properties as tensile, hardness, and flexural strength went down, but impact strength went up[103].

Wenying Zhou and Jiangtao Cai (2011) used hydroxyl-terminated polybutadiene (HTPB) liquid rubber and 2,4,6-tri (dimethylaminomethyl) phenol as a catalyst and methyl hexahydrophthalic anhydride as a curing agent to modify epoxy resin with a content of 5 to 30 phr. Fourier transform infrared (FTIR) was used to watch the reactions between HTPB and epoxy. The mechanical and dielectric properties of HTPB-modified epoxies were measured, and scanning electron microscopy(SEM) was employed to look at their shape . The FTIR analysis showed that the two parts were involved in a chemical reaction. The mechanical tests showed that the HTPB-modified epoxy had better impact strength than the pure epoxy. As the HTPB content went up to 10 phr, the best mechanical performances in terms of tensile and flexural properties were reached compared to the unmodified epoxy[104].

Muhammad M. Rahman et al., (2012). looked at the way a multifunction reactive diluent as well as toughener, an epoxy-terminated polyether polyol, and amino-functionalized multi-walled carbon nanotubes (NH_2-MWCNTs) affected the thermo-mechanical behavior of three-phase (epoxy/polyol/NH2-MWCNTs) toughened epoxy composites. But adding a very small amount of NH_2-MWCNTs (0.3wt.%) to the polyol-toughened epoxy greatly increased

the composites' glass transition temperature, storage and loss moduli, damping properties, and coefficient of thermal expansion (CTE). When the polyol (ten phr) was mixed in with the resin. a system, it made the system more flexible, but it also made the thermo-mechanical properties worse. But adding 0.3 wt.% of NH_2-MWCNTs to polyol-toughened epoxy composites made the features better than in neat and polyol-toughened epoxy composites. This was because the crosslinks between the NH_2-MWCNTs, epoxy-terminated polyol, and epoxy resin were better[105].

Wunpen Chonkaew et al., (2013)looked into how hybrid composites with rubber-like properties could be made from an epoxy that had been changed with either 2.5 phr or 15 phr of carboxyl-terminated poly(butadiene-co-acrylonitrile) (CTBN). From 0 to 5 phr of organo-montmorillonite clay was added. The morphology, including the shape of worn surfaces, was looked at; a dynamic mechanical analysis was done; and the resistance to impact was measured. Under dry sliding conditions, a pin-on-disc tribometer was used to measure the dynamic friction and wear. The smaller CTBN droplets in the material containing 2.5 phr CTBN led to a larger storage modulus compared to 15 phr CTBN. When compared to pure epoxy resin, all composites demonstrated superior Izod impact strength. While the addition of clay had no effect on the hybrids' dynamic friction, the wear resistance varied with clay concentration. At an applied stress of 5 N, EP/15-CTBN hybrids exhibited significantly higher wear rates than EP/2.5-CTBN nanocomposites. This may be due to the fact that EP/15-CTBN has a lower glassy storage modulus than EP/2.5-CTBN, which may explain the observed difference. To increase wear resistance at 5 N and 10 N typical loads, add less than 5 phr clay. It was found that the best way to improve the

mechanical and tribological properties of epoxy resin was to use 1 phr clay in an EP/2.5-CTBN matrix[72].

Hendrik Lützen et al., (2013) Incorporated of poly(caprolactone) (PCL) as a polymeric diol into cycloaliphatic epoxy resin transformed the brittle thermosetting polymer into a tough material dependent on the molecular weight and percentage of PCL that was (0–60 wt.%) in the polymer. Transparent polymers with improved toughness (tensile strength at break and elongation at break) were developed even at low PCL concentrations. With only a little bit of PCL added to the epoxy matrix, the polymer structure went from being a highly cross-linked hard epoxy network to one with a little lower crosslinking density. The polymers' increased strength and reduced brittleness, as well as their higher glass transition temperature and swelling behavior, provided evidence for this. Given that stress cracking may be substantially reduced and desirable thermal characteristics can be produced, PCL is an attractive substance that can be put to a wide variety of different uses[106].

Sajeev Martin George et al., (2014) An investigated epoxy based on diglycidyl ether of bisphenol A (DGEBA) and 4,4'-diaminodiphenylmethane (DDM) was used as a curing agent. when adding the epoxidation of styrene-block-butadiene-block-styrene triblock copolymer (eSBS47)to the epoxy matrix. The compositions included 10 and 20 weight percent of eSBS, respectively. The epoxy matrix included coreshell nanodomains of eSBS, as shown using transmission electron microscopy (TEM). The eSBS47-enhanced epoxy system features a nanophase-separated structure, which was verified by dynamic mechanical analysis (DMA). By adding eSBS47 to the

epoxy system, the fracture toughness of the nanostructured thermosets was increased. For example, the 20 wt% eSBS47-modified epoxy had a fracture toughness of 1.74 MPa.√m, which was much more than the unmixed epoxy but didn't altered its thermal stability or shape stability much[107].

K.C. Jajam et al., (2014) looked at how adding a reactive polyol diluent and amino-functionalized multi-walled carbon nano- tubes MWNTs to epoxy composites affected their fracture behavior. Epoxy, epoxy with carbon nanotubes (0.3 wt. %), epoxy with polyol (10 phr), and a hybrid epoxy with CNT(0.3 wt.) and polyol(10 phr) were the four types of samples developed . Overall, the changed systems had higher K_{IC} values than the pure epoxy did for quasi-static fracture initiation. Out of the four formulations tested, the hybrid epoxy/CNT/polyol system had the greatest K_{Ic} (70% improvement). Dynamic fracture experiments revealed that epoxy/polyol and hybrid epoxy/CNT/polyol composites had the lowest crack speeds compared to pure epoxy and epoxy/CNT. Composites made of epoxy and polyol or a mixture of epoxy and carbon nanotubes and polyol took far longer to break than pure epoxy and CNTs/epoxy. Compared to neat epoxy, the dynamic crack initiation toughness indices for epoxy/CNT, epoxy/polyol, and hybrid epoxy/CNT/polyol were 37%, 65%, and 92% better, respectively[108].

J. Abenojar et al., (2015) concentrated their research on the study of the surface damage caused by epoxy-based coatings applied to nanocomposites. The epoxy resin that was utilized was a commercial resin, and the fillers that were employed were boron and silicon carbides with a particle size of 60 and 100 nm, respectively. These fillers were used in two percentages (6 and 12 wt.%) (E6BC and E12BC, E6SC and E12SC) of the overall mixture. A

pin on disk test was performed in order to get a better indication of how much wear there had been. For the purpose of determining how efficient the nanoparticles/epoxy composites are as a wear-resistant coating, cavitation tests were carried out on aluminum specimens that had been coated with the composites. Scanning Electron Microscopy was used in order to investigate wear tracks as well as cavitation samples (SEM). The performance of nanocomposites containing 6% fillers is superior to that of nanocomposites containing 12% fillers. Between E6BC and E6SC, the results have demonstrated better properties in the E6BC, for its best anchoring with the matrix[109].

Fuzhong Wang et al., (2016) looked into how adding carboxyl terminated butadiene acrylonitrile (CTBN) to epoxy resins could improve the fracture toughness. Then, graphene nanoplatelets (GnPs) with diameters of 1 μm (GnP/C750) and 5 μm (GnP/5) were added to the CTBN/epoxy to make multi-phase composites. The amount of CTBN in the final composite was kept the same at 10 wt.% and 1 wt.%, and 3 wt.%. GnPs were put into the rubber-modified epoxy composite. By mixing 3 wt.% GnP/5 into 10 wt.%CTBN changed epoxy resins to make GnPs/CTBN/epoxy ternary composites with improved fracture toughness and thermal conductivity and stiffness corresponding to the value of the untreated resin. The high thermal conductivity of GnPs and strong interfacial adhesion between GnPs and the CTBN/epoxy matrix led to an increase in the composites' thermal conductivity, and the addition of GnPs also increased the storage, flexural, and Young's modulus of the rubber-modified epoxy. Based on the results of the investigation, GnP/5 improved the material's characteristics of CTBN/epoxy. There was a clear relationship between the improvement in properties and the size of the particles. For example, GnP-5 was better at

reinforcing than GnP/C750 because it had a more even distribution and a bigger aspect ratio. Incorporating 3 wt.% GnP-5 and 10 wt.% CTBN into the epoxy resin enabled the effective preparation of GnPs/CTBN/epoxy ternary composites with significant toughness (108%) and thermal conductivity (145%) increases while maintaining stiffness equivalent to the neat resin. SEM analyses suggested that CTBN prevented GnP/5 from detachment from the base matrix [110].

Nachiket G. Chanshetti1 and Anil S. Pol (2016) Examined the wear resistance and hardness of epoxy composites that have been supplemented with titanium dioxide (TiO_2) and tungsten carbide (WC). There were three distinct volume proportions of TiO_2 and WC put into the epoxy matrix: 5%, and 10%. The specimens were made using the hand layup method, which included pouring epoxy and a combination of reinforcements into wooden molds. The tests were conducted in accordance with ASTM G99-95a and ASTM D 2240 standards for wear and (shore-D) hardness, respectively. Specimen wear resistance was evaluated using a pin-on-disk setup at different loads and rotational speeds. It was shown that both types of reinforcement in an epoxy matrix result in a decreased wear rate compared to neat epoxy. When compared to unfilled epoxy and 5% TiO_2 filled epoxy, as well as 10% TiO_2 filled epoxy, the wear rate of the 10% TiO_2 filled epoxy is reduced at all amounts of load. When it comes to WC filled epoxy composites, both 5% and 10% of WC filled epoxy composites will provide outcomes that are superior to unfilled epoxy resin in terms of decreased wear rate[111] .

Lina Dong et al., (2017) looked at the possibility of modifying epoxy (EP) resin with carboxyl-terminated polybutadiene (CTPB) liquid rubber. The

chemical interactions that took place between the oxirane ring of (EP) and the carboxyl groups of CTPB while benzyldimethylamine served as a catalyst were confirmed by Fourier transform infrared spectroscopy. There is a possibility that the loss in thermal stability is attributable to the fact that CTPB has poorer thermal stability when compared to neat EP. The mechanical results revealed that CTPB-modified EP was better than pure EP, and 20 phr of CTPB was usually enough to get the best overall mechanical properties. Because the system has two phases, the impact strength of the system with 20 phr CTPB increased by 193%. The fact that CTPB-modified EP has better impact strength and elongation at break shows that the modified EP will last longer than pure EP. It has been shown that 20 phr of CTPB provides the optimal balance of mechanical performance in terms of tensile and flexural characteristics of EP. With increasing CTPB content from 0 to 20 phr, the elongation at break of the sample changed from 2.56% to 8.86%. The system containing a 20 phr CTPB had a maximum impact strength value of 21.1 J/m^2 which is about 193% higher than that of neat EP[112].

Fahriadi Pakaya1 et al., (2017) Studied the mechanical characteristics and thermal stability of thermoset epoxy as a function of room temperature vulcanization (RTV) silicone rubber content (5%, 10%, 15%, and 20% wt%). Thermoset epoxy with added RTV silicone rubber was subjected to testing and characterisation. Not only that, but RTV silicone rubber now has a lower tensile strength, elongation at break, and hardness. When 15% RTV silicone rubber was added, the best values for energy and impact strength were reached: 0.294 J and 6175 J/m^2, respectively. Additionally, thermoset epoxy's thermal stability may be enhanced by using RTV silicone rubber.

The inclusion of wt% RTV silicone rubber improves thermal stability. This is due to the presence of organosilane molecules in RTV silicone rubber[4]

Muzher T. Mohamed (2018) analyzed the effect of adding polysulfide rubber (PSR) as a toughener to a brittle base epoxy polymer on the toughness parameters of polymeric composites. Epoxy blended with 2, 4, 6, 8, and 10% PSR was tested, and a comparison to unmodifide epoxy specimens was made. These data are evidence that PSR added to polymeric resin improves epoxy's toughness. A similar series of experiments revealed that a mixing ratio of 6% PSR caused a good jump in the amount of composite strain at the loss of tensile strength and modulus of elasticity at fracture. Adding PSR to epoxy reduced its ultimate strength but increased its elongation and impact resistance. PSR mixed at 4% with epoxy yielded the best mechanical performance[113].

Zeyu Sun et al., (2019) studied using polysulfone (PSF) to strengthen and alter the epoxy. The samples were categorized as 5, 10, 15, and 20 phr based on the varying PSF to epoxy resin weight ratios. Optical microscopy, Fourier transform infrared spectroscopy, differential scanning calorimetry, mechanical testing, and a scanning electron microscope(SEM) were used to comprehensively examine the effects of PSF on the mechanical and thermal characteristics of the epoxy resin. It was found via experimentation that PSF is highly soluble in epoxy resin and has a high degree of compatibility with the resin. Because they have a bicontinuous phase structure, PSF/epoxy resin blends have better mechanical properties, such as higher impact strength and fracture toughness. The K_{IC} of the blend that contains 15 phr PSF shows that the material has reached its maximum fracture toughness. Increasing the PSF concentration is favorable to improving the fracture toughness. When

compared to unmixed epoxy resin, the PSF content of 15 phr yielded the maximum impact strength, with a value of 38.2 J/m^2. This represented an increase of 65.3% in comparison to the pure epoxy resin[114].

Ahmed J Farhan and Harith I Jaffer (2020) Prepared epoxy/RTV silicon rubber (SR) and unsaturated polyester/RTV silicon rubber (SR) blends are made by combining epoxy resins with SR and UPE resin with SR at weight percentages of 3, 5, 7, 10, and 20 respectively. This study aims to determine the mechanical characteristics of epoxy and unsaturated polyester as a function of RTV silicone rubber content (3, 5, 7, 10, and 20) wt%. Some of the mechanical parameters that were looked at were the impact strength, Shore D hardness, Young modulus, and flexural strength. The impact strength of the EP/SR and UPE/SR blends is maximized at 10%wt SR and 5%wt SR, respectively, according to the experimental data. In both EP/SR and UPE/SR, the hardness value was partially reduced as the SR component grew from 3% to 20%wt. As the SR component grew from 3% to 20%wt in both EP/SR and UPE/SR, flexural strength quickly declined[115]

M. Kameswara Reddy et al., (2020) Investigated tribological nanocomposites comprising an epoxy polymer and tungsten carbide (WC) nanoparticles. The polymer nanocomposites were made using the hand lay-up technique. The physical and wear characteristics of epoxy/WC nanocomposites were investigated by subjecting them to a set of erosive wear and hardness tests. Incorporating WC nanoparticles drastically lowered the erosion process. Adding WC nanoparticles to epoxy nanocomposites also made them harder. Nanocomposites with a 2% weight of WC nanoparticles performed better than those with a 1% weight of WC nanoparticles in terms of erosion wear characteristics and hardness. Due to

insufficient adhesive bonding between the matrix and the nanoparticles, hardness performance was lowest when WC nanoparticles made up only 3 weight percent of the material [116]

V Gavrish and et al., (2021) looked into the mechanical behavior of samples consisting of glass fiber Lavesan (Italy) and a binder-EPR 320 epoxy resin treated with tungsten carbide (WC) nanopowder. The favorable influence of nanopowder in terms of its tensile strength. The tensile of strength of fiberglass polymers (GRP) is increased by more than a factor of 1.5 when nanopowder is included in epoxy resin at a concentration of 1%. At a nanopowder level of 4% of the mass of epoxy resin, the strength of GRP is increased by more than 2.5 times over the range of values examined. This shows that these modifiers have a lot of potential to be used in the aerospace industry to make it easier to make parts stronger and easier to use[117].

2.16 Concluding Remark

This dissertation focuses on the mechanical properties and adhesion properties of epoxy resin those that have been altered by the different types of toughening agents. The wear properties for two systems of tungsten carbide nanoparticles WC/epoxy and WC/triblock copolymer (at 3% wt.)/epoxy were studied.

The aim of the research is to offer to a more complete understanding of action toughening agents for epoxy and modified (tungsten carbide particle reinforced) epoxy systems, will try to provide answers to the above raised questions and enable the targeted use of toughening agents in epoxies, i.e., manufacture tough, impact, mechanical strength, and wear resistant epoxies

by understanding the morphology of such versatile macromolecular species in high-performance resin systems.

To improve the fracture toughness of brittle polymer matrices, many studies used matrix toughening agents such as rubber, block copolymer, polyol, and thermoplastic toughening agents as liquids or particles. The results of these strategies were to make composites with two-phase modified matrices stronger and more resistant to damage from impacts.

In other studies, epoxy matrix was reinforced with various carbides and other nanoparticles to study the mechanical and tribological properties of epoxy nanocomposite.

A few studies have focused on adding liquid rubber and RTV silicon rubber to the modifier epoxy matrix. The epoxy/SiC/CTBN nanocomposite revealed a much higher Tg and greater thermal stability as compared with both pure epoxy and the epoxy/CTBN combination. Fewer studies have focused on the mechanical properties of polyether polyol-epoxy blends based on polyol content to study K_{IC} and impact strength of the blend.

Other studies have used thermoplastic and block polymers to enhance the brittleness of epoxy resins with studied mechanical , thermal, and phase-separate morphologies. Another studies have focused on the effects of nano reinforcement on epoxy resin, e.g.,tungsten carbide , boron carbide ,silicon carbide, and studying different properties such as tensile ,fracture toughness, impact , hardness, and wear properties.

In this study, use five mixtures (TBCP,PU polyol, LSR, PVC and PSR) with epoxy to improve the toughness, and the best material that give stiffness and improved toughness at the same time was triblock copolymer at a mixing

ratio of 3%wt. After that, tungsten carbide nanoparticles/epoxy nanocomposite was prepared once with epoxy and once more for a mixture of epoxy and triblock copolymer with a ratio of 3%wt. The mechanical properties, wear and adhesion properties of the composite materials were studied, and give good properties.

Chapter Three

Experimental Part

Chapter Three

Experimental Part

3.1 Introduction

The present chapter covers all the most important details about the methodology that was used in this study, starting with materials selection and specification, preparation of samples, and the instruments of inspection. The research plan that was carried out is shown in figure (3.1)

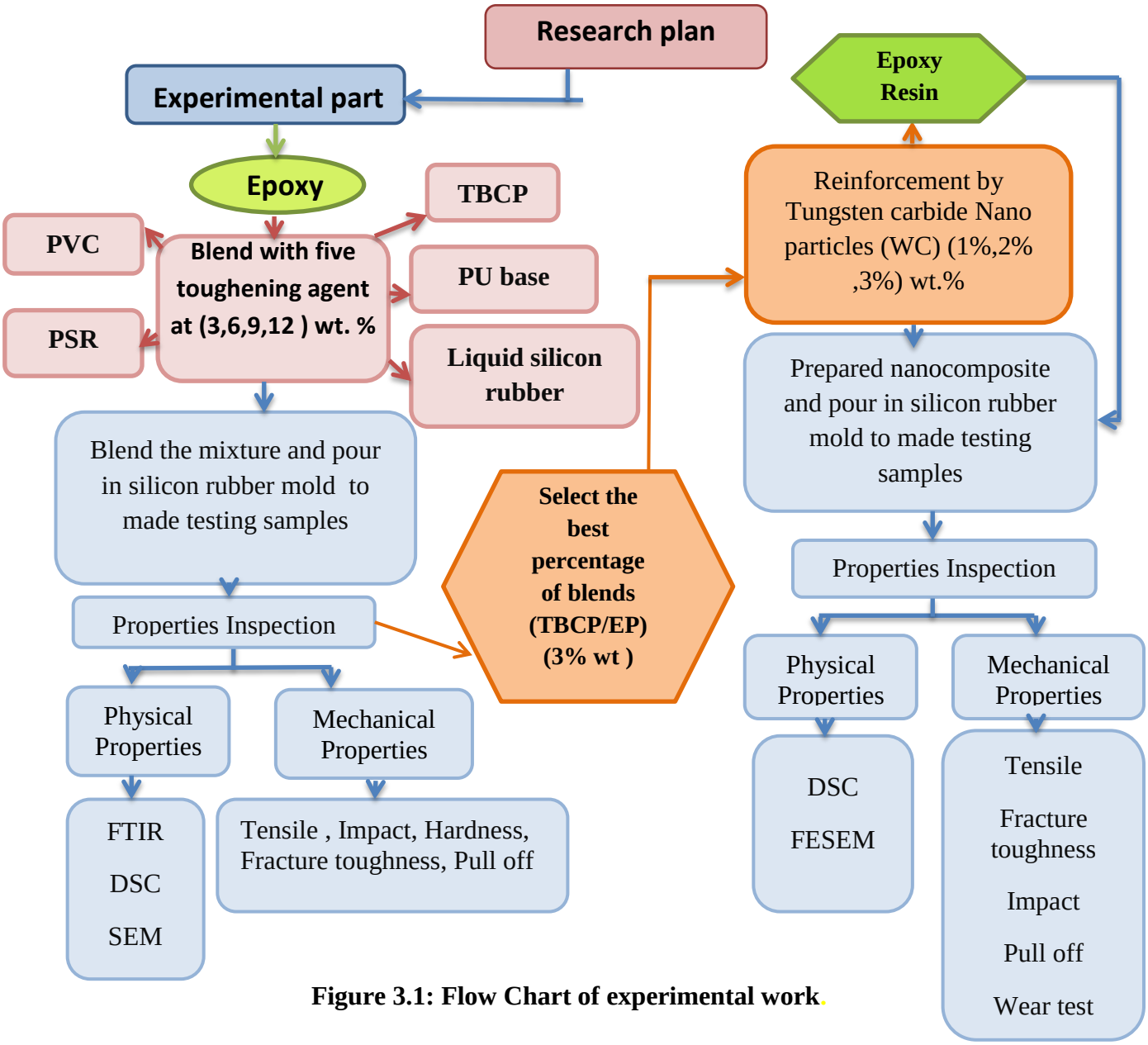

Figure 3.1: Flow Chart of experimental work.

3.2 Materials

3.2.1 Epoxy Resin

Epoxy Sikadur 52 (TR Produced) was purchased from the company's agent in Sikadur, Hilla, Iraq. Sikadure 52 with the properties maintained in table 3.1.

Table 3.1: Epoxy sikadur 52 properties[118].

Property	Data
Form	Liquid
Chemical Base	two-part epoxy resin. Part A: bisphenol F-(epichlorohydrin) Part B: ((izoforon diamine), (1-methylethyl)-1,1'-biphenyl))(hardner)
Color	Part A: Transparent Part B: Brownish Part A+B mixed: Yellowish-brownish
density	1.1 kg/l (at +20°C)
Compression strength	52 N/mm^2
Flexural Strength	61 N/mm^2

3.2.2 Toughnening Agents

3.2.2.1 Triblock copolymer (TBCP)

The softer segment of a polyethylene glycol-block-polypropylene glycol-block-polyethylene glycol structure, also known as EO-PPO-EO, was used in this study as a toughening agent. It had a number average molecular weight (Mn) of 2000 g/mol and a functionality of 2.0[119] (See figure 3.2). Dow Chemicals was the company that supplied the material.

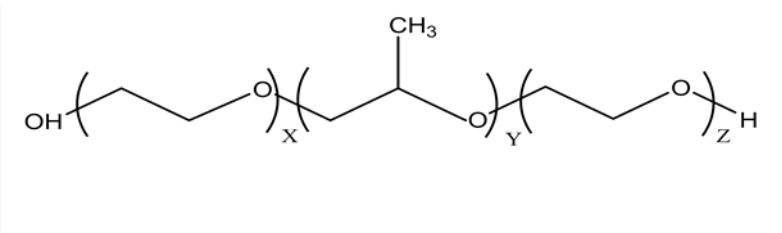

Figure 3.2: EO-PPO-EO Structural style[120,121].

3.2.2.2 Quickmast 120 PU Polyol

Another toughening agent (polyol) that is used in the preparation of the samples is the Quickmast 120 type (PU base resin), which is supplied by the company agent DCP, Hilla, Iraq. Manufactured by DCP Saudi Co. The properties of 120 Quickmast polyol base liquid are as follows: yellowish green, relative density (1.1-1.2 at 25 °C), insoluble, and stable.

3.2.2.3 Liquid Silicon Rubber (LSR)

silicone rubber is a kind of liquid silicone elastomer. Liquid silicone, which curing at room temperature with good self-leveling ability, was purchased from HONG YE JIE, China, has Shore A hardness can be modulated from 18 to 65. Elongation at break can range from 150% up to 700%[122].

3.2.2.4 Liquid Polyvinyl Chloride Adhesive (PVC)

The type of polymer used in the work is a commercial PVC adhesive type(local material). It is in a fluid form as an adhesive. It contains tetrahyrofuron 109-99-9, methyl ethyl ketone 78-93-3, and cyclohexanone 108-94-1.

3.2.2.5 Polysulphide Polymer

The polysulphide polymer is a two-part adhesive, the base, and the hardener. The base that was used in this study (Flexseal PS660 – base) was purchased from the company agent DCP, Hilla, Iraq. Manufactured by DCP Saudi Co. It is a viscous liquid with, off-white color. Its relative density at 25 °C is 1.50 and it has insoluble water solubility.

3.2.3 Tungsten Carbide (WC) Nanoparticle

Tungsten Carbide nanoparticles were purchased from US Research Nanomaterials, Inc., Houston, TX USA with the properties maintained in a table (3.2). See figure 3.3 illustrated SEM image of pure carbide tungsten nanoparticles standard and sample test.

Table 3.2: Properties of Tungsten Carbide nanoparticle

Properties	Value
Form	Nano particle (Hexagonal)
Density	15.63 g/cm^3
Color	Grey Black
Nanoparticle grain size	55 nm
Nanoparticle APS	150 – 200 nm
Purity	99.9 %

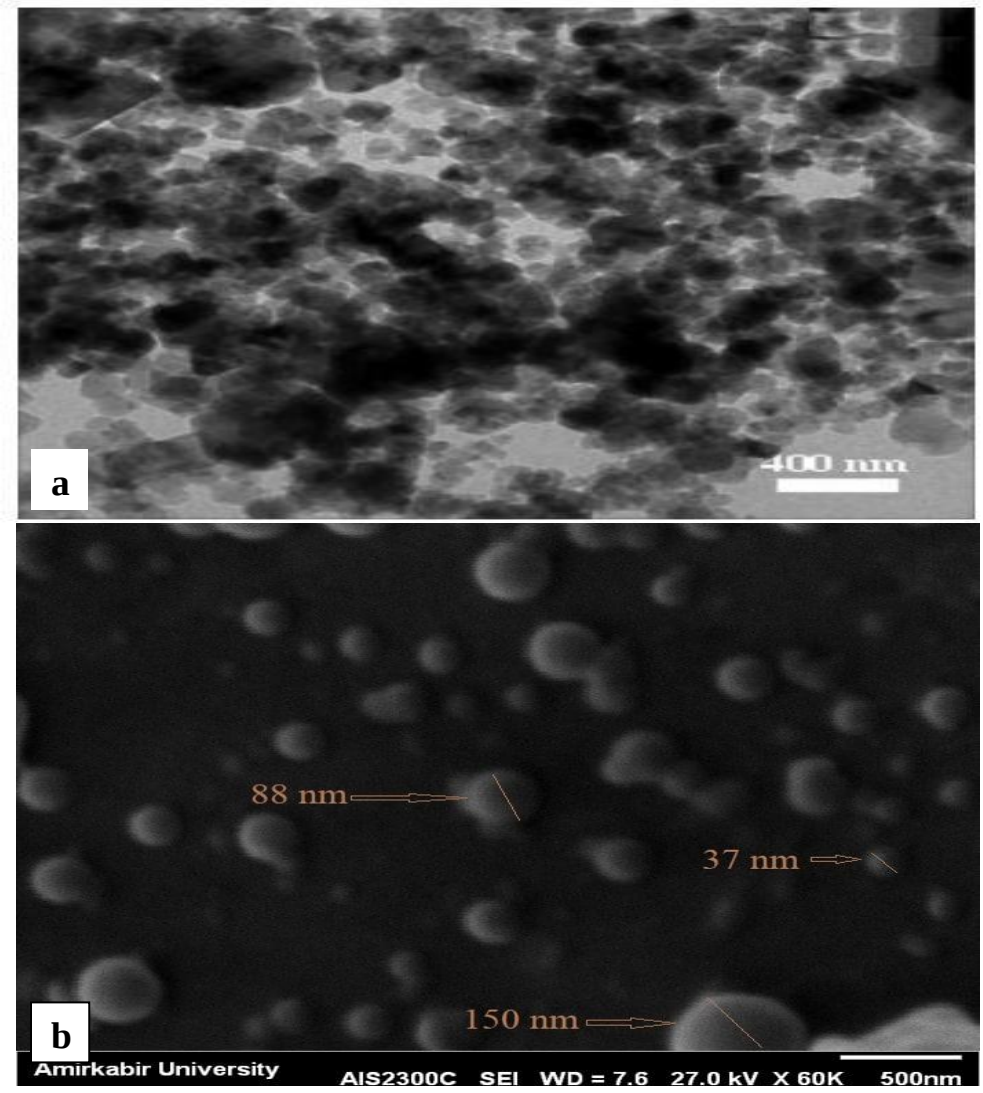

Figure 3.3 : SEM image of pure carbide tungsten nanoparticles a)standard from company b) sample test .

3.3 Samples Preparation

3.3.1 Unmodified Epoxy (neat epoxy EP)

Epoxy resin/harder was mixed (with a ratio of 2:1) for 10 minutes using a mechanical stirrer, and the mixture was put in the degassing system under vacuum at room temperature for 10-15 minutes to eliminate bubbles. After that, the materials were put into the mold made of silicon, which was previously prepared, and left for 24 hours at room temperature to obtain unmodified epoxy samples. Figure (3.4) shows the procedures used to prepare unmodified epoxy samples.

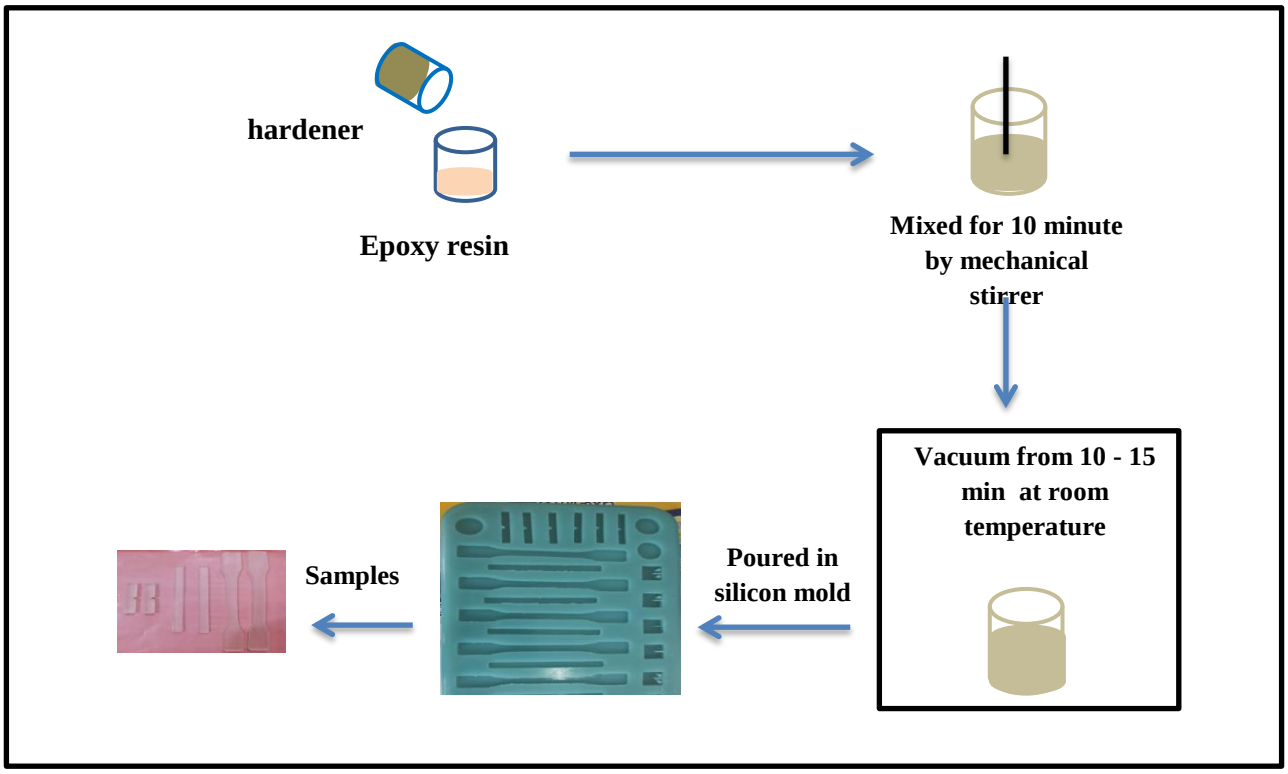

Figure 3.4: The procedure of preparing unmodified epoxy samples

3.3.2 Epoxy Blends

3.3.2.1 Preparation of Samples Using Matrix Toughening Agents

- Group A**:** Epoxy with TBCP blend.
- Group B: Epoxy with 120 quick maste (PU base) blend.
- Group C: Epoxy with liquid PVC adhesive blend.
- Group D: epoxy with liquid silicon rubber blend.
- Group E: epoxy with polysulfide polymer blend.

Blends were prepared using different ratios of toughening agents (five groups A-E), 3%, 6%, 9%, and 12% wt, as shown in table (3.3). The toughening agent added to epoxy was carried out using a mechanical stirrer for 10 minutes, then the hardener (with a ratio of 2:1) was added and mixed for 10 minutes using a mechanical stirrer. The prepared mixture is put in the degassing system under vacuum at room temperature for 10–15 minutes to eliminate bubbles. After that, the materials were put into the mold made of silicon, which was previously prepared, and left for 24 hours at room temperature, at which point different samples of modifier epoxy polymer blends were obtained. Figure (3.5) describe the procedure used to prepare the modifier epoxy polymer blend samples.

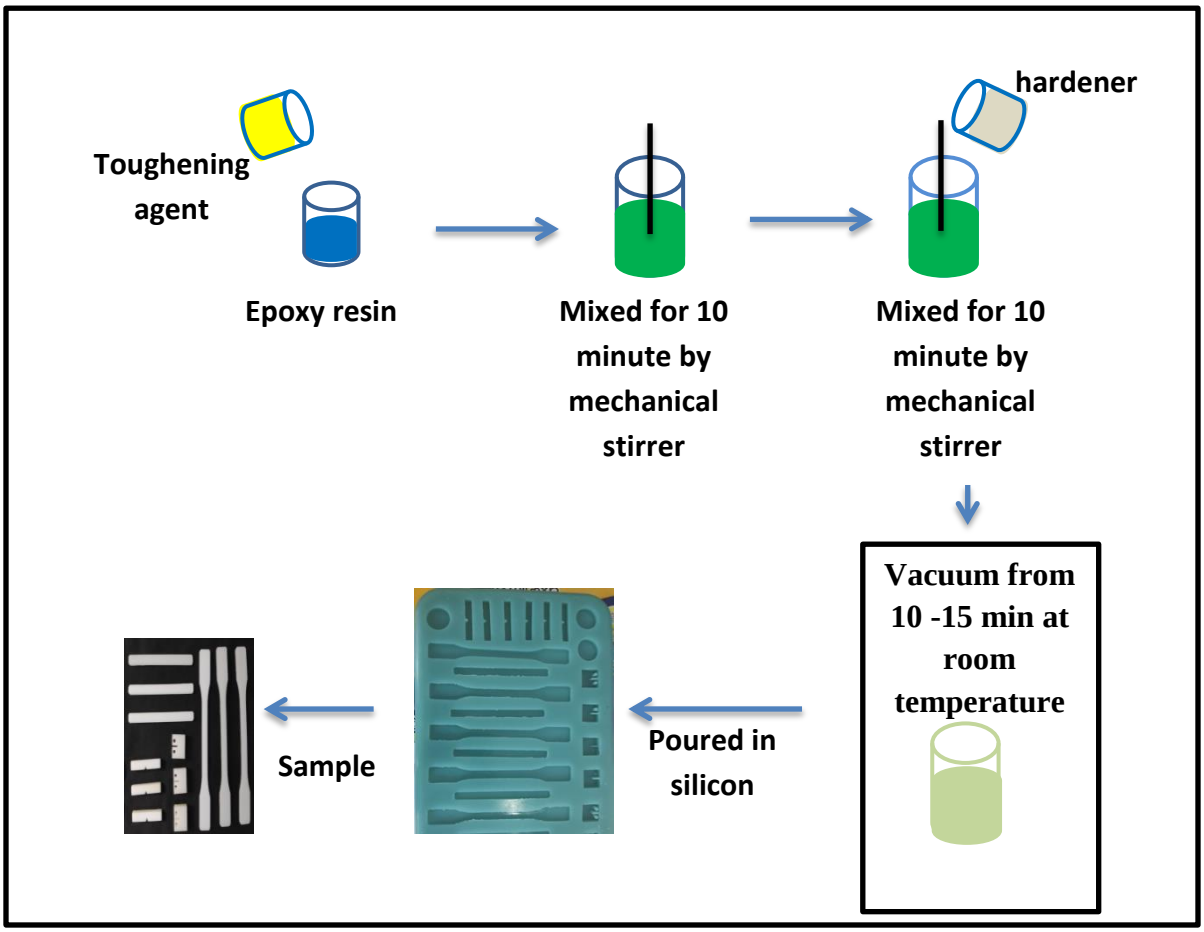

Figure 3.5: The procedure used to prepare modified epoxy blends

Table3.3:Toughening agent/epoxy blend sample composition prepared in this study

Sample number	Matrix Polymer blends	Toughening agent	Samples Composition
1	Unmodified epoxy (neat epoxy)	No toughening agent	**EP**
2	Modified epoxy	(EO-PPO-EO) TBCP	**3% TBCP/EP**
3	=	=	**6% TBCP/EP**
4	=	=	**9% TBCP/EP**

5	=	=	**12% TBCP/EP**
6	=	120 Quickmaster (polyol)	**3% PU/EP**
7	=	=	**6% PU/EP**
8	=	=	**9% PU/EP**
9	=	=	**12% PU/EP**
10	=	Liquid silicon rubber	**3% LSR/EP**
11	=	=	**6% LSR/EP**
12	=	=	**9% LSR/EP**
13	=	=	**12% LSR/EP**
14	=	Liquid polyvinyl chloride	**3% PVC/EP**
15	=	=	**6% PVC/EP**
16	=	=	**9% PVC/EP**
17	=	=	**12% PVC/EP**
18	=	Polysulphide polymer	**3% PSR/EP**
19	=	=	**6% PSR/EP**
20	=	=	**9% PSR/EP**
21	=	=	**12% PSR/EP**

3.3.3 Preparation of Nanocomposites

Two groups were prepared from nanocomposite material. The first group was mixing epoxy with nano-tungsten carbide(WC), while the other group was mixing tungsten carbide nanoparticles with a blend of epoxy with 3% TBCP(sample numbers 4, 5, and 6 in table 3.3). The material was weighted according to the weight fraction ratio according to the table (3.4) and then the WC nanoparticles were dispersed in ethanol by an ultrasonic device at 35°C and energy 40% (sonic frequency 40 (kHz)) for 30 min. Then, the matrix (epoxy, TBCP/epoxy) was added to the nano solution simultaneously with mixing using a mechanical stirrer for 15 min. To get the ethanol to evaporate, the mixture was put on a magnetic stirrer and heated to 70 degrees Celsius for more than one and a half hours until the weight was fixed. After that, let the mixture cool down at room temperature. Following this, added hardener and put it under a degassing vacuum to avoid bubbles, and lastly, they poured it into the silicon mold to obtain samples. Figure (3.6) shows the schematic of the WC/epoxy nanocomposite preparation process.

Table 3.4 shows the sample composition of the WC/epoxy nanocomposite prepared in this study.

Sample number	Type of composite	Matrix nanocomposite	Reinforcement Nanoparticle reinforcement	Samples composition
1	Epoxy Nanocomposite	Neat epoxy	Tungsten carbide	**1% WC/ EP**
2	=	=	=	**2% WC/EP**
3	=	=	=	**3% WC/EP**
4	Modified epoxy Nanocomposite	Epoxy/3% wt TBCP	=	**1% WC/TBCP/EP**
5	=	=	=	**2% WC/TBCP/EP**
6	=	=	=	**3% WC/TBCP/EP**

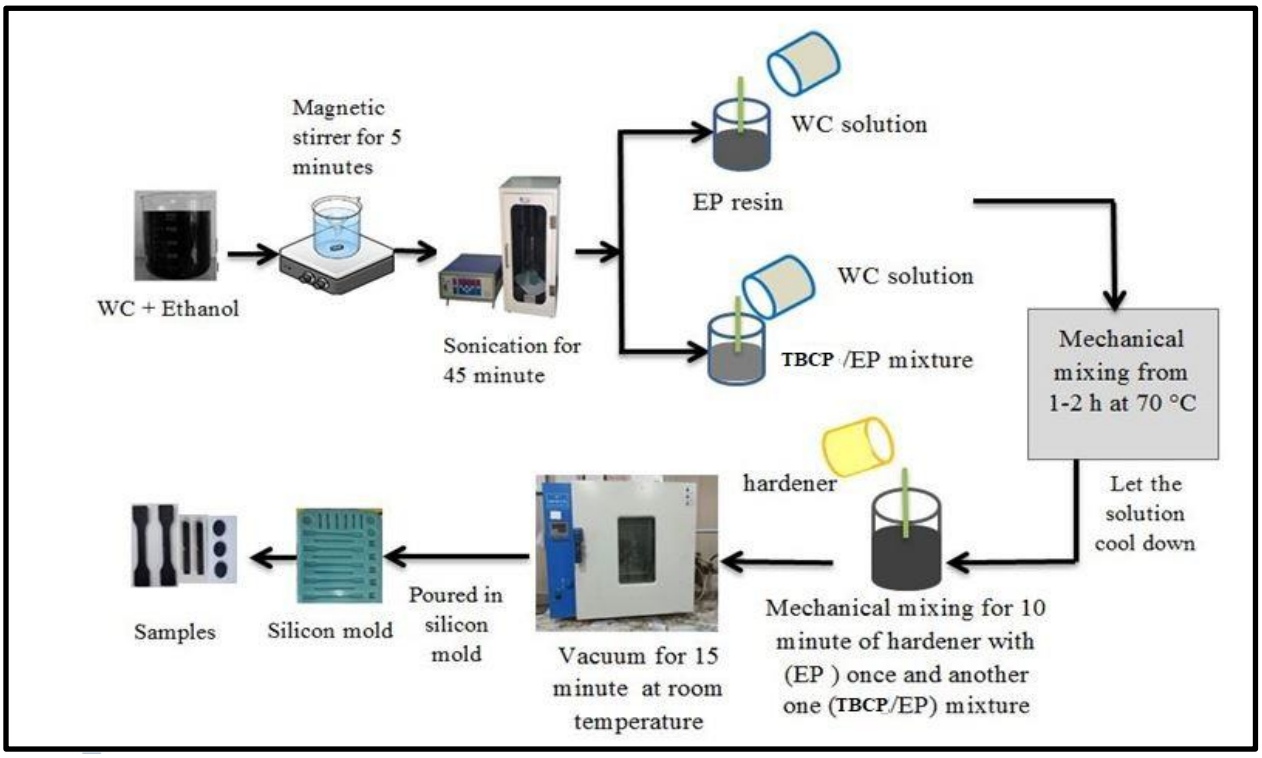

Figure 3.6: Schematic of the WC /epoxy nanocomposite preparation process.

3.4 Physical Inspection

3.4.1 Fourier Transform Infrared Spectroscopy (FTIR) Test

The test of FTIR was achieved using a Fourier transform infrared spectrometer and was used to obtain specific information about the chemical bonds and molecular structure of epoxy system samples. The (FTIR) test is performed according to (ASTM E1252) by using FTIR instrument type IR Affinity-1 (made in Japan)[123]. It is available in the laboratory of the Materials Engineering Faculty/Polymer Engineering and Petrochemicals Industries Department/ University of Babylon. It is supplied with a DTGS detector that operates at ambient temperature and a KBr beam splitter. The infrared spectrum was used within a range of (400–4000)cm^{-1}.FTIR was performed on a spectrum of neat epoxy polymers, epoxy blends, and WC/epoxy nanocomposites.

3.4.2 Differential Scanning Calorimetry (DSC)

Differential scanning calorimetry measurements (DSC) were carried out according to ASTM D3418-03[124],. using the SHIMADZU model FC-60A made in Japan. The prepared samples had a weight of (8-10)± 0.5 mg. It was inserted into aluminum pans and has a temperature range of 25 to 250 degrees Celsius with a heating rate of 10 degrees Celsius per minute. The test was done in the laboratory of the Polymer Engineering and Petrochemical Industries Department at/ University of Babylon

3.4.3 Morphology Test

The techniques of SEM and FESEM have been employed in current work to characterize the toughening agents/epoxy blends fracture surfaces, tungsten carbide nanopowder, and also study the surface of fracture of prepared

nanocomposite materials. Thus, to get good tribology properties, composite materials were spluttered with gold. Electronic pictures were recorded, and the working voltage was held at (20 kV). The FESEM device product, TA company, model Q600, made in America, and the SEM device used to analyze the fracture surface of epoxy/blends, was from Seron Technology Company, South Korea Manufacturing, AIS2100 Model.

3.4.4 X-Ray Diffraction Analysis

An X-Ray diffraction test (XRD) is a non-destructive technique for determining the crystalline nature, chemical content, and physical properties of a material. The technique relies on the constructive interference of monochrome X-rays and a crystalline specimen. X-rays are a type of electromagnetic radiation with shorter wavelengths that are produced when electrically charged particles with enough kinetic energy are decelerated. An X-ray diffractometer (XRD) uses incident X-rays that have been focused and collimated on a sample of nanomaterial. The resulting diffracted X-ray is then identified, evaluated, and recorded. Diffraction patterns are displayed by plotting the intensities of photons that have been diffracted and then dispersed at different angles within a material[125].

3.5 Mechanical Tests

3.5.1 Tensile Test

A microcomputer-controlled electronic universal testing machine model (WDW-5E) from China with a 5 N load cell, was used to perform tensile tests according to ASTM D-638-03[126]. The force was applied until the specimen failed, and the cross head was 2 mm/min. Stress and strain information were recorded. Each time a sample was tested, three were taken,

and their combined results were used to determine its mechanical features. The images and the dimensions of tensile samples were shown in figure 3.7.

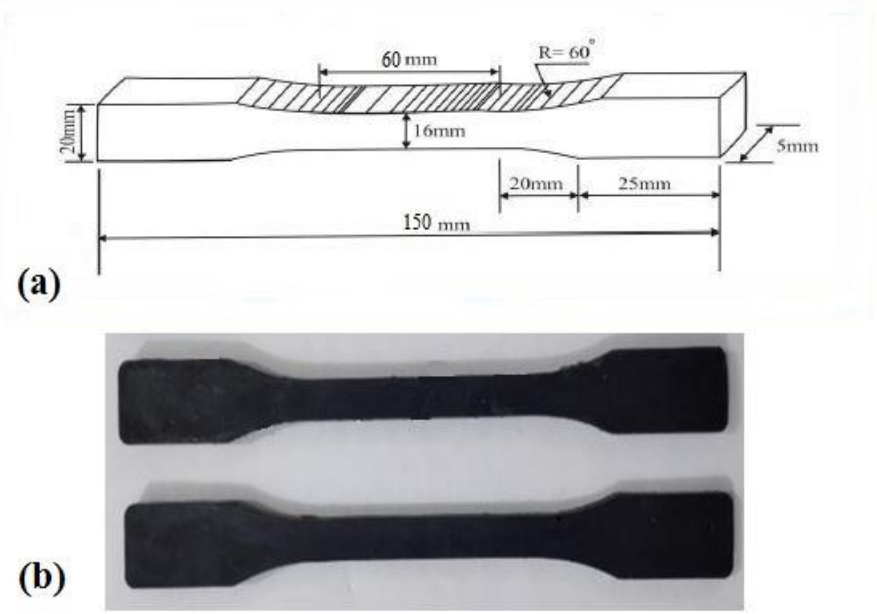

Figure 3.7: (a) Schematic tensile specimen, (b) Prepared tensile specimens

A stress/strain curve was obtained after applying the load until the test sample broke. The tensile strength and elastic modulus were calculated using the following equation :

$$\sigma = P/A \text{……..……(3.1)}$$

- **σ** is the tensile strength in the MPa unit
- P is the force required to break in N unit
- A is the cross-sectional area in mm^2 unit

$$E = \sigma_2 - \sigma_1 / \varepsilon_2 - \varepsilon_1 \text{.....……..(3.2)}$$

- E is the modulus of elasticity (representing the slope of the stress-strain curve up to the proportionality limit) in the MPa unit

- where the stress (σ) is calculated by dividing the applied force by the cross-sectional area of the specimen.
- Strain (ε) is the percentage length change over the initial gauge length of a material.

3.5.2 Impact Test

One of the most common tests for determining the impact resistance of polymers. Specimens were prepared according to ISO 179[127]. Figure (3.8) shows standard [128]and prepared un-notched samples.

Figure 3.8: (A) Schematic Impact Specimen. (B) prepared impact specimens.

The Charpy is used method to test impact samples. After laying out the test specimen on a horizontal plane, we raised the pendulum to its highest possible point, where energy stored would have been converted to kinetic energy, and firmly fastened it in place. The used instrument of Charpy Test, German, Gunt (HAMBURG) company, Model WP 400, is in the Department of Polymer Engineering and Petrochemical Industries/Material Engineering faculty/Babylon University.

Calculating the necessary energy for fracture was crucial to determining the impact strength(a_{CU}) in this test. In order to calculate the impact strength in(KJ/m^2) that would be produced by a Charpy test on an unnotched specimen, we use the following formula (Eq.3.3) [127].

$$a_{cU} = \frac{W_B}{bh} \times 10^3 \qquad \text{.....(3.3)}$$

h represents the thickness of the test sample measured in millimeters,

b represents the width of the specimen measured in millimeters,

and W_B represents the energy at break measured in joules.

3.5.3 Hardness Test

A hardness test is required to measure the resistance of a material to indentation. A Shore D durometer instrument model (TIME 5431) made in China was used to test hardness samples. The specimen is circular in shape, as shown in figure 3.9[129]. The test was done according to ASTM (D2240) [130]. The Shore device has a needle applied in a perpendicular direction to the sample. To obtain correct readings, the surface of the sample must be smooth and clean with a thickness of not less than 3 mm. Each specimen was tested six times at different positions on each specimen at the same time, and the final hardness is an average of them.

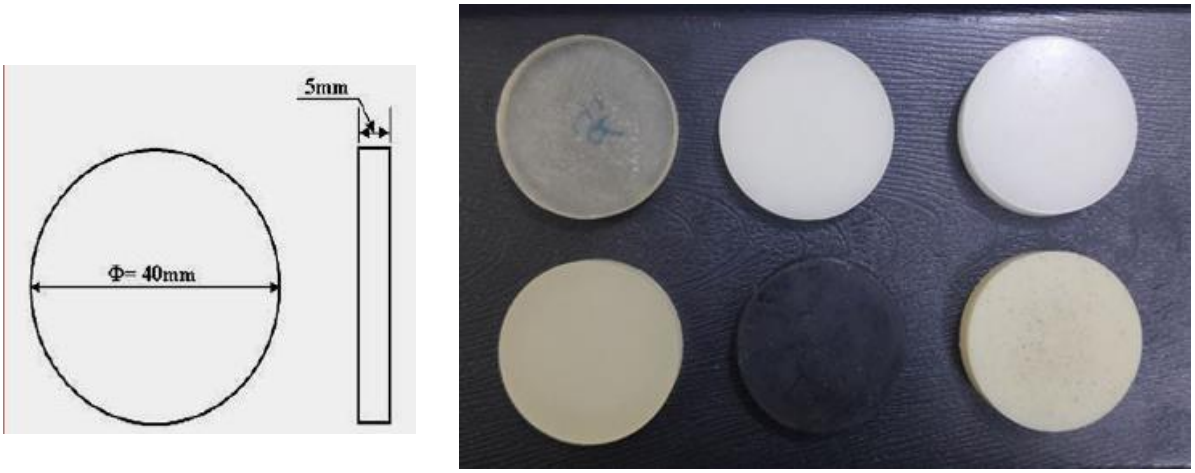

(A (B)

Figure 3.9: (A) Dimensions of the hardness test samples,(B) Samples used in hardness test.

3.5.4 Single Edge Notch Bending (SENB) Fracture Toughness Test

After completing the preparation process of fracture toughness (SENB type) samples, an incision was made in the center of the original slit of the sample called a "sharp crack introduced by the razor." The sample was placed using a certain weight and a force called the force of the hand, as shown in figure (3.10). This method is used in many studies to create a stress center incision with a length of 2 mm.

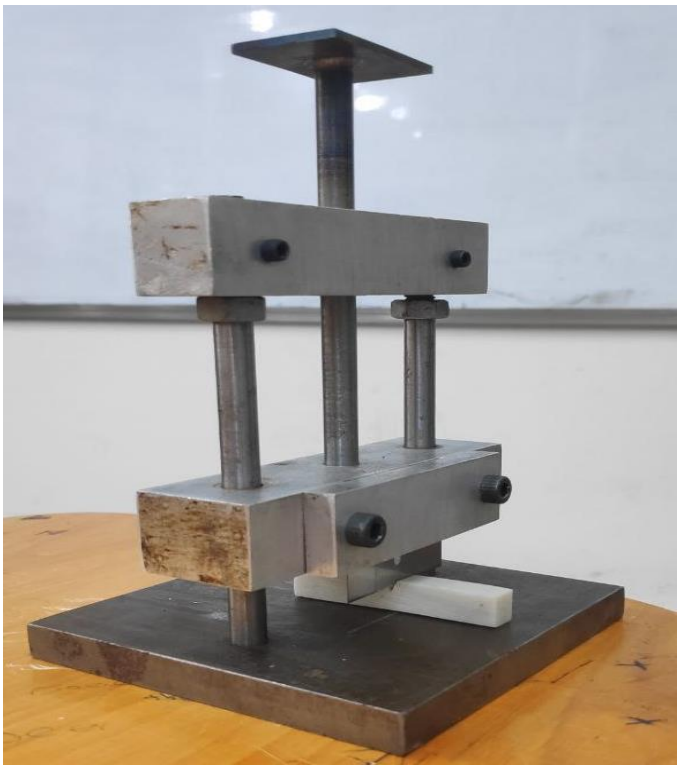

Figure 3.10:Method of creating incision for SENB fracture toughness samples

For the purpose of determining the fracture toughness of each specimen, a single edge-notched three-point bending test was carried out. The test was conducted using a universal testing machine type (WDW/5E) at 5 KN. The test was carried out according to the ASTM D5045[131] procedure at a crosshead speed of ten millimeters per minute. The samples were bars that

were 53 mm long, 9 mm wide, and 8 mm thick. The bars had a V-shaped notch in the middle that was about 4 mm long, the crack tip was started with a clean razor blade, and a support span of 40 mm was used(show figures 3.10 and 3.11). At least three accurate measurements were carried out in order to confirm the data's dependability. The critical stress intensity factors, also known as K_{IC}, were analyzed using the equation(3.4):

$$K_{IC} = \frac{P_{max}}{BW^{1/2}} f\left(\frac{a}{w}\right) \quad \text{.....(3.4)}$$

$$f\left(\frac{a}{w}\right) = \frac{\left(2+\frac{a}{w}\right)\left\{0.886+4.64\left(\frac{a}{w}\right)-13.32\left(\frac{a}{w}\right)^2+14.72\left(\frac{a}{w}\right)^3-5.6\left(\frac{a}{w}\right)^4\right\}}{\left(1-\frac{a}{w}\right)^{3/2}} \quad \text{.....(3.5)}$$

Where: Pmax is the greatest load that the specimen was subjected to before it failed in kilo-newtons, B is the thickness of the specimen measured in millimeters, and W is the width of the specimen measured in millimeters, (a) is the crack length that was measured in millimeters, and f(a/W) is the expression that given in ASTM D5045[131] in which the shape of the sample itself is taken into consideration.

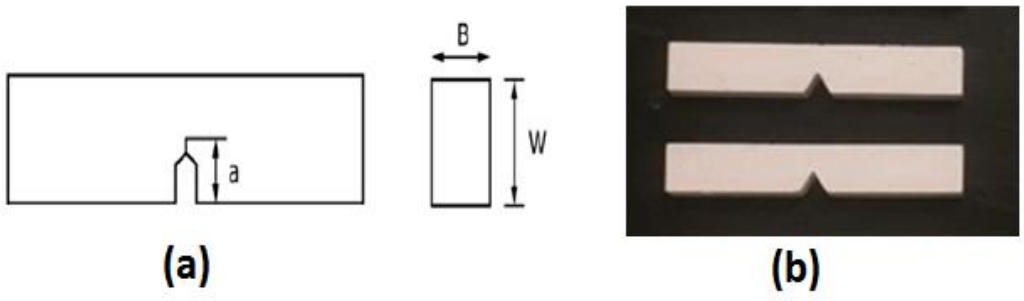

Figure 3.11 :(a) Standard sample geometries of SEBN test,(b)Test samples.

3.5.5 Pull-off Adhesion Test

A satisfactory pull-off test according to ASTM D-4541[132] is a common method for testing coating and adhesion quality; it entails adhering a dolly to a substrate (metal) with glue (as shown in figure 3.12). Then, the dolly and the adhesive or coating are taken off the substrate by pulling perpendicular to the surface. Epoxy, epoxy mixtures, and WC/epoxy nanocomposite are used as coatings.

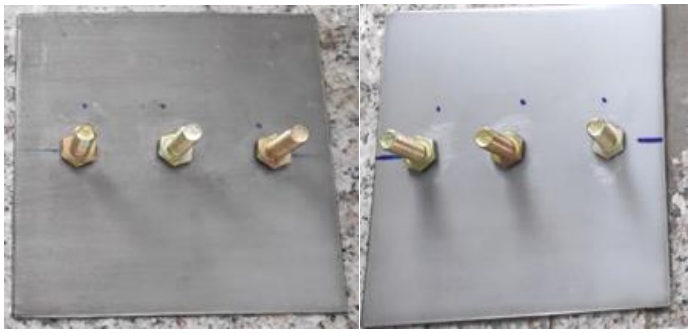

Figure 3.12: A substrate for a pull-off adhesion test, which is a sample of metal that has been coated.

The metal studs (d = 16 mm) were washed multiple times in acetone before being glued to the coated metal surfaces for the pull-off test. Seventy 15 x 15 cm^2 panels were cut for each coating formula. For the purpose of improving the mechanical anchoring of the glue, the coated surface of each panel was given a little sanding using sandpaper numbered 80 and 1200. After that, the studs were adhered to the coated surface substrates in a perpendicular direction using glue that was allowed to cure at room temperature for 24 hours. A hand drill was used to remove the coating and the cured adhesive that was around the stud before beginning the pull-off test. Pull-off measurements were taken with a Microcomputer Controlled Electronic Universal Testing Machine Model WDW-5E (Tensile Equipment) at a velocity of 1 mm min^{-1}. The amount of force needed to peel the coating

away from the substrate was measured and analyzed as a function of the stud's position change.

3.5.6 Wear Test

The wear test was achieved according to ASTM G99-17 [133] using a pin-on-disc machine U.S.A MT4003 version 10 micro-test. A polymer disc with dimensions of 40 millimeters in diameter and 4 millimeters in thickness was moving around a steel pin(16 Mn Cr5) with dimensions of 6 millimeters in diameter, a hardness of sphere of HRC 56, and a surface roughness of R=3.2 micrometers in a vertical configuration under a load of 30 newtons. At a speed of 300 rpm, a sliding distance of 235 m, and a time of 25 min, the pin was gliding along a track that was 24 millimeters in diameter. The wear specimen is shown in figure (3.13)[128]. The test was done in the laboratory of Babylon University/College of Material Engineering/Department of Metallurgical. The investigation into the wear rate, which is shown below, uses the following relations[134,135]:

$$\mathbf{W.R = \Delta W / S.D} \quad \ldots\ldots\ldots\ldots\ldots\ldots\ldots\ldots\ldots\ldots \quad (3.6)$$

Where:-

W.R: The weighted measure of sliding wear is expressed as grams per millimeter

The following relationship will be used to compute the change in weight (ΔW) that occurred during the experiment: -

$$\mathbf{\Delta W = W1 - W2} \quad \ldots\ldots\ldots\ldots\ldots\ldots\ldots\ldots\ldots\ldots\ldots\ldots \quad (3.7)$$

Where:-

W1: Before the analysis, the sample's weight (g)

W2: The sample's final weight after being tested (g)

S.D: a sliding distance that is determined from the lows that are presented below :

S.D=S*t ……………………………………….(3.8)

S: the rate of sliding (in millimeters per minute).

t: the time of test (min).

(a) (b)

Figure 3.13 :(a) Aschematic of wear specimen, (b) wear test sample.

Chapter Four

Results and Discussion

Chapter Four

Results and Discussion

4.1 Introduction

This chapter covers a detailed discussion of all the results which were obtained from the experimental work. It includes the results of mechanical tests: tensile, fracture toughness, impact, pull-off adhesion, and hardness tests. Moreover, the present chapter contains the results of structural and morphological tests: X-Ray, FTIR, SEM, and FE-SEM. It also includes the results of the tribological test: a wear test used to study the wear rate of WC nanocomposite materials prepared in this study. DSC results are also presented in this chapter.

4.2 Toughening agents /Epoxy Blends Result and Discussion

4.2.1 Fourier Transform Infrared Spectroscopy (FTIR) Results of Blends

The FTIR spectra of polyethylene glycol-polypropylene glycol-polyethylene glycol blocks copolymer (EO-PPO-EO) studied shown in figure(4.1a). Multiple peaks arising from PEG and PPG are observed in the region of OH and CH stretching modes [136]. The wavenumbers related to the vibrational spectra of the different groups present in the sample are identified: a broad peak between 3400 and 3600 cm^{-1}, due to the stretching of the O-H groups from the terminal hydroxyl groups of PEG polymer chains as shown in table 4.1[137,138]. The ether bonds (C–O–C) stretching vibrations are presented at 1230 $cm^{-1}$to 1099cm^{-1} in PEG and PPG respectively as a broad peak. FTIR spectra of a sample displayed bands in the region from 2600 to 3000 cm^{-1}, which are characteristic of the C–H group stretching vibrations[139].

The main characteristic bands of the polymer (PPG) appear at 2985 cm^{-1} to 2947 cm^{-1} (C-H stretching of the CH_3 group), and 1481 to 1414 cm^{-1} (C-H bending)[140].

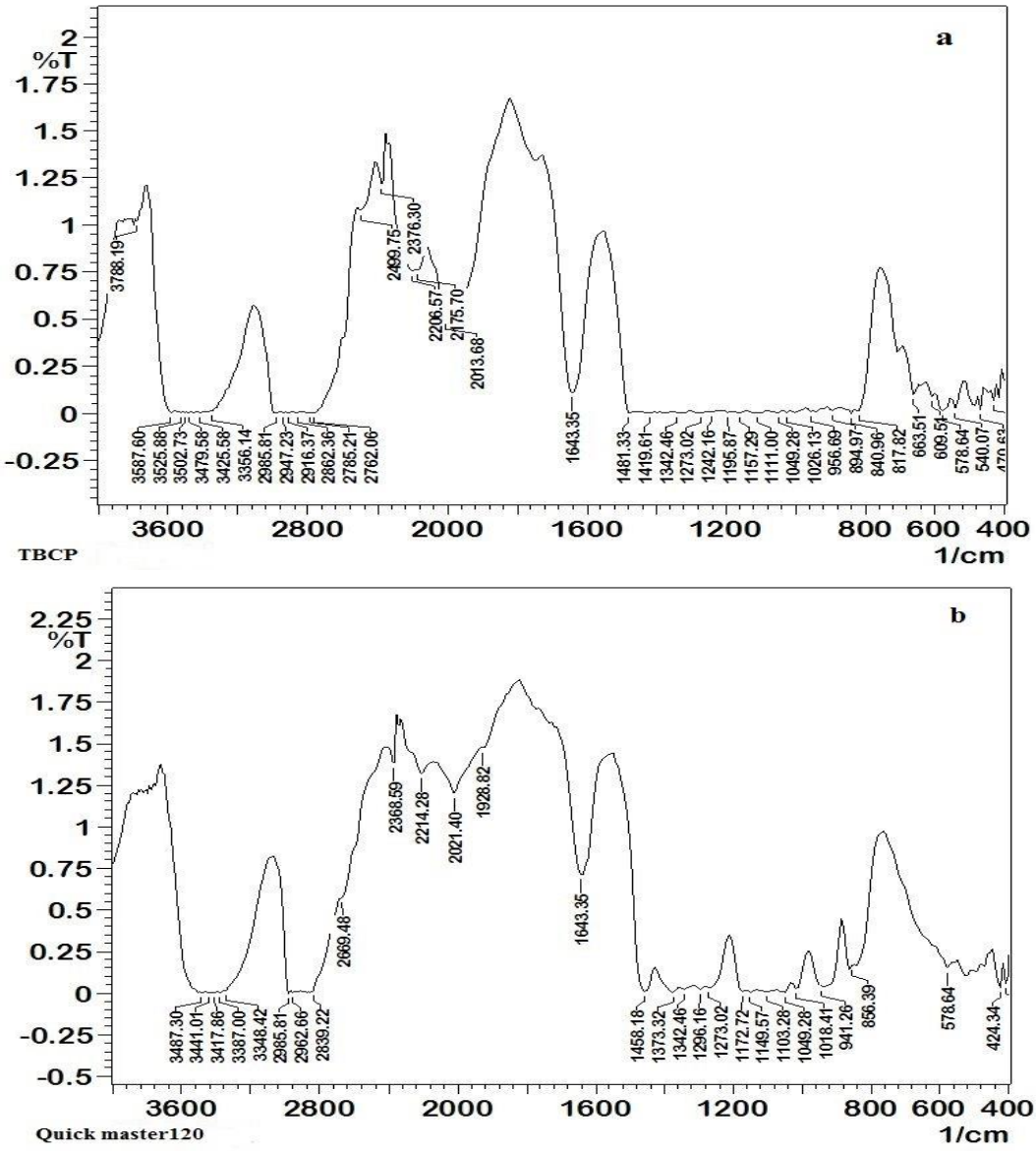

Figure 4.1. The FTIRs Spectrum for (a) Triblock copolymer and (b) Quick mast 120 (PU base)

Table (4.1) The Transmission Bands of FTIR Spectrum Characteristic of polyethylene glycol-polypropylene glycol-polyethylene glycol blocks copolymer (EO-PPO-EO)

Type of bond	(EO-PPO-EO) cm^{-1}
the stretching of the O-H groups	3400 - 3600
(C–O–C) stretching vibrations	1230 - 1099
C–H group stretching vibrations	2600 -3000
C-H stretching of the CH_3 group	2985 - 2947
(C-H bending)	1481 to 1414

The structural function groups for quickmast (120) polyol were analyzed by Fourier Transform Infrared Spectroscopy (FTIR). The FTIR spectra in figure 4.1 (b) are recorded for the quickmast (120) polyol, which shows the main peaks. The peak around 3487 cm^{-1} corresponds to the vibration stretching of –OH (free hydroxyl groups) and becomes a broad peak, indicating the rise in hydroxyl content [141]. The symmetrical and asymmetrical stretching vibrations of –CH corresponds to CH_2 at 2962 and 2839 cm^{-1} [142], respectively. In addition, the absorption peak at 1373 cm^{-1} corresponds to the symmetrical bending vibration of –CH in CH_3. The band at 1273 cm^{-1} is the characteristic absorption of C–O–C (ether bond) stretching vibrations. An absorption peak at 1643 cm^{-1} is attributed to the vibration stretching of C=O (carbonyl group) as shown in table 4.2 [143]. The molecular structure of polyol is characterized by the presence of hydroxyl –OH and ether bonds C–O–C [144], and 120 quickmast (PU base) is thought to have a polyether structure, which agrees with[139,145].

Table (4.2) The Transmission Bands of FTIR Spectrum Characteristic of quickmast (120) polyol

Type of bond	quickmast (120) polyol cm^{-1}
the vibration stretching of –OH	around 3487
symmetrical and asymmetrical stretching vibrations of –CH corresponds to CH_2	2962 and 2839
symmetrical bending vibration of –CH in CH_3	at 1373
C–O–C (ether bond) stretching vibrations	at 1273
C=O (carbonyl group)	at 1643

The FTIR spectra of liquid silicone rubber (LSR) are shown in figure 4.2 The peak around 3425.58 cm^{-1} is related to the O-H group and the peaks at about 2962.66 cm^{-1}, 802.39 $cm^{-1,}$ and 694.37 cm^{-1}which indicated to the C-H bonds, $Si(CH_3)_2$ and $Si(CH_3)_3$, respectively)[146]. In the presence of absorption peaks of methyl silicon at 1265.30 cm^{-1}, three peaks around 1100-1000 cm^{-1} are related to silicon-oxygen bonds [147]. In general, the IR bands located at about 890-860 cm^{-1} and 1100-1000 cm^{-1} indicate the presence of Si-H bending and Si-O-Si stretching modes, respectively see table 4.3 [148].

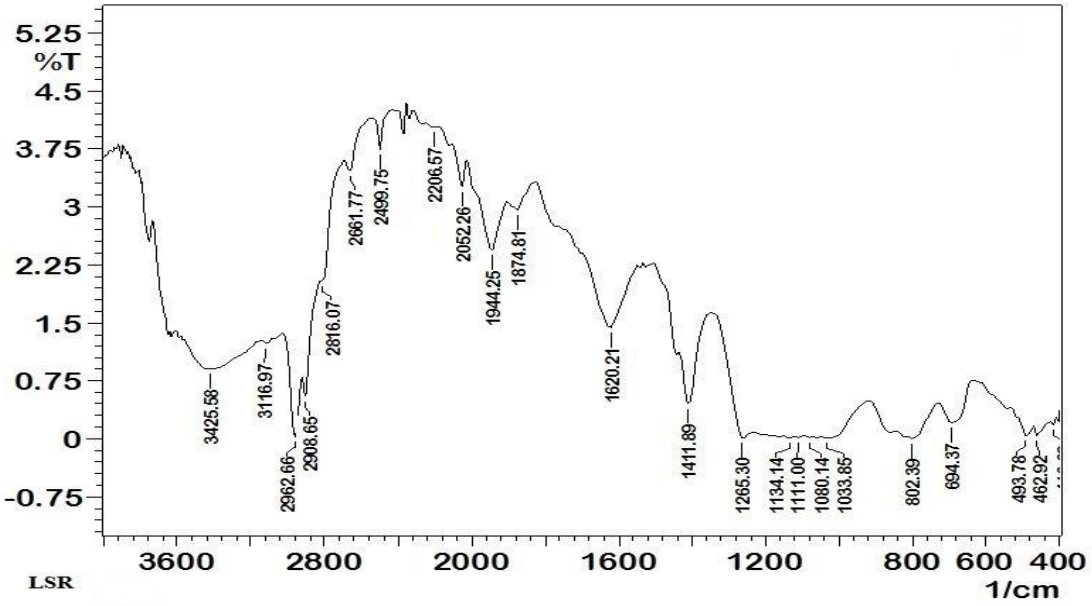

Figure 4.2: The FTIRs Spectrum for liquid silicon rubber (LSR)

Table (4.3) The Transmission Bands of FTIR Spectrum Characteristic of liquid silicone rubber (LSR)

Type of bond	Liquid silicon rubber cm^{-1}
the O-H group	3425.58
C-H bonds	2962.66
$Si(CH_3)_2$	802.39
$Si(CH_3)_3$	694.37
Si-H bending	890-860
Si-O-Si stretching	1100-1000

Figure 4.3 shows the Fourier transform infrared spectroscopy (FT-IR) spectra of pristine PVC adhesive. As shown in Figure 4.3, the characteristic peaks of the PVC molecules can be seen; including peaks for C-H bands (1427.32 cm^{-1}), C-C vibrations (941.26 cm^{-1})[149], a band (695.2and 678.96 cm^{-1}) between 500 cm^{-1} and 696 cm^{-1} is observed which is assigned

to the stretching vibrations of the C-Cl bond [150]. Peaks at 2970.38 cm^{-1} consist of the CH_2 asymmetric stretching vibration mode (see table 4.4). This peak shows the asymmetric stretching bond of C−H and the peak at 1273.02 cm^{-1} is attributed to the bending bond of C−H near Cl. Finally, the C−C stretching bond of the PVC backbone chain occurs in the range 1000−1100 cm^{-1}[151]. From these FT-IR results, PVC is expected to be strongly polarizable due to C–Cl[152,153].

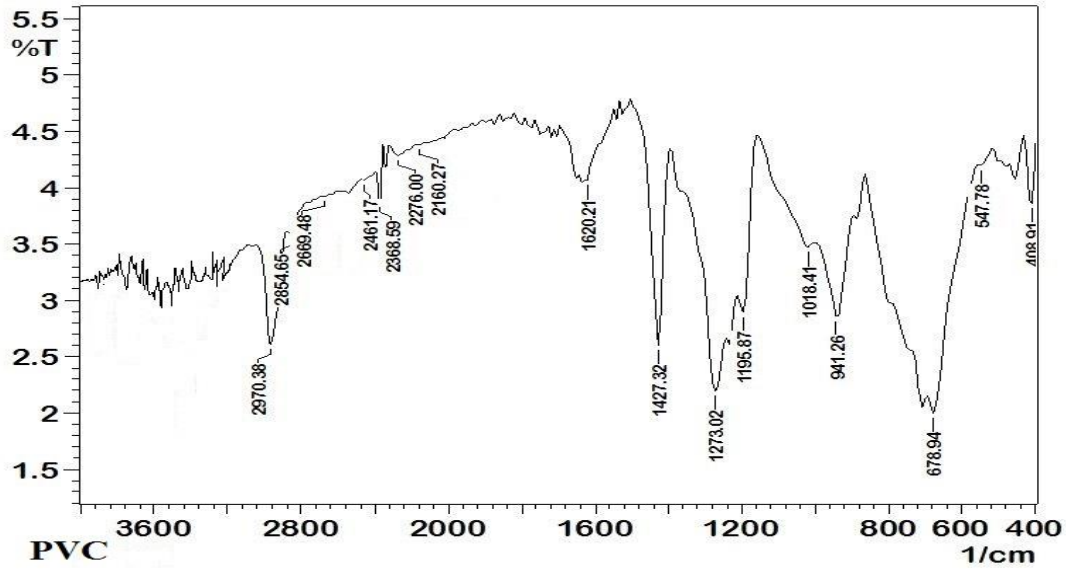

Figure 4.3: The FTIRs Spectrum for polyvinyl chloride adhesive (PVC)

Table (4.4) The Transmission Bands of FTIR Spectrum Characteristic of pristine PVC adhesive

Type of bond	PVC adhesive cm^{-1}
C-H	1427.32
C-C vibrations	941.26
stretching vibrations of the C-Cl bond	500 - 696
the CH_2 asymmetric stretching vibration	2970.38

The FTIR spectra of the unmodified epoxy (epoxy/hardener) system are shown in figure 4.4. The typical absorption bands, including the OH-bond characteristic absorption band at 3417.86 cm^{-1}, are present in the spectra of a pure epoxy system (between 3600 and 3200 cm^{-1})[154] see table 4.5. Since there are many OH groups in the molecules of this resin, the observed peak is rather broad. An epoxy group can be identified by the band at 933.55 cm^{-1} (in the 950 to 860 cm^{-1} range), while an aromatic ether group can be identified by the peak at 1110 cm^{-1}[155].

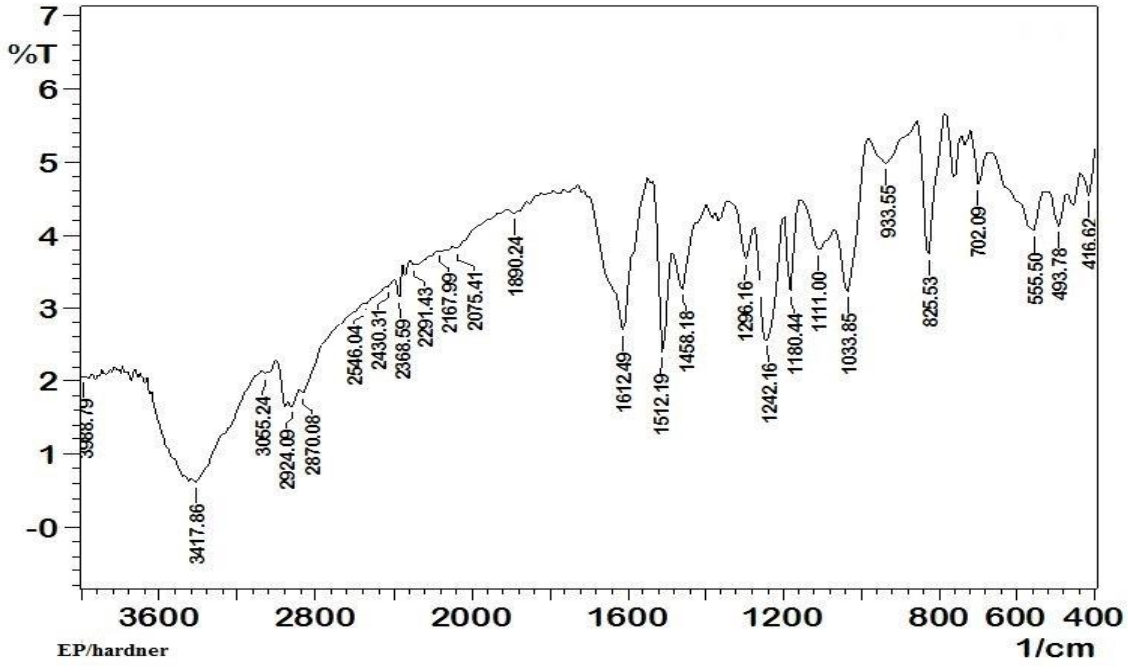

Figure 4.4: The FTIR Spectrum for unmodifed epoxy (neat epoxy)

Table (4.5) The Transmission Bands of FTIR Spectrum Characteristic of the pure epoxy system

Type of bond	Pure epoxy cm^{-1}
the OH-bond	3600 - 3200
epoxy group	950 - 860
an aromatic ether group	1110

It is important to add that the stretching frequencies of the functional groups in the FTIR spectra of the TBCP/epoxy blends see figure 4.5 (a), are identical to the unmodified epoxy (neat epoxy) system. This implies that there is no new bond formation or chemical interaction between the epoxy and TBCP[156,157]. Analysis of polymer blend systems by means of FTIR spectroscopy is a standard procedure for investigating hydrogen bonding interactions. In order to determine if hydrogen bonding was happening in the TBCP/epoxy blend system, FTIR spectroscopy was utilized. During the epoxy-amine reaction, many free hydroxyl groups are generated. These free hydroxyl groups of cured thermoset can form hydrogen bonding with ether groups of PEG the miscibility of TBCP with the crosslinked epoxy system can be explained in terms of intermolecular hydrogen bonding. In figure (4.5a), blends were found to have broad signals in the FTIR spectra in the region of OH stretching, indicating the presence of hydroxyl groups bonded to hydrogen atoms[158]. Pure epoxy's spectra showed a strong unresolved broad peak at 3417.66 cm^{-1}, which corresponded to the signal of its free OH groups; this peak's strength faded with time. Since the epoxy's broad peak at 3417.66 cm^{-1} broadened when mixed with TBCP, this observation is suggestive of hydrogen bonding between the epoxy's OH groups and the ether groups of the PEO and PPO segments[159]. Thus the FTIR result confirms the role of hydrogen bonding in generating rather a transparent epoxy blend matrix [158].

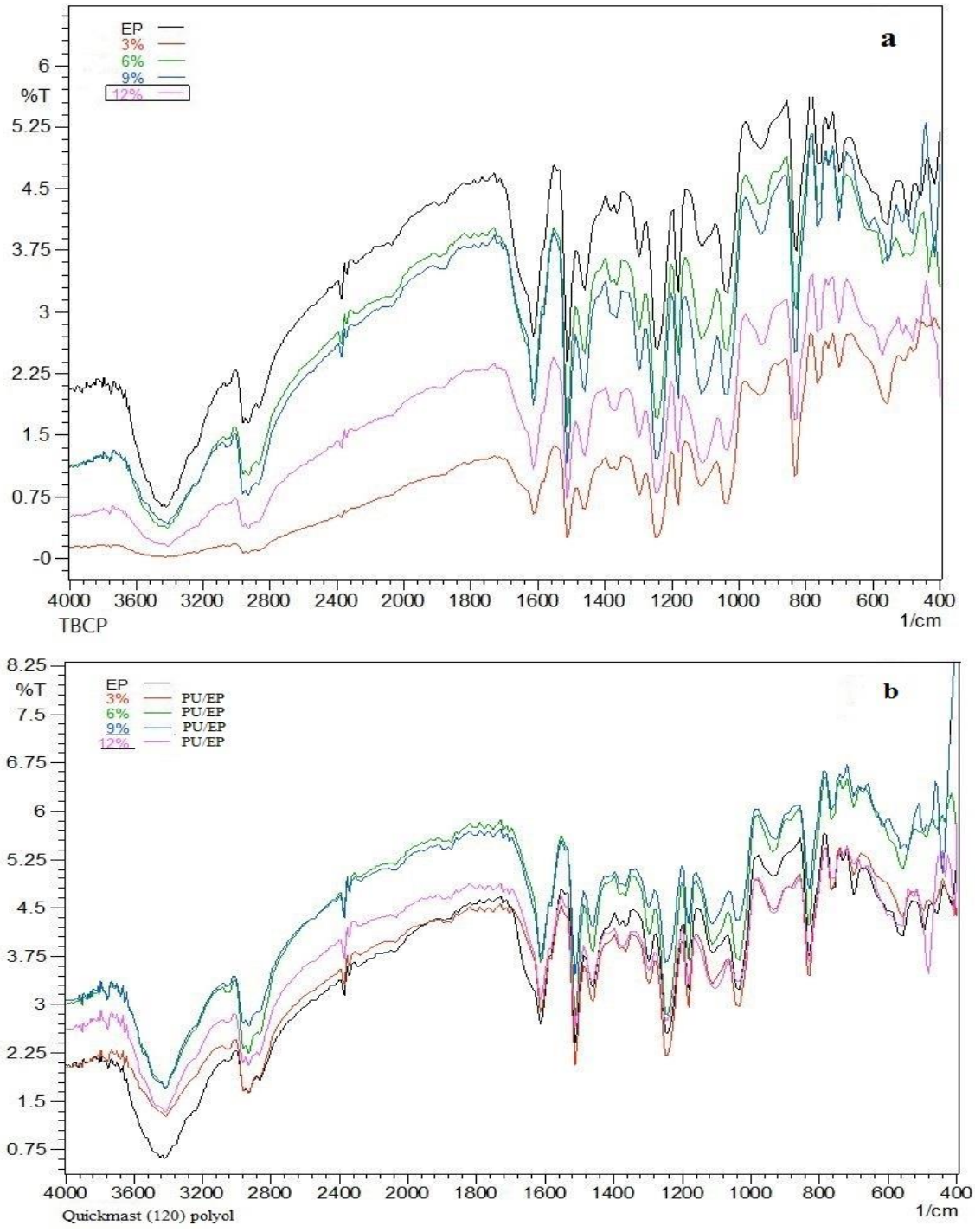

Figure 4.5: The FTIR Spectrum for (a) TBCP/EP blends (b)PU/ EP blends

The FTIR spectra of unmodified epoxy figure 4.4 and PU/epoxy blends are shown in figure 4.5(b). The FTIR spectra indicate the possible intramolecular hydrogen bonding interactions that may arise from combining the epoxy matrix with the quickmast(120) additive. Identifiable peaks at around 3417.66 cm^{-1} for hydroxyl and amine groups, and around 933.55 cm^{-1} for epoxy groups, are attributed to the various functional groups of epoxy (EP)[160]. Figure 4.5(b) reveals that the epoxy group peak arises at a frequency of 933.55 cm^{-1} for the untreated EP, which has about the same intensity as the epoxy blends changed with various weight percents of quickmast 120.The ether bonds (C–O–C) stretching vibrations are presented at 1230 $cm^{-1}$to 1099cm^{-1}[139] as shown in table(4.6). In the FTIR spectra, the absence of a peak at 915 cm^{-1} (indicating complete cure) and a shoulder at 3620 cm^{-1} (ruling out the presence of free hydroxyl groups) in the hydroxyl groups formed by the epoxy-amine curing reaction are of particular interest This indicates that the majority of secondary hydroxyl groups produced by the curing reaction participate in intramolecular hydrogen bonding interactions. More importantly, the ether group of PU polyol and the free hydroxyl groups of the cured epoxy system are kept from forming intermolecular hydrogen through these interactions. As predicted, the lack of intermolecular hydrogen bonds leads to the conclusion that PU polyol/epoxy complexes become immiscible as agreed with[161]. Meanwhile, the network polymer containing ether bond structure generated by the curing reaction can help to form a three dimensional network structure and enhancing the mechanical characteristics of modified epoxy.

Table (4.6) The Transmission Bands of FTIR Spectrum Characteristic of the PU/epoxy blends

Type of bond	PU/ EP blends cm^{-1}
hydroxyl and amine groups	3417.66
epoxy group	950 - 860
(C–O–C) stretching vibrations	1230 -1099

FTIR spectrum from thermosetting epoxy with the addition of 3, 6, 9 and 12 wt% silicone rubber can be seen in figure 4.6. For LSR/EP, the characteristic absorption peaks at 1438, 1247, 1132, 913, and 933.55 cm^{-1} are attributed to the Si-C_6H_5, Si-CH_3, Si-O-C, and the terminal epoxy groups, respectively[162,163]. Compared to blends with unmodified epoxy peaks, these peaks ultimately are nearly the same. This indicates that a small amount of the epoxy groups have reacted with Si-O-H [164]. Stretching intensity of Si-O-Si and Si-O-R at 1018 cm^{-1} peak increases with increasing weight percent of silicone rubber in thermoset mixture. The thermoset epoxy/silicone rubber exhibits a rising C-H ratio from Si-CH_3, as seen by an intensifying peak at 780 cm^{-1}. It can be deduced from the FTIR results that the addition of silicone rubber enhances the intensity of the peaks at 1018 and 780 cm^{-1}, indicating that the number of bonds formed between Si-O-Si, Si-O-R, and Si-CH_3 rises, see table 4.7[165].

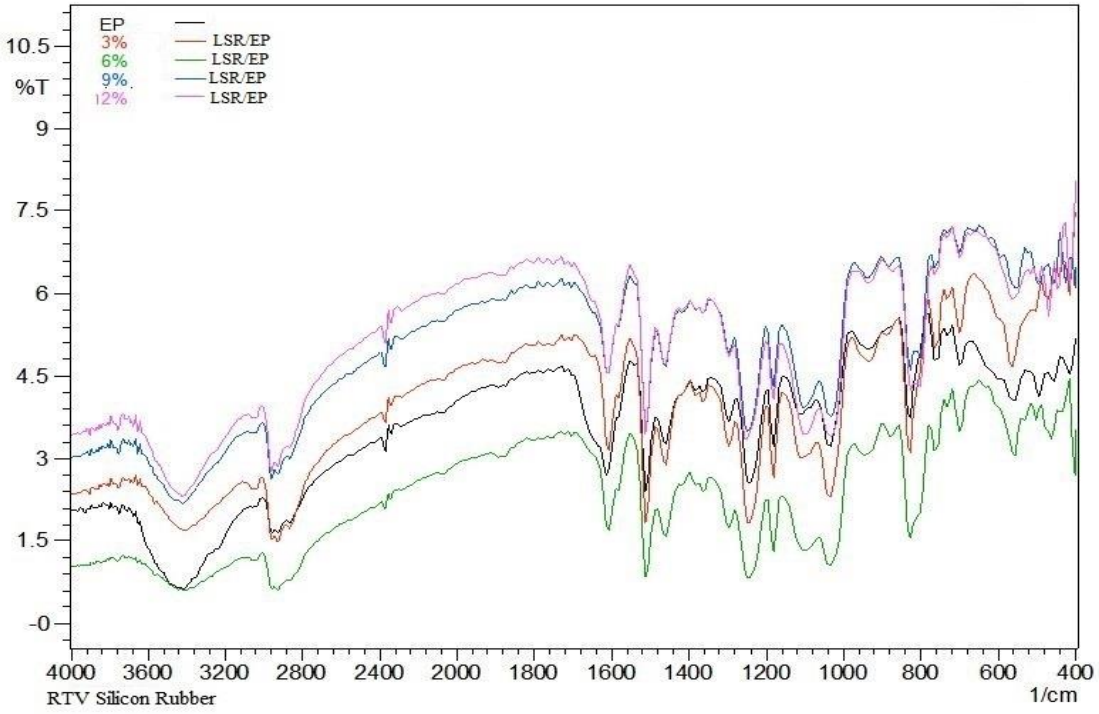

Figure 4.6: The FTIR Spectrum for LSR/epoxy blends

Table (4.7) The Transmission Bands of FTIR Spectrum Characteristic of the LSR/ epoxy blends

Type of bond	LSR/ EP blends cm^{-1}
Si-C_6H_5	1438
Si-CH_3	1247
Si-O-C	1132
terminal epoxy groups	913-933.55

The FTIR spectrum of PVC/EP blends shown in figure 4.7 explains no new bond appearance when PVC is combined with the epoxy resin. Complexation may shift the polymer peak frequencies. The characteristic peaks of pure EP 3417.86 cm^{-1} are shifted to 3425.58 cm^{-1} in the PVC/EP blend and the peak of pure PVC at 941.26 cm^{-1} is shifted to 933.55 cm^{-1}, respectively.

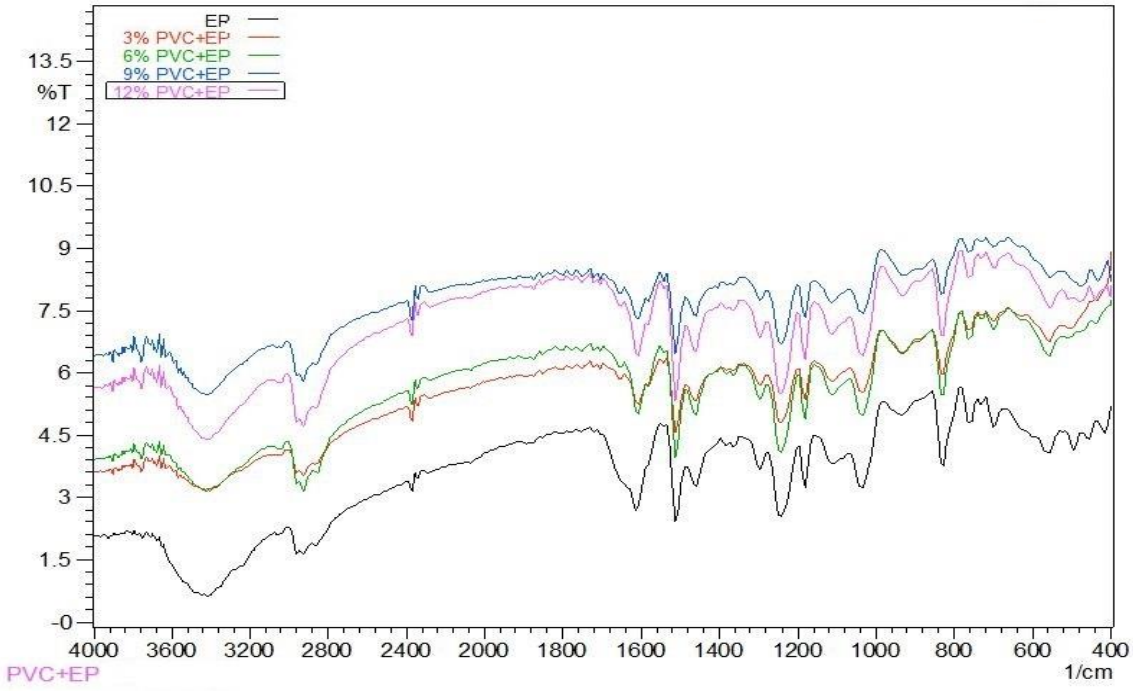

Figure 4.7: The FTIR Spectrum for PVC/ epoxy blends

Figure 4.8(a) shows FTIR of pure PSR. The absorption band at 540.07 cm^{-1} can be ascribed to the S-S group of polysulfide rubber [166]. As can be seen in figure 4.8(b), FTIR spectroscopy was applied in order to investigate the modification reaction that occurred when polysulfide was combined with epoxy. Epoxy's thiol group had an interaction with its oxirane ring, which resulted in the consumption of the thiol group (also known as the -SH group) and the formation of the hydroxyl group. Absorption at 2550-2700 cm^{-1} (S-H stretching) and 3200-3450 cm^{-1} (O-H stretching) are used to characterize

thiol and hydroxyl groups, respectively [167,168] see table 4.8. The thiol group of PSR reacts with the epoxide group of epoxy resin to give S-CH_2 linkage and –OH groups[169,170]. Modifying epoxide with polysulfide increased the strength of the O-H stretching and decreased the strength of the S-H stretching. According to the FTIR analysis, the polysulfide and epoxy had bonded[168].

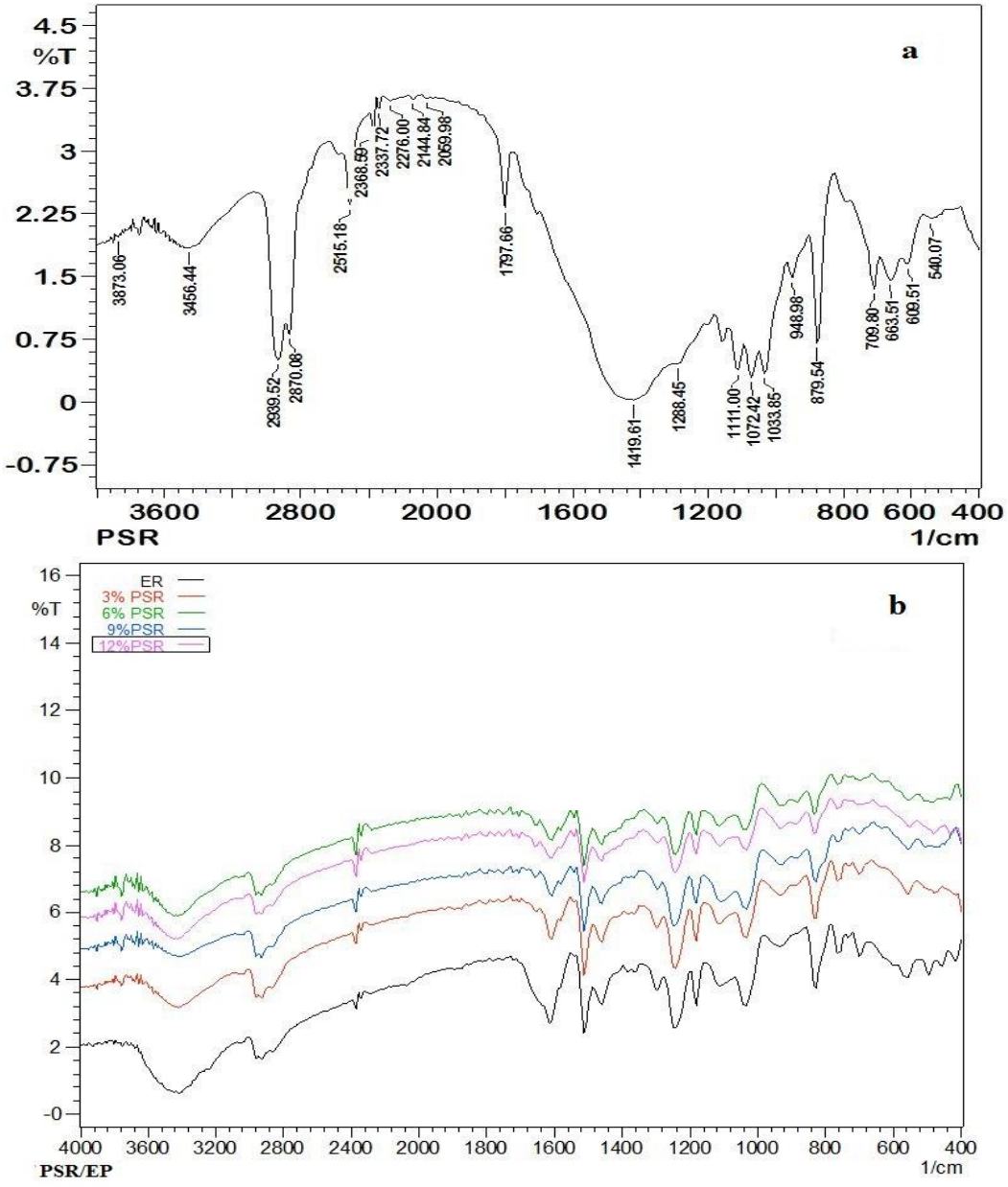

Figure 4.8: The FTIR Spectrum for (a) Pure PSR (b) PSR/ epoxy blends

Table (4.8) The Transmission Bands of FTIR Spectrum Characteristic of the PSR/epoxy blends

Type of bond	PSR/ EP blends cm^{-1}
S-S	540.07
S-H stretching	2550-2700
O-H stretching	3200-3450

4.2.2 Morphology Test Result of epoxy blends

A scanning electron microscope can provide information on the morphology and structure of neat epoxy(unmodified epoxy) and modified epoxy blends. Figure 4.9(a and b) exhibits the image of neat epoxy at two scales 5 and 50 μm scale, respectively. SEM micrographs demonstrate a typical featureless one-phase morphology, consistent with the amorphous single-phase structure of epoxy networks. Similar SEM pictures have previously been observed[171,172].

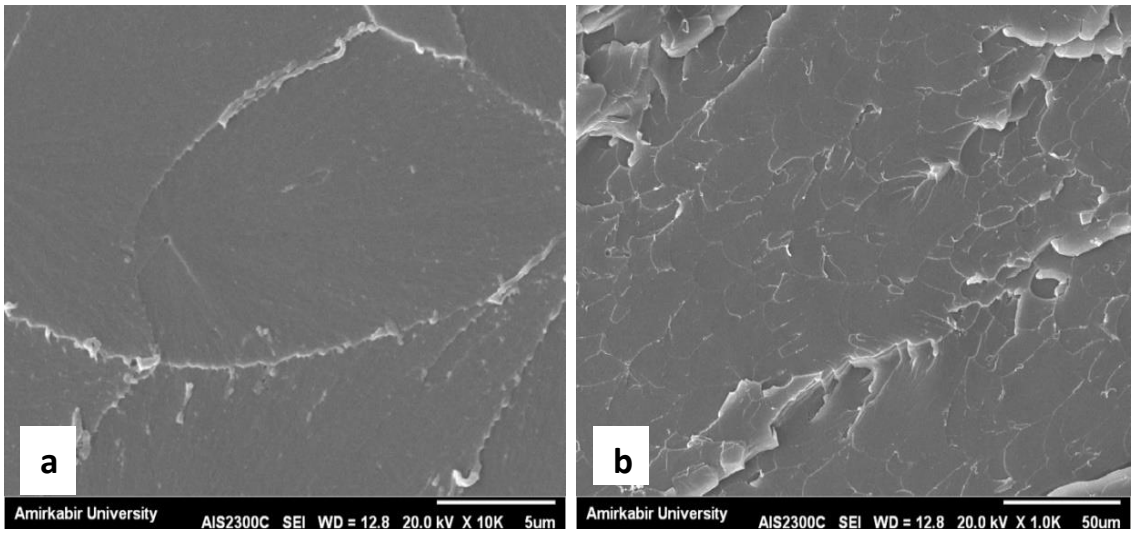

Figure 4.9 :SEM micrographs of a and b) unmodified epoxy at 5μm scale and 50 μm scale ,respectively

Figure 4.10 (a and b) shows the fracture surface of the TBCP/EP blends at low(3%wt.) and high(12% wt.) load content TBCP at a 5μm scale. Several spherical formations are seen, indicating phase separation and the creation of immiscible TBCP structures in the matrix[173]. At low and high percentages of TBCP, a microphase separation can be detected. PPO micro-separated phase that is not miscible with the epoxy matrix, which is represented by dark areas[174]. Furthermore, the PEO block is spread across two phases since it is miscible with the epoxy matrix while still being covalently connected to the segregated PPO block. In the case of a 3wt% TBCP/epoxy system, certain black spherical domains are tiny in size and evenly dispersed, however when the concentration of block copolymer increased at (12%wt.), these spherical domains got larger, wider, and more apparent in the epoxy matrix [175].

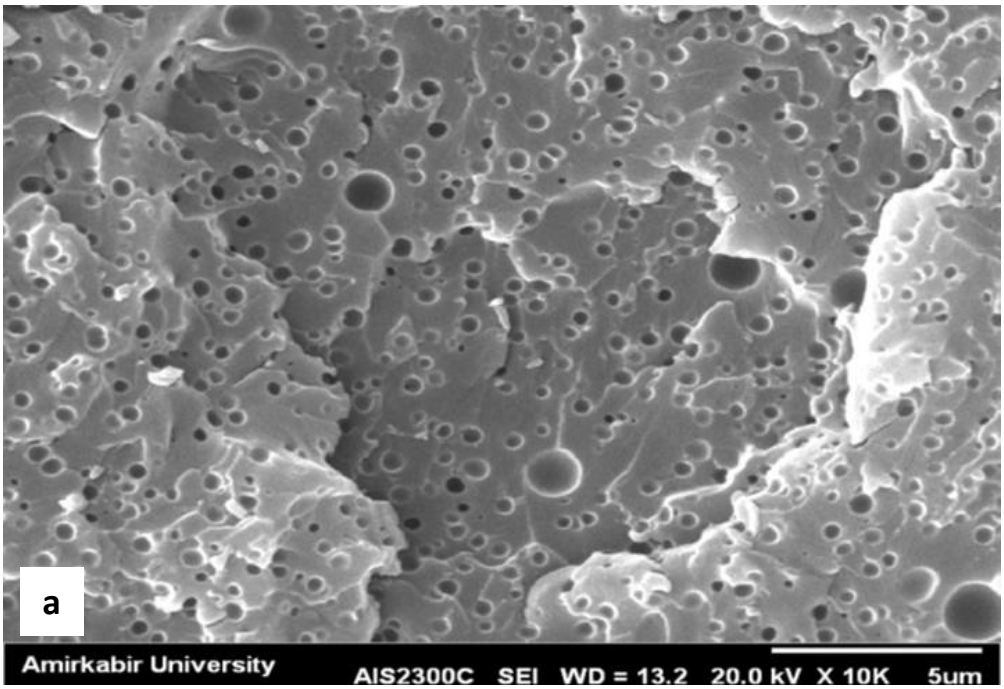

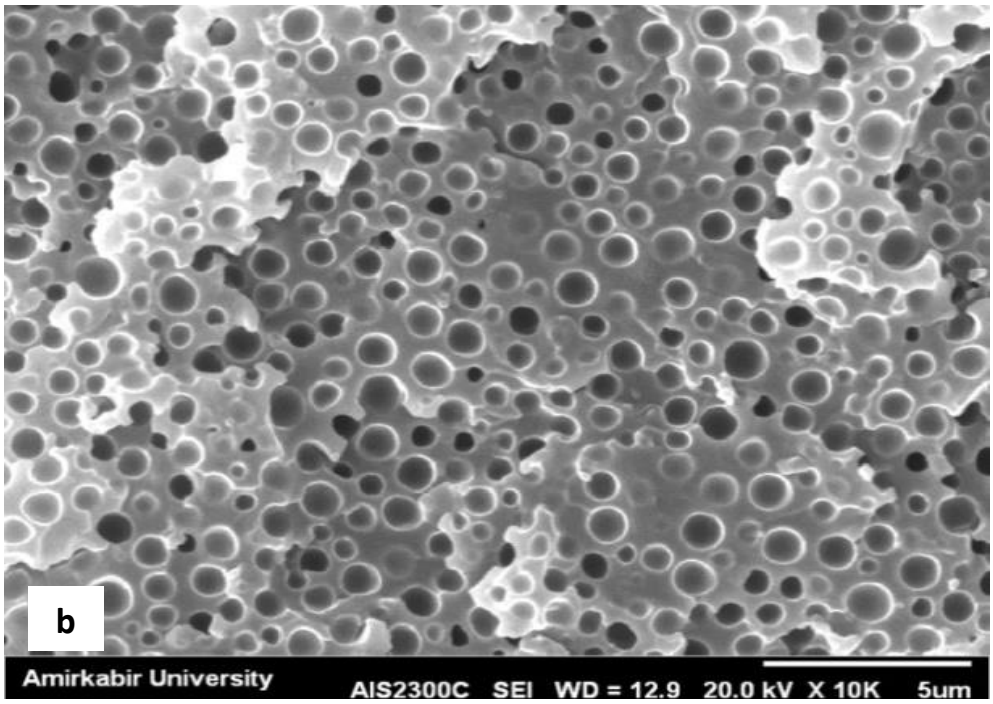

Figure 4.10: SEM micrographs of a) 3 wt % TBCP/EP blend, b) 12 wt % TBCP /EP blend

Figure 4.11(a and b) displays SEM morphology of fracture surface of epoxy blended with quick mast120 (PU base) at low (3%wt) load content and high (12%wt) load content of PU polyol. During the curing process, the polyol phase separates as it becomes less miscible with the epoxy matrix. The finely distributed sub-micron size polyol domains as (spherical zones) in epoxy structure can be observed in the inset along with the presence of riverbed markings and the shear band features responsible for strain energy absorption similarity with[108,176]. The uniform distribution of spherical polyol domains throughout the epoxy matrix allows uniform plastic deformation and considerable shear yielding, as expected for ductile systems [177].

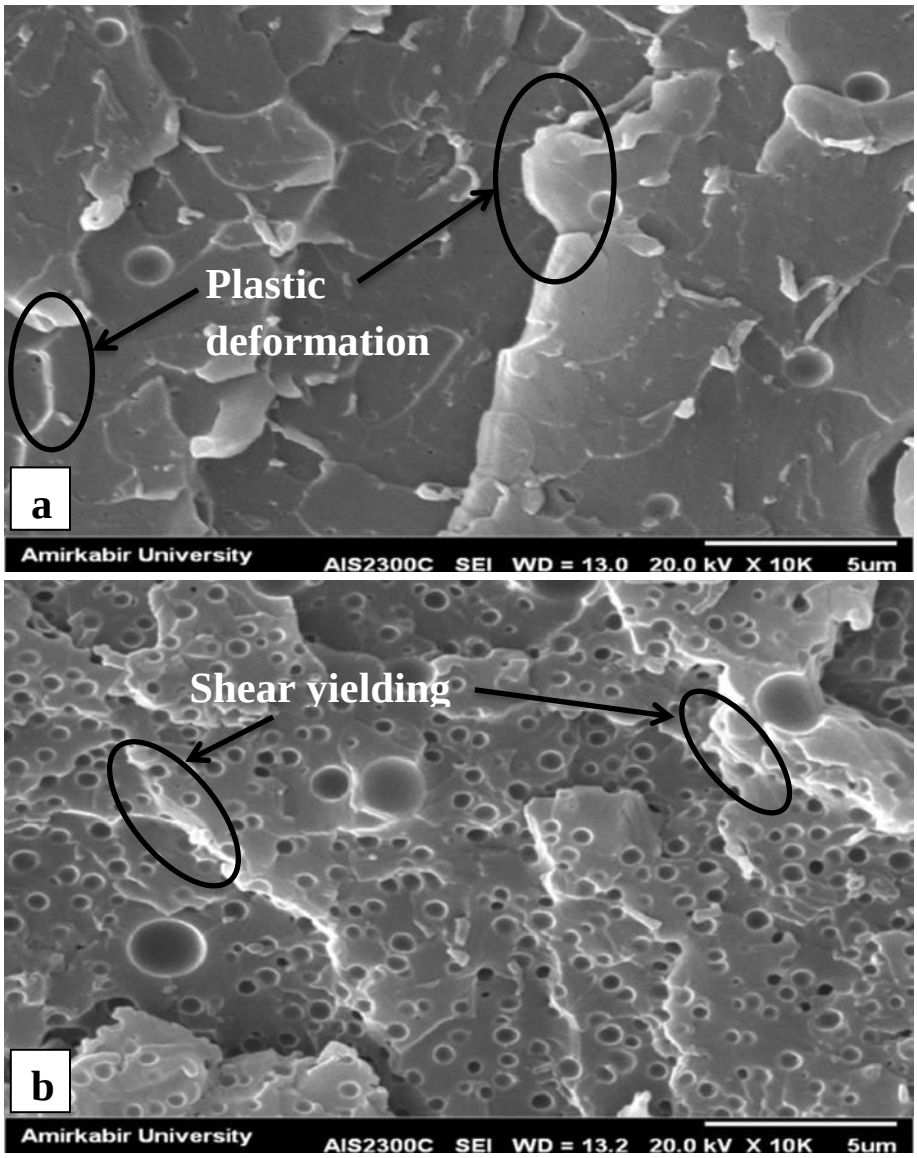

Figure 4.11: SEM micrographs of a) 3 wt % PU/EP blend, b) 12 wt % PU /EP blend

The fracture surface of liquid silicon rubber (LSR)/epoxy blend was analyzed using SEM as shown in figure 4.12 (a and b) at low (3%wt) load content and high (12%wt) load content of LSR. The analysis of the scanning electron microscope pictures indicates the existence of (a sea-island structure) in the epoxy resin similar to [164]. Figure 4.12 displays the beginning of two-phase separation. The majority of the compound is a thermosetting epoxy, while the other is a bit and gathering silicone rubber.

As the LSR load content rises, the portions gradually grow much larger agrees with[178].

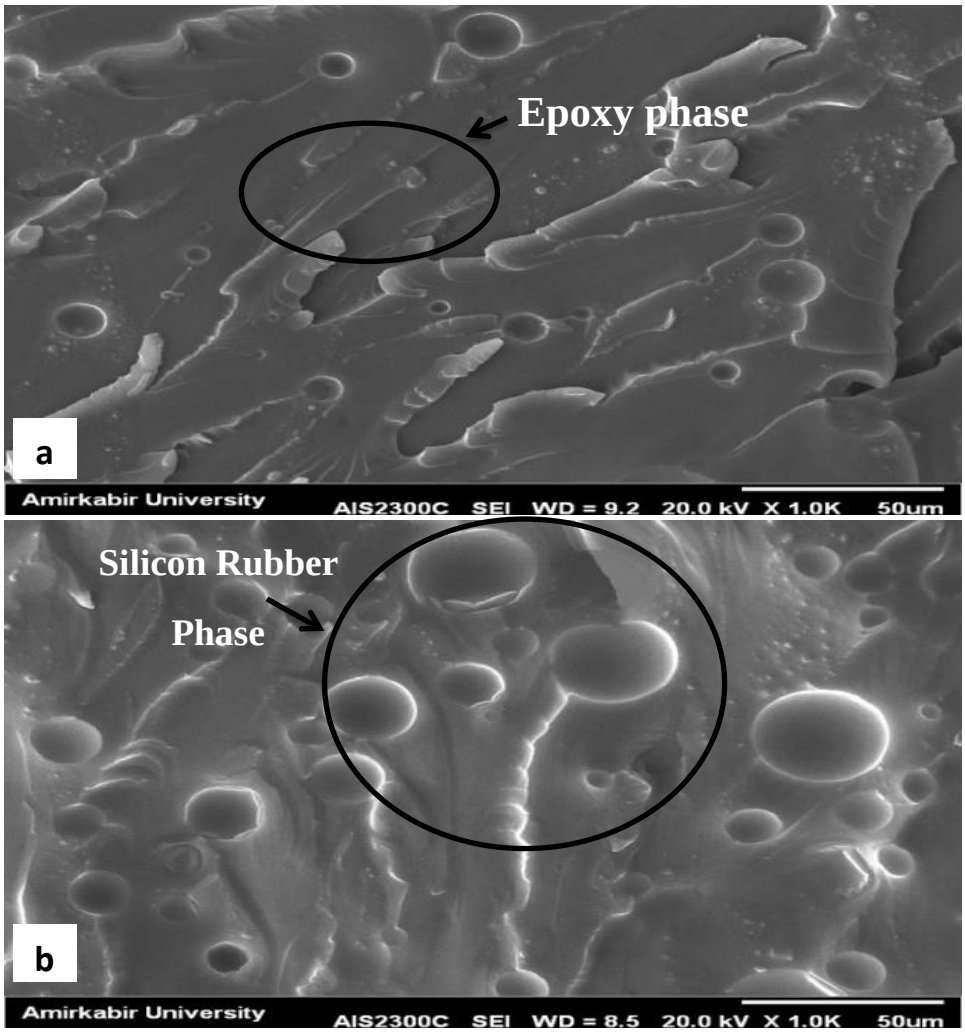

Figure 4.12: SEM micrographs of a) 3 wt % LSR/EP blend, b) 12 wt % LSR /EP blend

Epoxy resin is mixed with liquid silicon rubber to create a rubber zone that, after cured, has the shape of a sphere. Due to its low compatibility with epoxy resin, LSR's particles exhibit a less uniform distribution, however the presence of rubber zone limits fracture growth and improves toughness agreeing with [179].

Likewise, the diameters of the spheres show variation as a function of LSR concentration. As the LSR concentration is increased from 3% wt to 12% wt, it is revealed that the diameter of the spherical zone grows, suggesting the presence of plastic void development mechanisms. These results are consistent with those relating fracture toughness, where the K_{IC} value increases with increasing LSR concentration. Other researchers have found that rubber-toughened epoxies are susceptible to rubber cavitation and void formation[180].

The fracture surface of the pure epoxy samples is too smooth, as shown in the SEM images in figure 4.4, while the fracture surface of the PVC-modified epoxy specimens is slightly rough, as seen in figure 4.13(a and b). In the absence of a cavity on the fracture surfaces, phase separation did not take place[181,182]. The EP-PVC fracture surfaces also exhibit large shear yields and plastic deformations, which is indicative of a typical toughness character[183]. In the case of low load (3%wt) and high load (12% wt) PVC/EP, the fracture surface becomes rougher compared with EP also some micropores are observed owing to the evaporation of solvents during the curing process[184]. PVC stabilized with epoxy resin exhibits two-phase morphology and a compatible system. In addition, these samples do not contain cracks or micro-cracks in polymer bulks. This phenomenon is responsible for the action of epoxy derivative during sample processing leading to less brittleness and more flexible sample agree with[185].

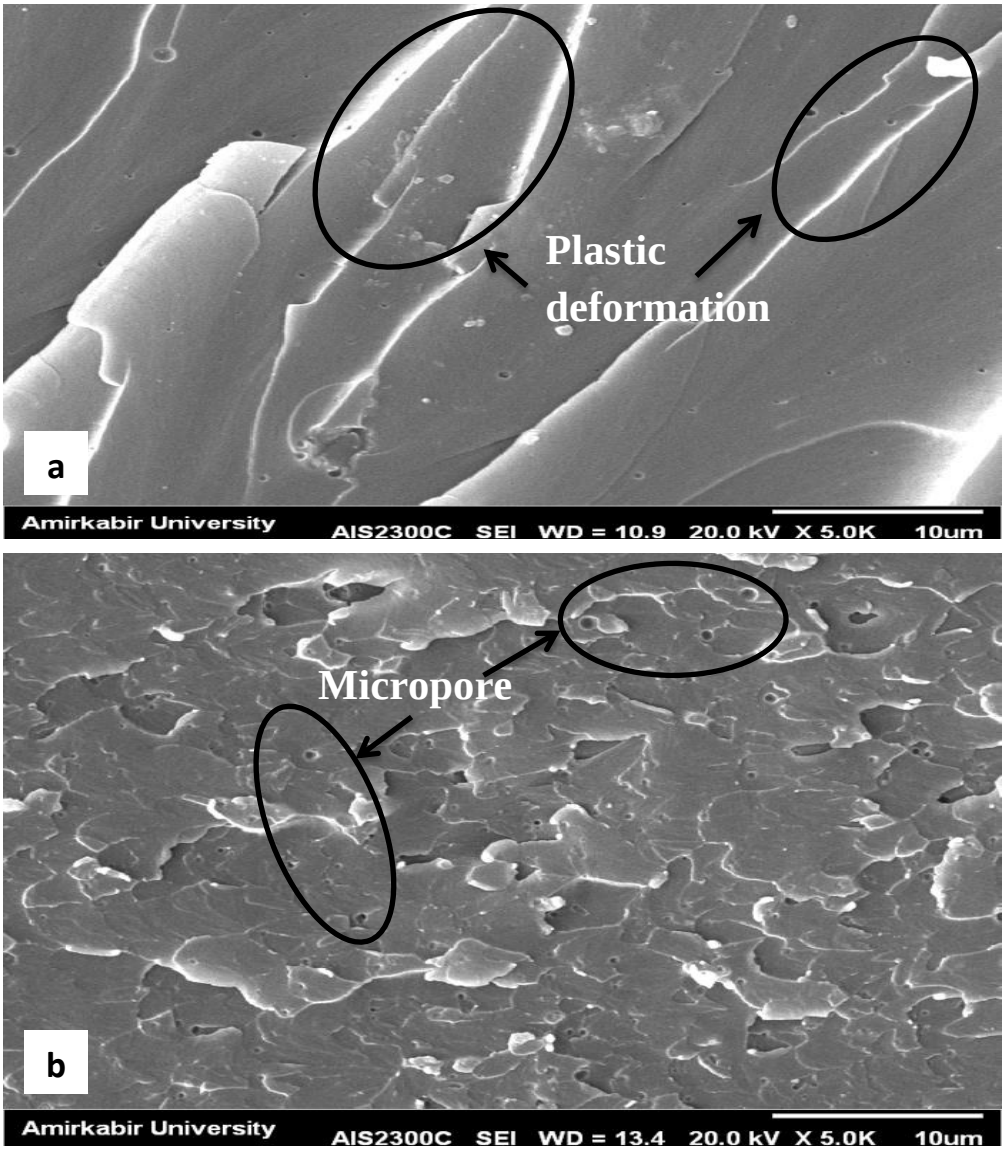

Figure 4.13: SEM micrographs of a) 3 wt % PVC /EP blend, b) 12 wt % PVC /EP blend

SEM studies were also carried out for modified epoxy containing low load content (3 wt%) and 12wt % (high load content) PSR. The corresponding micrographs are shown in figure 4.14. Figure 4.14 (a) shows a micrograph of a large area of the fracture surface. It shows the degree of roughness in PSR/epoxy blends. In addition, a multilevel fracture with ridges and a wavy crest is observed [186].

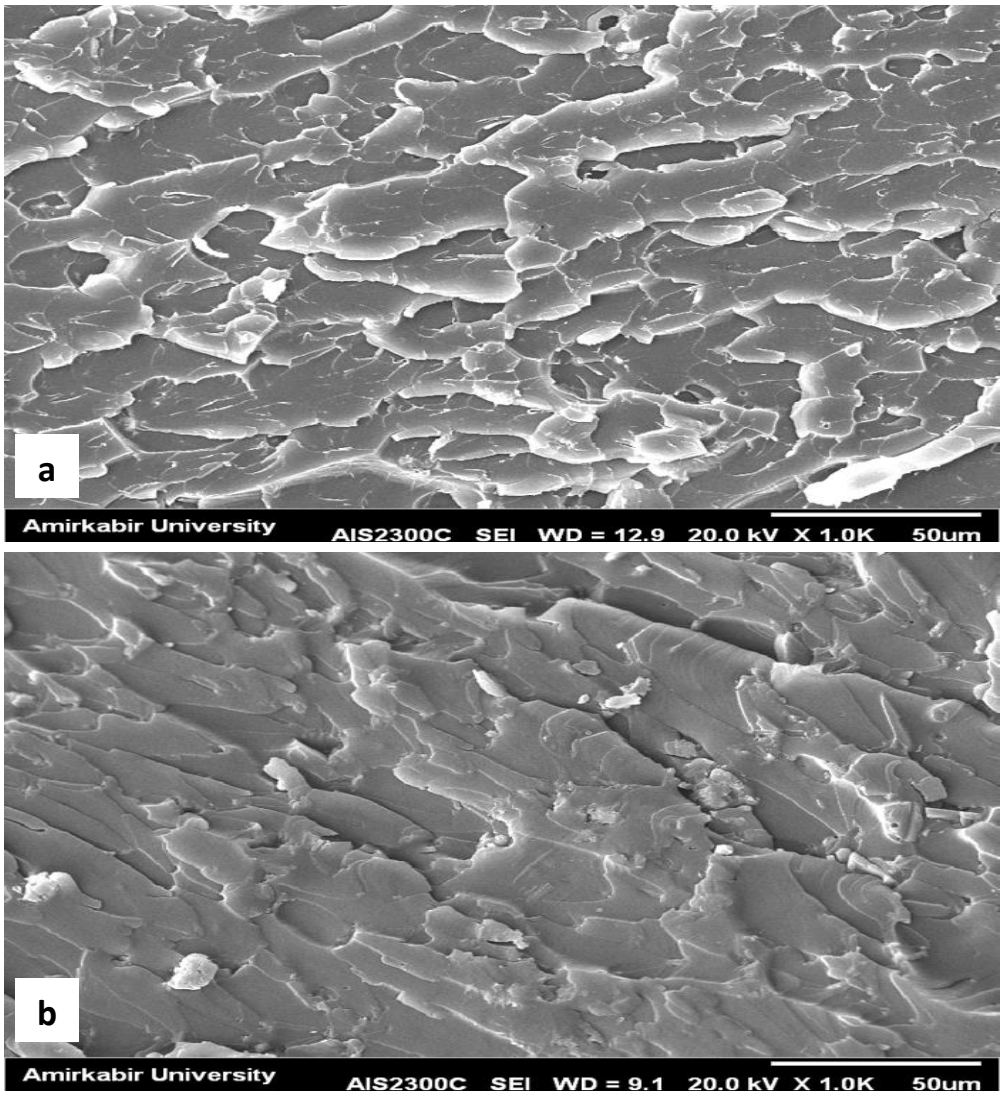

Figure 4.14: SEM micrographs of a) 3 wt % PSR /epoxy blend, b) 12 wt % PSR/epoxy blend

Where parabolic marking is observed all over the fracture surface. It is interesting to note that a 3 wt% PSR modified epoxy system exhibits entirely different co-continuous phase morphology, very similar to a thermoplastic elastomer[187] with little plastic deformation and a few long threads of a deformed material occasionally discernible similarity with [188]. The SEM micrograph of polysulfide modified blends shows that in both cases (a)and (b),increased fracture toughness and impact strength can be traced back to the increased roughness and considerable plastic yielding of the polymer

matrix seen at the fracture surfaces, along with distorted leaf-like structures and more cavitations[189]. It can be seen that with rubber levels of 12% wt, the second rubbery phase gets more and more aggregated leading to that phase being less distinguishable from the epoxy matrix. This situation leads to flexibilization of the matrix resulting in the reduction of tensile properties[166].

4.2.3 DSC test result of epoxy blends

Figure 4.15 displays the DSC curves of TBCP/epoxy blends. As can be seen, all curves show a drop in heat flow indicating the presence of a curing reaction between epoxy and the hardener as shown in figure 4.15. The reaction was considered complete when the isothermal DSC thermograms leveled off to the baseline[190]. As the percentage of block copolymer in epoxy resin rises, the curing reaction was slowed down, resulting in a noticeable decrease in heat flow drop. Increased block copolymer content obviously slowed down the curing reaction in agree with [175].

The results were tabulated as shown in (appendix A/ table 4.9). It is observed that for the unmodified epoxy system, the glass transition temperature T_g is 83.76 °C. With the addition of block copolymers, the temperature has started decreasing with increased load content TBCP %. This is about a 36 % decrement compared with the unmodified epoxy system. It can be concluded that the addition of TBCPs affects the T_g of epoxy resin due to the lower crosslinking degree of the PEO-rich areas and the highly mobile microphases of PPO similarity with [191].

One possible explanation for this phenomenon is that the development of a second phase is presenting an obstacle to the increase of thermoset cross-link density[192]. Furthermore, Wang et al.[60] suggest that[193] some free

TBCP molecules may remain in the cured structure of the epoxy, which, due to insufficient and incomplete conversion, could not be fully assembled during the curing process, and consequently may bring mechanical properties and the matrix T_g down. Also, some TBCP chains are miscible with epoxy, while other chains were phase separated from the epoxy, and this may suggest a matrix plasticization action that led to the observed lower T_g [193,194].

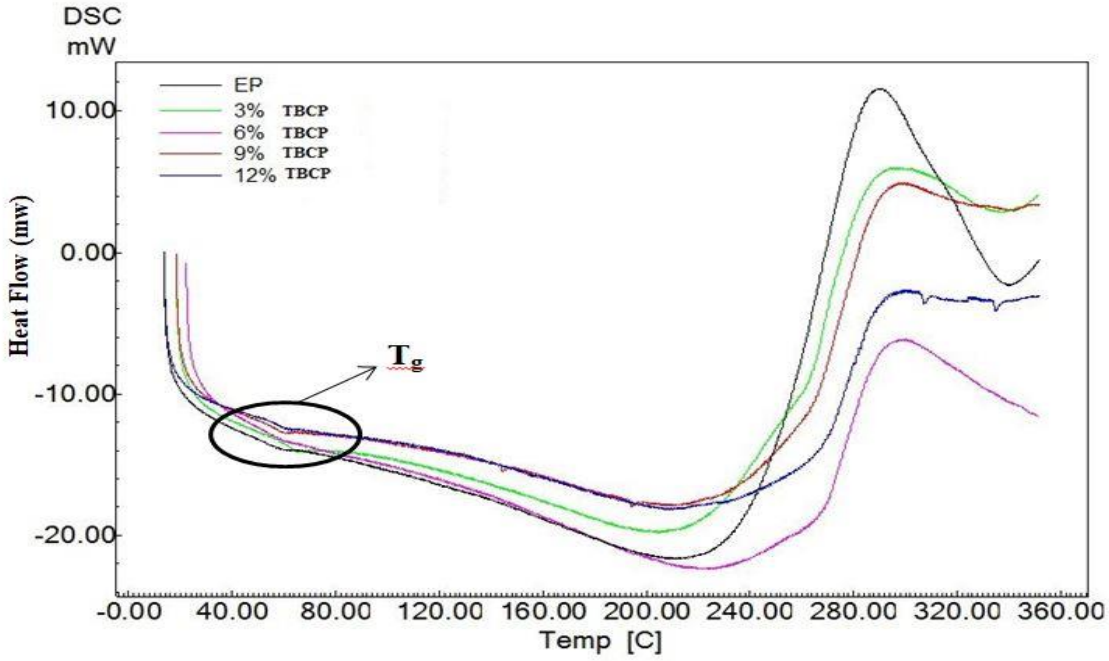

Figure 4.15: DSC curves of TBCP/EP blends.

The glass transition temperature (T_g) of PU/epoxy with varying PU concentrations was analyzed using DSC to determine the effect of PU on the thermal characteristics of epoxy resin. As shown in figure 4.16, the addition of polyol PU decreased the T_g of the epoxy resin. The glass transition temperature (T_g) of cured epoxy is mainly governed by the material's chain flexibility, crosslinked structure, and the amount of intermolecular hydrogen bonding interaction. The modified epoxy resins' T_g would drop because the addition of PU's flexible segments would loosen the crosslinked structure.

As a result, the T_g of PU/epoxy blends is less than that of pure epoxy in agreement with [195].

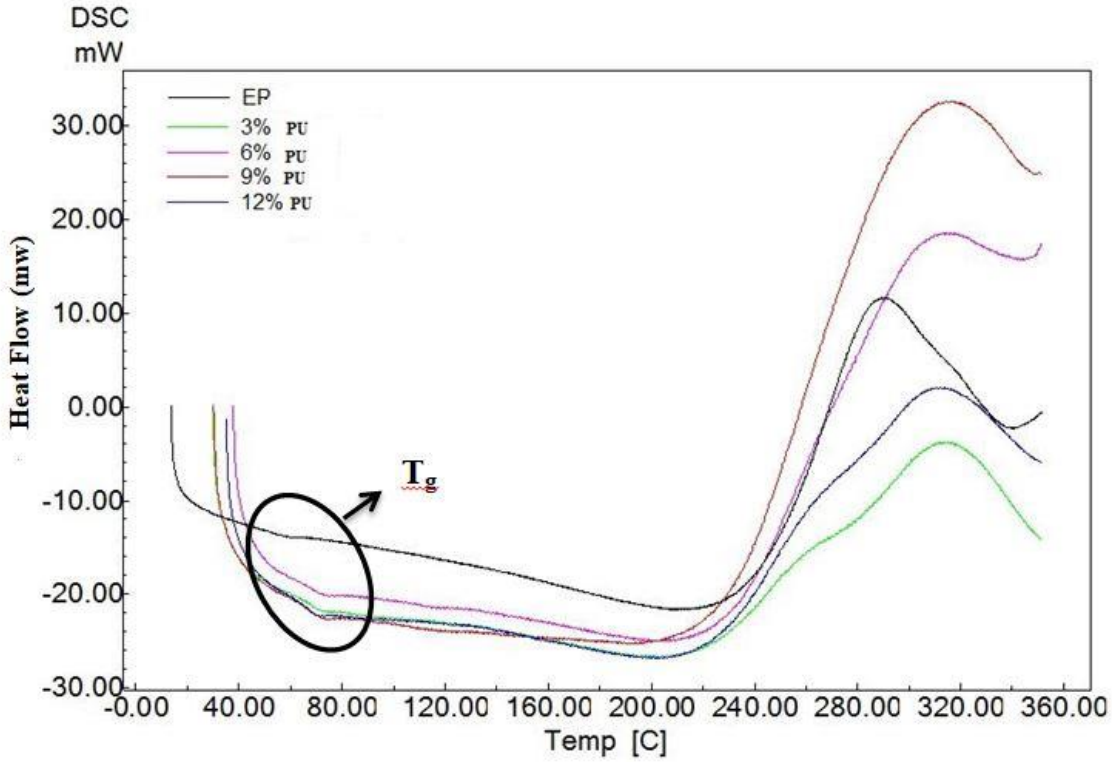

Figure 4.16: DSC curves of PU/EP blends.

On the other hand, figure 4.17 shows that the T_g values of epoxy are reduced when silicon rubbers are added to the epoxy systems. This is a common side-effect of EP that has been modified with LSR, as mentioned in a number of studies. This fact could be explained by the presence of a liquid silicon rubber phase, which caused a decrease in the cross-link density. This, in turn, led to an internal plasticizing effect in the modified epoxy resin, in addition to the incomplete conversion of epoxy groups in LSR-modified samples[196]. The presence of discrete rubber phases inhibits the creation of the cross-linking structure of epoxy resin, hence lowering the cross-linking degree. A lower degree of crosslinking enhances the free volume of the material and facilitates the mobility of the chain segments, resulting in a decrease in glass transition temperature[197]. In addition, it can be observed

a decrease in the transition temperature value with more silicon rubber loading may be due to acting as a plasticizer phase in the matrix consequence of reducing the stiffness of the blend[198,199].

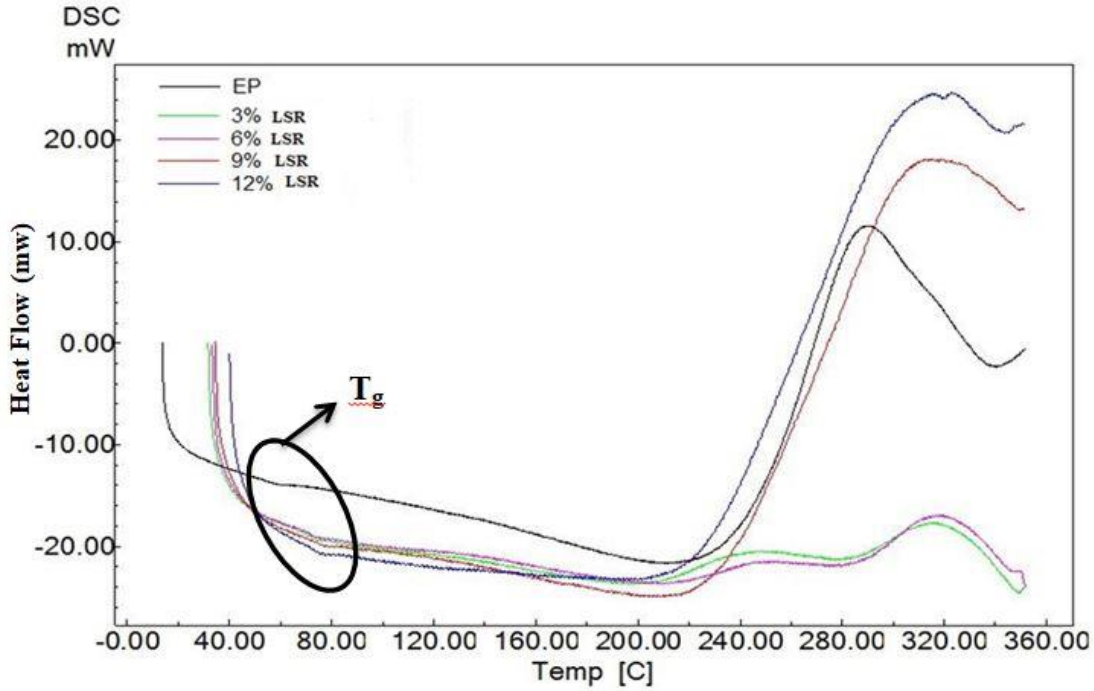

Figure 4.17: DSC curves of LSR /EP blends.

The physical state of PVC adhesive used was a viscous liquid and it is expected that it may work as plasticizer for epoxy. A PVC adhesive may be considered as a substance, breaking intermolecular bonds in an epoxy network, or even as a lubricant, reducing intermolecular friction and by this increasing deformability of the structure [200]. Figure 4.18 illustrated T_g of PVC/epoxy blends. Despite the fact that the plasticizer can inhibit reactive species in the epoxy resin and/or crosslinking agent (hardener) due to the size of its molecules, a minor drop in T_g is seen[201].

Thus, a plasticizer improves the molecular mobility of polymer chains, and this increased mobility decreases the glass transition temperature (T_g). An increase in the excess free volume and a decrease in the crosslinking density as a result of some reactive sites being blocked by the big PVC plasticizer

molecules are both potential causes of this decrease in the T_g in the case of a thermoset like an epoxy resin[202,203].

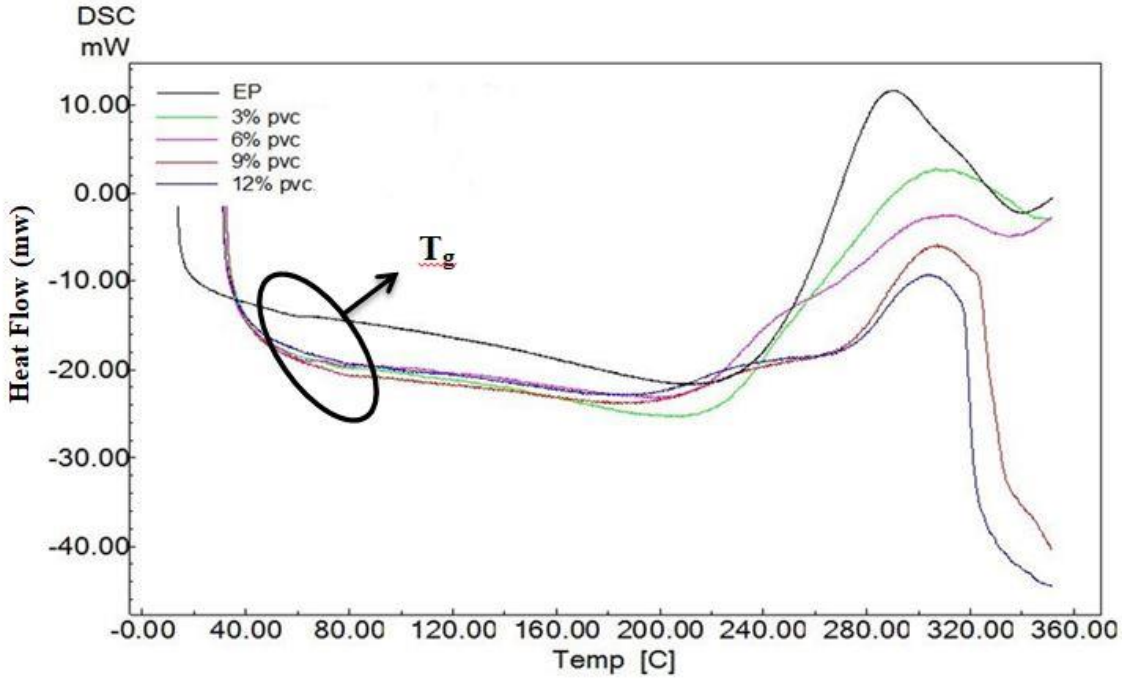

Figure 4.18: DSC curves of PVC /EP blends.

The glass transition temperature (T_g) of the polysulphide/epoxy blends is determined by the DSC test and the results show that the Tg decreases with increasing polysulphide load content, see figure 4.19 and (appendix A/ table 4.9). This is attributed to more elastic behavior due to increased flexibility[204]. It can be related to a reduction in network crosslink density accompanied by a rise in modifier weight ratio[205].

In the case of polysulfide polymers, they act as both modifiers and diluents for epoxy resins, and polysulfide polymer as rubber phase is utilized to toughen hard and brittle epoxy resin[206]. The reduction in the epoxy T_g is due to the polysulphide polymers being reactive modifiers. Both the mercaptan and epoxy end-groups are capable of reacting in a normal epoxy/amine system. As polysulphide polymers are flexible, rubbery

polymers. the overall rigidity of the matrix is reduced, hence producing a lower T_g in agreement with[207,208].

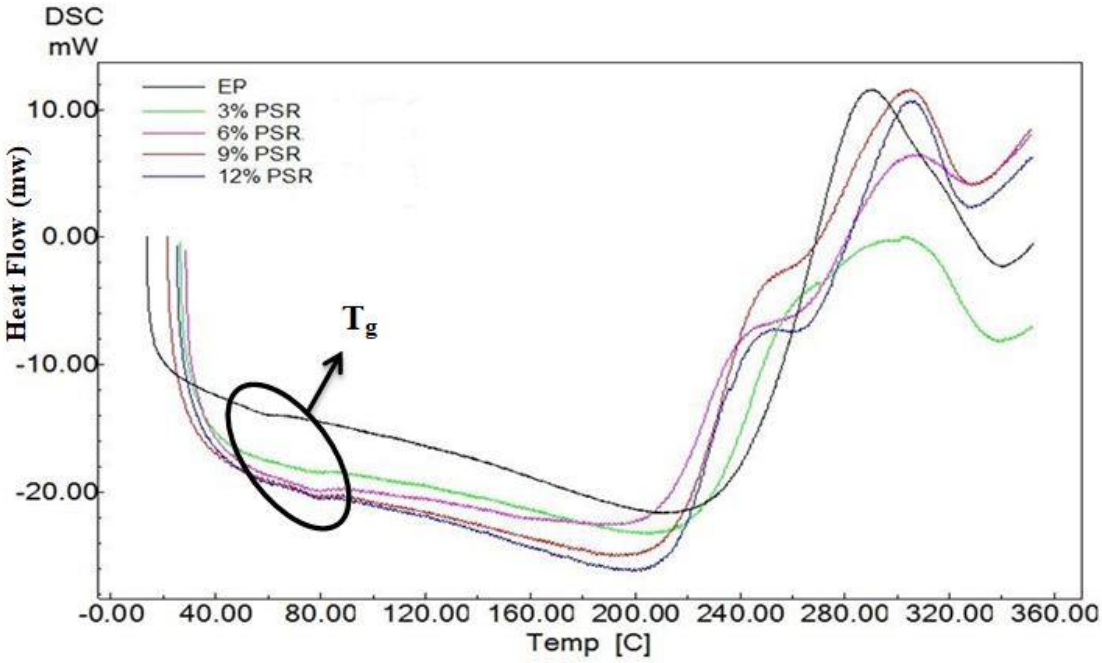

Figure 4.19: DSC curves of PSR/EP blends.

4.2.4 Mechanical Tests Results and Discussion

4.2.4.1 Tensile test

Figures 4.20(a,b, and c) shows the tensile properties of toughening agents /epoxy blends. From graph 4.20 (a and b), it is observed that the addition of 3% and 6% of TBCP increase the tensile strength and elastic modulus of epoxy thermoset, and then higher than 6% of TBCP decreases these properties. This is because TBCP chains which have low molecular weight overlap between the epoxy network, giving an impediment to movement inside the matrix, leading to an increase in both the modulus of elasticity and tensile strength of the epoxy. Similar results were found by [158,173], which were justified based on the compatibility between TBCP and epoxy. Figure 4.20 (c) shows that elongation of TBCP/epoxy blends decreases slightly with an increase in the TBCP content, especially at a high percentage related to the

quantity and size of the chains that hinder the movement and prevent it from elongating significantly.

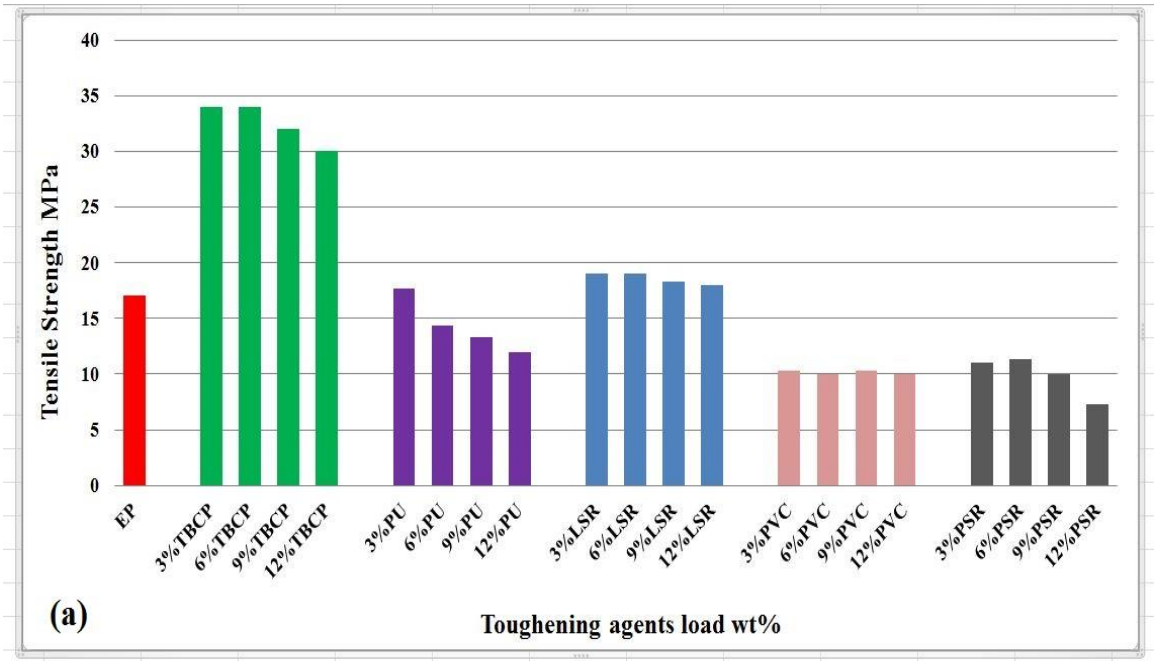

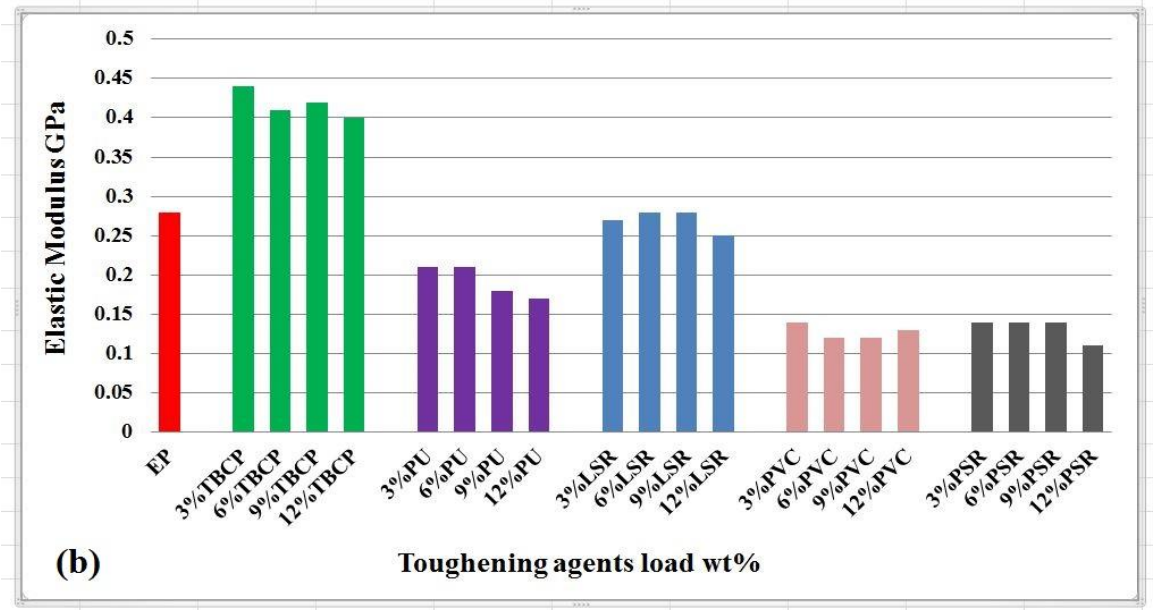

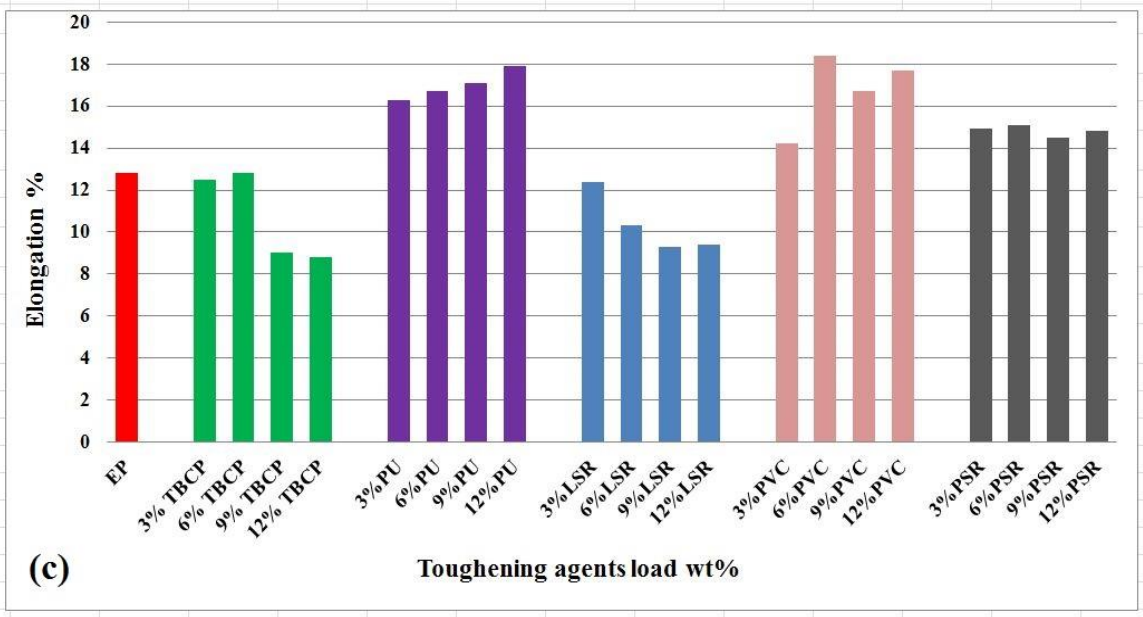

Figure 4.20 : Tensile properties (a) tensile strength (b) elastic modulus(c) elongation of toughening agents /EP blends

To investigate the influence of PU polyol addition on mechanical properties of the epoxy, the tensile strength, elastic modulus, and elongation were studied. Figure 4.20 (a, b, and c) demonstrates the tensile characteristics of epoxy that has been mixed with varying amounts of PU polyol. When polyurethane polyol is added, the tensile strength and elastic modulus of the material both decrease, with the tensile strength dropping by a significant amount.. Thus, the crosslink densities of the epoxy/polyol blend samples may be low, leading to a decrease in elastic modulus. See (appendix A/ table 4.10) displays a decrease in tensile strength of 29.4 percentage points and a modulus reduction of 39 percentage points when 12 wt% is added. In contrast, the elongation at the break of the blended system increases significantly with an increase in the PU content. This is attributed to PU polyol which works as a plasticizer. The incorporation of PU polyol toughening agent between epoxy chains breaks some extent of the polymer segment interactions, enabling increased segment flexibilities and therefore

allowing the polymer matrix to sustain large deformations before fracture. Consequently, the elongation of the tested samples is improved[209].

The tensile strength of the LSR/EP blends is significantly improved(see figure 4.20 (a)). An epoxy matrix is a cross-linked structure with a very brittle system. When the sample was put under tensile force, the matrix could not handle enough tensile force because the molecular chain between the cross-link points was too small to conform, which would be essential to reduce stress concentration and transfer stress. When liquid rubber was added to the system, the crosslink density fell and the system became more flexible than when it was just EP. When tensile stress was laid on the cured blends, the molecular chain was able to change its shape to relieve stress concentration and transfer stress. This made the matrix less sensitive to flaws [210]and gave the blends a fairly high tensile strength. As the rubber content of the epoxy matrix increases, the matrix becomes plasticized, and the tensile strength drops to a value higher than that of neat EP. Adding liquid rubber to the epoxy resin leads to improving tensile strength and toughness. The young's modulus (E) is a measure of stiffness (rigidity) of the material. The greater the young's modulus, the smaller the elastic strain resulting from the application of given stress [115] (see figure 4.20 (b)). The tensile modulus of the LSR/EP blend decreases with increasing silicone rubber content. The reason for this reduction is the increase in the flexibility of the polymer chains for the blends compared with that of pure (EP). This implies an increase in the strain rate and reduction in the stiffness (rigidity), which means, these blends will have a new prospect of application, similar to [115]. The tensile modulus of a polymer has a tight relationship to the molecular chain structure, and the crosslink density is established by the number of chemical crosslink points (covalent bonds) and physical crosslink

points in the material (hydrogen bonds and molecular chain entanglement points). With an increase in silicone rubber content, the tensile modulus lowers because of a decrease in the blends' content of rigid segment structure and crosslink density. Other systems have shown similar results[211]. Regarding the LSR-modified blends' elongation-at-break, the same pattern figure 4.20 (c) is also found, when the loading content of the LSR goes from loading (3 wt%) to loading (12% wt) the size of the spherical regions is large and becomes a point defect, resulting in a reduction in the elongation of LSR/EP blends this agreed with[212].

In this study, PVC was also employed to enhance the epoxy resin's mechanical and thermal qualities. As a result, tensile strength and other mechanical properties of the PVC/epoxy blends against the variation of PVC content carefully are illustrated in figure 4.20(a and b), When PVC is added, both the tensile strength and the modulus go down. As the PVC content goes up, the tensile modulus goes down and the tensile strength stays about the same. This is because there isn't enough interfacial adhesion between the PVC phase and the epoxy resin matrix, which makes the ability to transfer loads weaker similarity[114,213] All these indicate that PVC has an effective toughening modification to EP.

The percentage of elongation and its relationship to the PVC concentration are illustrated in figure 4.20(c). Elongation increases significantly with increasing PVC content. This phenomenon is due to the polar bonds contained in PVC, which allow for a large movement into the chain. Epoxies, on the other hand, have a three-dimensional structure with covalent bonds, and individual molecules are bound to the net with no significant mobility possible. The high amount of PVC acted as a plasticizer for the epoxy resin, thereby reducing Young’s modulus and tensile strength, and

increasing the elongation at break, owing to its effect on the enhanced distance between the EP molecules agree with[214].

The tensile mechanical properties of all PSR/ epoxy thermoset blends are shown in Figure 4.20. As can be seen in figure 4.20 (a and b), tensile strength and Young's modulus both drop when PSR concentration rises. This is due to the addition of PSR reducing the cross-linking density and enhancing ductility, The altered specimens are much less sensitive to deformation, resulting in a reduction in Young's modulus[183,215,216]

Figure 4.20 (c) displays a rise in elongation-at-break from 16% (at 3% wt PSR) to 18% (at 6%wt PSR), indicating an increase in the material's toughness. This shows that PSR can make the epoxy curing system toughen. This is because the modifier is flexible, which can stop cracks from getting bigger and cause crazes[217]. The addition of liquid rubber to an epoxy matrix causes the epoxy network to become plasticized, resulting in a larger free volume and, as a result, easier polymer chain movements, allowing for greater ductile deformation prior to sample fracture. In addition, it is well known and shown that the interaction of rubber particles with the stress field in front of the moving crack tip induces the rise in epoxy resin strain at break. It is claimed that rubber particles suffer partial cavitation, hence promoting yielding and plastic flow in epoxy resin[189].

4.2.4.2 Fracture toughness and Impact strength results

The results of fracture toughness and impact strength tests for unnotched specimens of epoxy and epoxy blends are summarized in (appendix A/ table 4.11). All of the modified epoxy blends exhibit much higher impact strength than the unmodified epoxy network.

The fracture toughness values of TBCP/epoxy blends that are shown in figure 4.21 increase with increasing in the TBCP load content . Compared to the neat epoxy formulation, TBCP-modified epoxy system shows that the surface is very coarse and rough, which is a good sign for crack resistance and energy dissipation as shown in figure 4.10. In these formulations, the microspherical shape of TBCP may be seen. The main toughening process is thought to be the debonding of particles from the matrix, which is caused by cavitation, followed by shear yielding[218]. It seems that for 3 wt% TBCP formulations, a tiny, uniformly distributed spherical zone inside the matrix may improve the effective transfer of stress between the matrix and the spherical zone, resulting in a significant increase in fracture toughness[219].

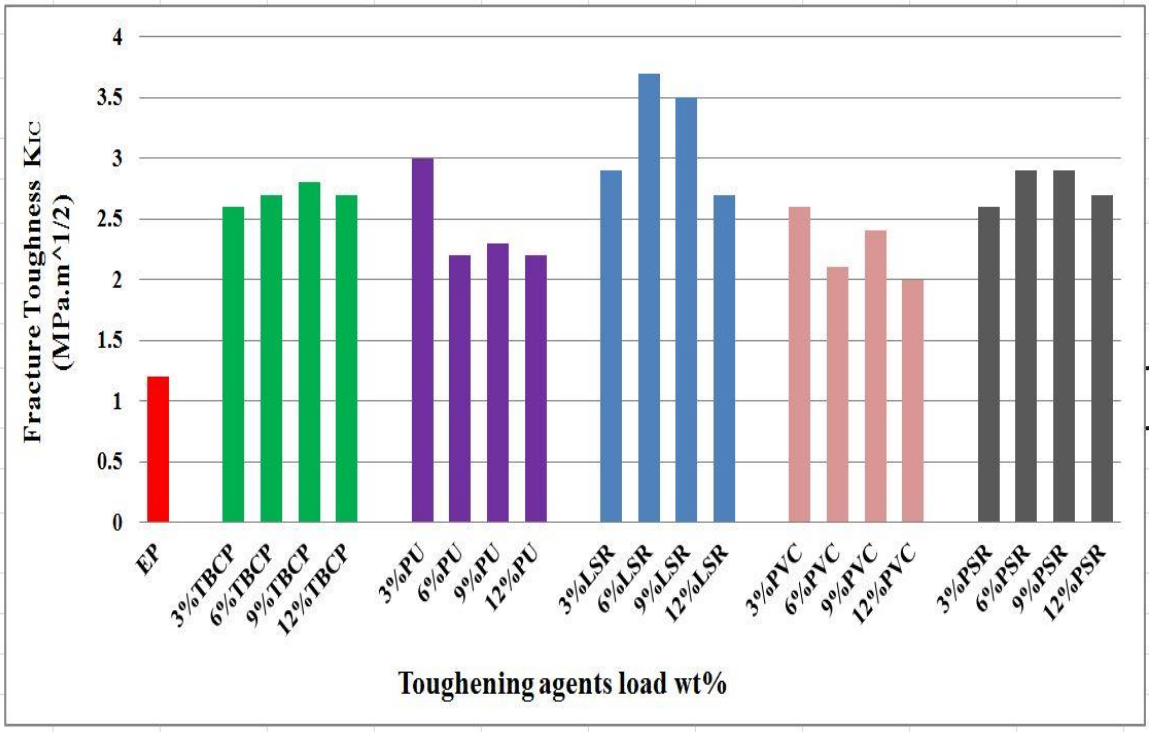

Figure 4.21 : Fracture toughness of all toughening agents /EP blends

The impact strength of the epoxy increases by the addition of TBCP at 3% wt. (see figure 4.22 that shows the impact strength of TBCP/epoxy blends). Then, the impact strength decreases with increasing the TBCP content but remains higher than the impact strength of pure epoxy. Phase separation morphology, in which the TBCP phase forms dispersed domains in an epoxy matrix, allows the blend to achieve this effect. The slight improvement in mechanical characteristics brought about by the addition of TBCP may be explained by the compatibility and interfacial adhesion between the matrix and dispersed phase, as well as the softening effect of the flexible TBCP chains in the rigid epoxy matrix[161]. Impact energy is kinetic energy, and when it hits a material that has a second phase with plastic deformation, like TBCP, it will absorb the impact energy and release it through vibration because its chains are flexible. This makes the material more strong to impact.

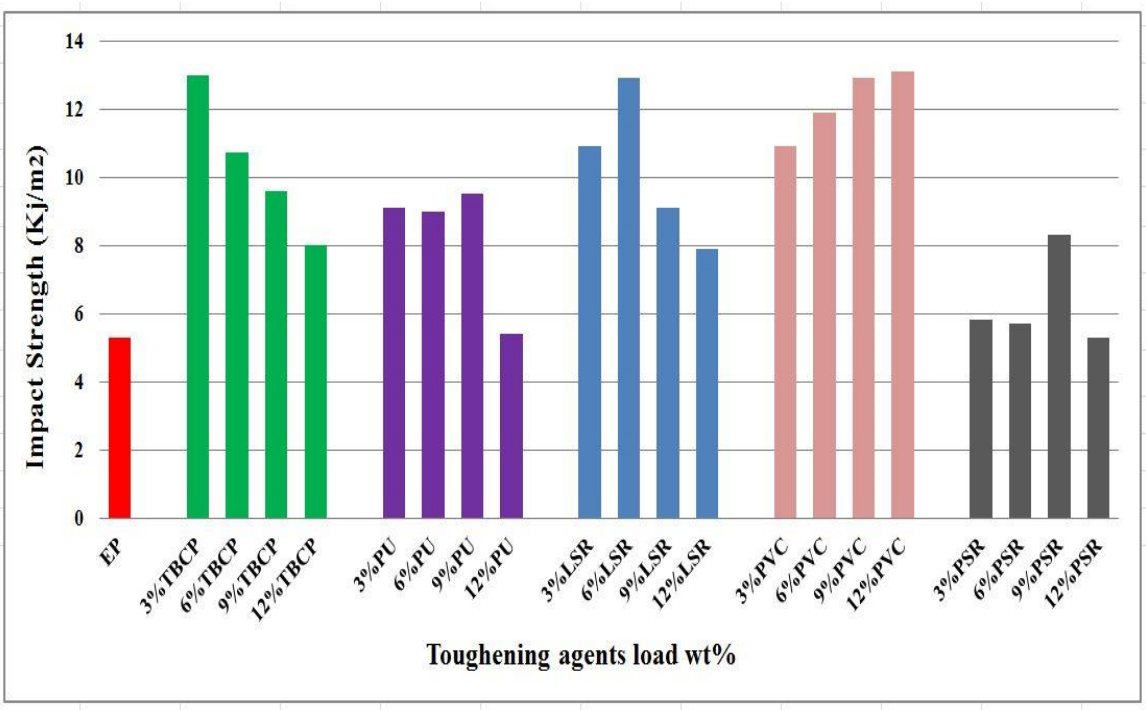

Figure 4.22 : Impact strength of all toughening agents /EP blends

The fracture toughness values of PU polyol /epoxy and LSR/epoxy blend are shown in figure 4.21. The results show that the K_{IC} values of epoxy resins blended with PU polyol and LSR are significantly improved as compared to neat epoxy, and epoxy resins blended with LSR are higher than with PU polyol. A maximum increase in the K_{IC} is around 208% for epoxy samples with LSR content of 6% wt. as compared to neat epoxy. The improvement of K_{IC} value for PU/epoxy blends may be attributed to the incorporation of flexible modifier chains, which resulted in an increase in the free volume available. In point of fact, a liquid modifier may perform the function of a plasticizer for the polymer matrix, leading to increased energy required to crack it similarity with [160]also plasticizers hinder polymer molecules from interacting with each other by breaking the attachments along the chains. Hence, plasticizers reduced the self-crosslinking density of epoxy [176]. Cavitations of the LSR spherical zone can absorb energy and hence increase fracture energy that requires to fracture so increase fracture toughness by lowering the local yield stress and provoking extensive shear yielding[220]. The cavitation of rubber-rich zones has been attributed to be the main driving force behind shear yielding to be activated in the matrix by[3].

The impact strength of PU /epoxy and LSR/epoxy blends for all the percentages are shown in figure 4.22. The impact strength of the neat epoxy resin is improved in the presence of polyether polyol. The incorporation of the PU (polyol) molecules between polymer chains to some extent breaks polymer segment–polymer segment interactions, enabling increased polymer segment flexibilities and therefore allowing the epoxy matrix to sustain large deformations before fracture. The enhancement of impact strength of epoxy with PU polyol (plasticizer) might be attributed to some extent to the excessive shear yielding and the large ductility of modified samples [221].

As shown in figure 4.22, compared to the neat epoxy (unmodified epoxy) the 6 wt % LSR-modified epoxy resin displays a 143% increase in the impact strength, demonstrating that the silicon rubber provides a good buffer and dispersion against the instantaneous impact and LSR improves the fracture toughness and impact performance of epoxy similarity with[222]. When silicone rubber is added to a material, the impact strength and energy both increase, leading to the production of a second phase that serves to prevent cracking and slow the propagation of existing cracks. Due to its extreme flexibility, elastomer has a high impact strength agree with[178].

The fracture toughness is the resistance of a material to crack initiation and propagation. The increase in fracture toughness is caused by a variety of factors, such as the quantity of the modifier in the mixture, the interfacial adhesion between the phases, the curing conditions, etc. A two-phase morphology is an essential need for enhancing the fracture toughness of a thermoset/thermoplastic blend. In this study, all the blends were heterogeneous, which was a requirement that had to be satisfied in order to get the desired result of improved fracture toughness[223]

Factor of stress intensity K_{IC} measures the fracture toughness of cured systems. As can be seen in figure 4.21, the fracture toughness of PVC/blends improves as the PVC load content rises. Improvement in fracture toughness equal to 117% is reported at 3 wt% percentage of PVC. Fracture toughness of epoxy resins was shown to improve with a rise in thermoplastic phase concentration, according to reports[224,225]. Specifically, the continuous thermoplastic phase exhibited inverted phase morphology. Here, however, the fracture toughness of all blends is improved in comparison to that of pure epoxy-amine systems. Increased fracture toughness has been attributed, in

part, to enhanced interfacial adhesion between the epoxy resin and the dispersed thermoplastic phases[226,227].

As may be observed in figure 4.13(a) and (b), the fracture surfaces are rough, and river markings have developed on the surfaces. These phenomena are indicative of the matrix's plastic deformation, the crack's ductility, and the crack's deflection. When PVC diffuses into the epoxy, it makes the epoxy more flexible near the PVC dispersed phase. Local shear deformation of this dispersed PVC phase zone might lead to stress relief. The ductile drawing process of the PVC dispersion phase also absorbs deformation energy as a consequence, the surface area of the crack increases, which in turn leads to an increase in the fracture toughness[223].

Figure 4.22 shows the impact strength of unmodified epoxy and PVC/epoxy blends. The impact strength of blends increases with increasing PVC content load. compared with neat epoxy the increment in impact strength reaches 147 % percentage (12wt% PVC). This indicates that the introduction of thermoplastic PVC has more influence on the impact strength. This result may be related to the PVC phase in the epoxy matrix acting as stress concentrators to absorb the external energy and mitigate the crack growth[228,229]. When the crack occurs, the PVC-rich domains are plastically deformed at the crack tip to prevent crack propagation and increase the impact strength of modified PVC/epoxy blends agreed with[230].

Fracture toughness of PSR/epoxy blends was measured and analyzed as a function of PSR concentration, as shown in figure 4.21. Compared to pure epoxy resin, the blend samples all show a remarkable increase in fracture toughness. The K_{IC} of the blend with 9 wt% PSR represents a maximum

fracture toughness, and the K_{IC} increases as the PSR concentration rises. Incorporating a rubbery phase into an epoxy matrix results in a less dense crosslinking reaction. When epoxy resins are cured in the presence of polysulfide modifiers, the resulting structures have two distinct "domains": the epoxy/amine crosslinking and the linear segment of the modifier. Reducing crosslink density and improving chain stiffness are two ways to improve the fracture toughness of epoxy systems agree to [205]. In addition, the plasticizing act of the polysulphide rubbery phase might occupy the free volume of the epoxy network, leading to ductility. This may contribute to an increase in fracture toughness in the PSR/epoxy blends system[231]. This means that the increase in fracture toughness is caused by many different things happening at the same time in the epoxy matrix when a load is put on it[68,107].

The experimental data shown in figure 4.22 indicate that the impact resistance of PSR/epoxy is enhanced by 57% at a PSR concentration of 9% when compared to the epoxy value in (appendix A/ table 4.11). An increase in impact resistance is also attributable to some degree of polymer chain entanglement.This is related to the fact that polysulfide rubber has the ability to improve the flexibility of the blend matrix, therefor the resultant blend matrix can absorb and dissipate the impact energy load before fracture agrees with[232,233]. Micrograph fracture of samples for additional PSR rubber phase in the epoxy matrix are similar to those presented in Figure 4.14, with the only discernible difference being the degree of roughness. This makes it easier for the blend to create plastic deformation zones along the direction of the crack so that it can absorb more energy. As a result, the blends' impact resistance went up, which was a good thing[186]. According

to Wang et al.[234]an increase in the entanglement of the molecule chain enables the blend to absorb more energy when destroyed.

4.2.4.3 Hardness test results and discussion

The hardness of the samples is determined with a Shore D durometer which indicates the relative resistance of a material to indentation with a load applied to the indenter[235].

It is noted that the shore D hardness values of all prepared toughening agents/ epoxy blends as shown in figure 4.23 and (appendix A/ table 4.12), are slightly increased or decreased compared to pure epoxy. This is because the hardness property depends on the penetration of the durometer to the surface of the sample and as a result of using small amounts of the toughening agent in the thesis. The maximum addition is 12wt% inside the epoxy matrix, due to the distribution and spread of the second stage inside the epoxy, when the test performed , once needle will hit the secondary phase, so notice a decrease in the hardness value, and when it encounters the epoxy matrix, will notice an increase in hardness, so the toughening agent do not significantly affect the hardness property.

Figure 4.23 : Hardness (shore D) of all toughening agents /EP blends

4.2.5 Pull off adhesion of epoxy blends result and discussion

An investigation into the effects of coating strength on metal was carried out via the use of a pull-off adhesion test. In the pull-off adhesion test, a coated film of a certain diameter is separated from its base and the force that results is measured as shown in figure 4.24. To determine the adhesion strength, a coated sample was pulled off from underneath a rounded loop that was loaded with increasing quantities until the coating was removed away from the surface of the substrate[236]. The results are presented in (appendix A/ table 4.13).

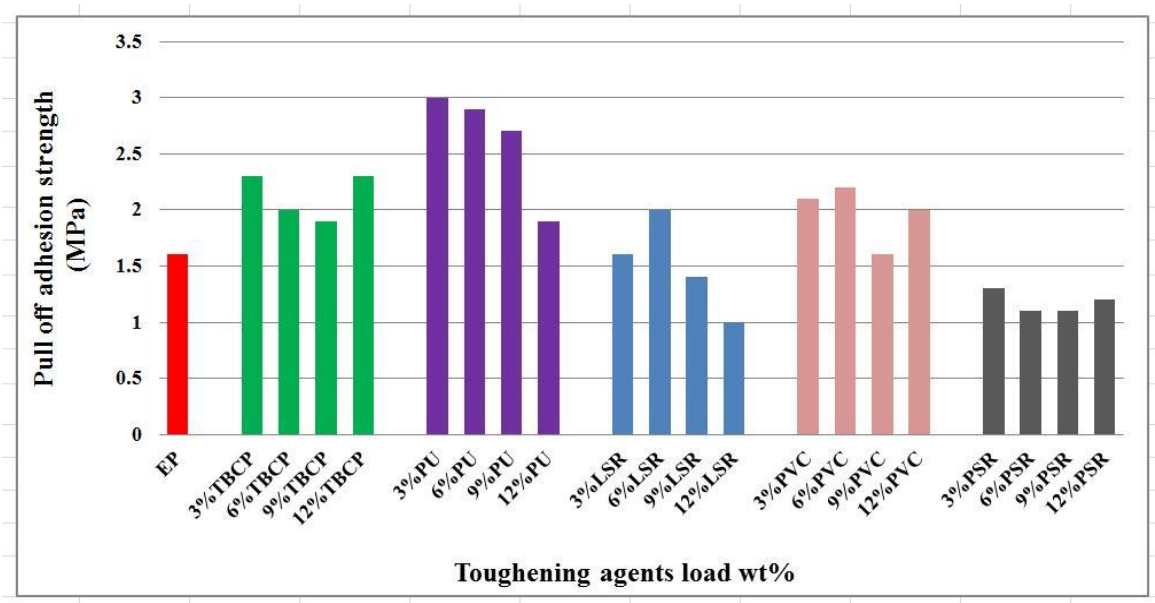

Figure 4.24: Pull off adhesion strength of different toughening agent /EP blends

The TBCP/EP, PU/EP, and PVC /EP coating samples display good adhesion properties as shown in figure 4.24. It is possible for the coating to come off during the pull-off test due to adhesive failure at the epoxy/steel interface or cohesive failure at the epoxy layer itself, as seen in figure 4.25. Cohesive failure happens when the bond between the coating and the substrate is strong, while adhesive failure happens when the bonds between the coating and the substrate are weak[237].

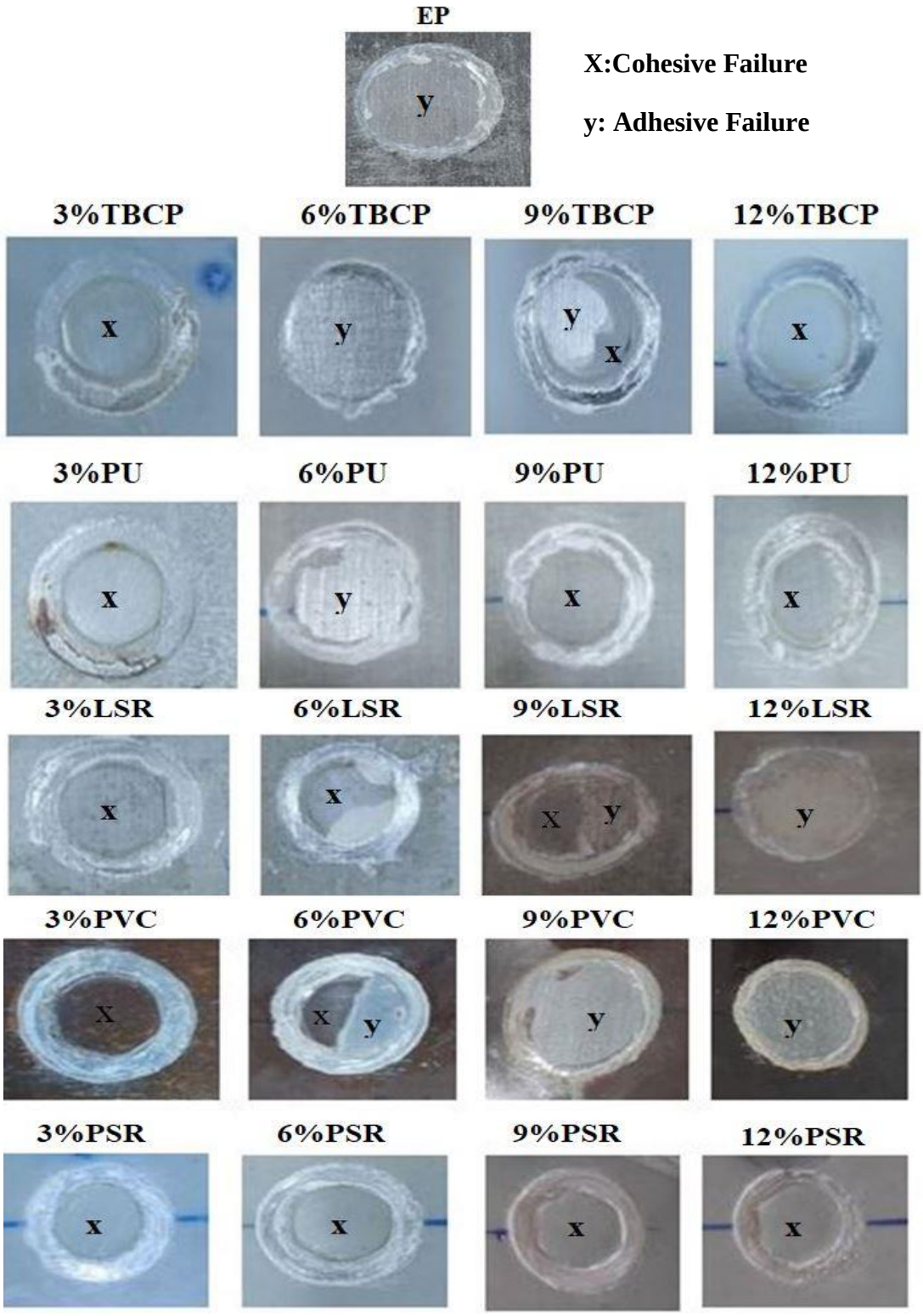

Figure 4.25: Visual inspection of samples EP, TBCP/EP, PU/EP, LSR/ EP, PVC /EP and PSR/EP after pull-off test

The most prevalent adhesion forces involved in adhesion bonds between epoxy and steel can be classified into three groups: mechanical (mechanical interlocking bond), physical (hydrogen bonding, dipolar interactions, weak, secondary or van der Waals forces), and chemical (covalent, ionic, and metallic bonding)[238]. Epoxy resin's epoxide groups may react with the oxide film's active hydrogen to form chemical bonds[239–241].In TBCP/ EP samples the maximum increase in pull-off adhesion strength is at 3 and 12 % wt about 2.3 MPa compared with neat epoxy resin at 1.6 MPa. This can be attributed to the maintenance of the stiffness of the blend as confirmed by the higher E value, which leads to the increment in stress capacity and diminishes local detachment between the coating and the substrate[242,243].

The pull-off strength of PU/EP and PVC /EP, are sensitive to the number of functional groups, such as hydroxyl groups, ether group, and Cl-group(polar group) which form strong bonds with Fe atoms on the substrate surface (metal surface) and make a good adhesion to the substrate for epoxy based coatings[244,245].

In the case of LSR and PSR addition in epoxy resin, pull-off adhesion strength decreases as shown in figure 4.24. Figure 4.25 shows the apparent results along with the adhesion strength of several samples. There are generally two sorts of failure on this test. EP adhesion failure at the EP/metal interface is the first type and occurs when the adhesion strength between the EP and the substrate is insufficient. Cohesive failures occur inside the EP rather than at the metal/coating contact and are the second form of failure [246]. These materials have a rubber phase that does not contain polar groups or ions, and therefore their interaction on the metal surface is produced by physical bonding by Vander Waals attraction, which is low energy compared to hydrogen bonding or ionic bonding, Coating material

will penetrate cavities on the surface with displace trapped air at the interface to occur mechanical interlocking with the metal surface and thus coating adhesion strength of this LSR and PSR toughening agent is low compared to other materials.

4.3 Epoxy Nanocomposite Result and Discussion

In this part of the work was prepared two epoxy nanocomposite, WC/EP and WC/(3%wt TBCP)/EP nanocomposite with addition carbide tungsten nanoparticles percentage 1%,2%,3% wt. and the results obtained is:-

4.3.1 Analysis of X-ray Diffraction Result of WCnanoparticles

An X-Ray diffraction test (XRD) is a non-destructive technique for determining the crystalline nature, chemical content, and physical properties of a material. The technique relies on the constructive interference of monochrome X-rays and a crystalline specimen. X-rays are a type of electromagnetic radiation with shorter wavelengths that are produced when electrically charged particles with enough kinetic energy are decelerated. An X-ray diffractometer (XRD) uses incident X-rays that have been focused and collimated on a sample of nanomaterial. The resulting diffracted X-ray is then identified, evaluated, and recorded. Diffraction patterns are displayed by plotting the intensities of photons that have been diffracted and then dispersed at different angles within a material[125].

In order to confirm that the nanopowder is tungsten carbide, an XRD test was carried out. Figure 4.26(b) displays the XRD pattern that was recorded, which consists of several distinct phases of tungsten carbide (WC) nanoparticles. All of the principal reflection planes of WC nanoparticles can be seen in clear detail in the spectrum, corresponding to (001), (200), (100), (101), and (110), respectively[247–249]having phases that are comparable to

those that were revealed earlier[250]. The XRD spectra of WC nanoparticles, which can be seen down, demonstrate that they have a hexagonal phase[251] agree with[252].

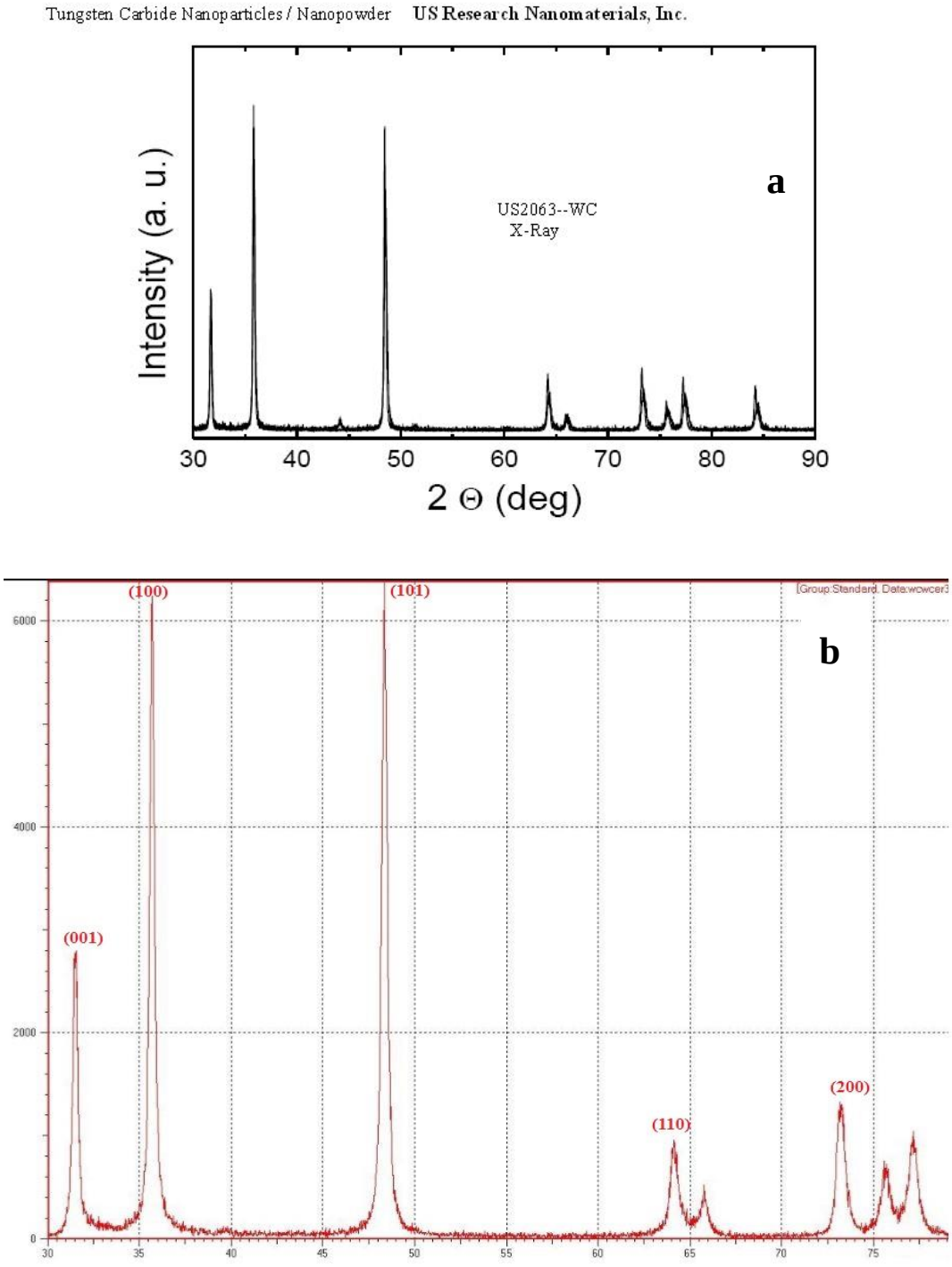

Figure 4.26: X-ray diffraction profiles of tungsten carbide powder (a) stander from company (b) WC sample test in laboratory.

4.3.2 Morphology Test Result

FESEM micrographs of two epoxy nanocomposites are shown in figures 4.27 and 4.28,in figure 4.27(a,b, and c) demonstrate that the nanoparticles utilized with block copolymers have no effect on the distribution of the copolymer in the matrix, nor do they interfere with miscibility at the circumstances used in this work. It can suggest that 3%wt TBCP may be enhancing the nanoparticle's adherence to the matrix. Martin-Gallego et al.(2015) discovered the same thing[174]. It is observed in figure 4.27(b)for 2 percent wt WC/TBCP/epoxy systems a lower agglomeration degree, good spread of nanoparticles, and distribution inside the matrix, this relates to the presence of TBCP which aided uniformly distribution nanoparticle and possibly affected the interaction between the nanoparticle and the matrix as recommended in [253]. As a result of their amphiphilic nature, the block copolymer presents between the tungsten carbide nanoparticle (WC) partly inhibits the nanoparticles from adhering back together after dispersion. As a result, at 2 wt. percent of WC nanoparticles for two systems nanocomposites prepared the dispersion of nanoparticles inside the matrix is more regular and homogenous. As the tungsten carbide loading percentage is raised, the quantity of agglomerations rises, as does their size. It also demonstrates that at large nanoparticle loadings, the likelihood of lump formation is quite high due to a deterioration in material characteristics caused by the heterogeneous dispersion of WC nanoparticles in the matrix(as shown in figure 4.27b and 4.28f). Many other studies have made similar observations.

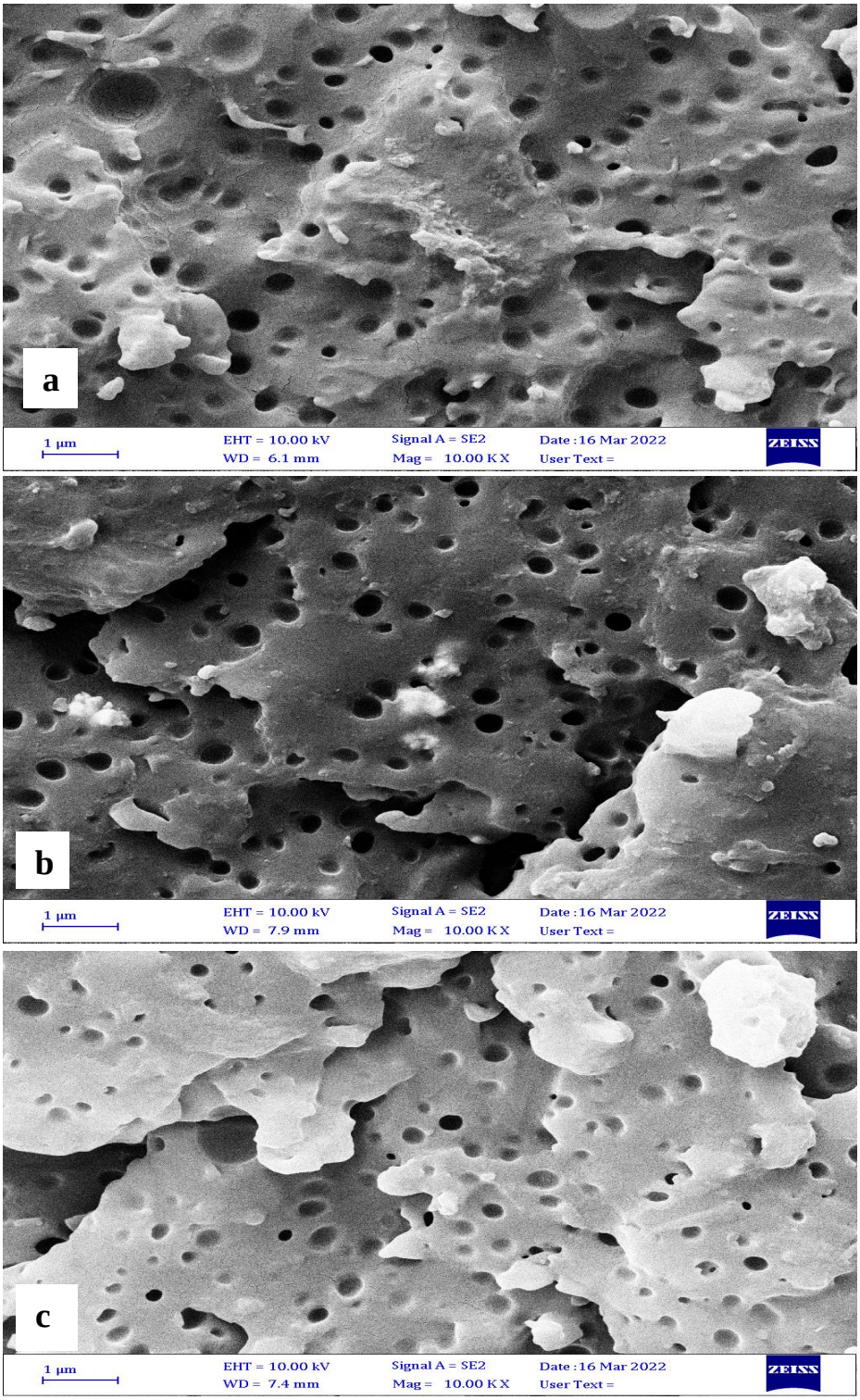

Figure 4.27: FESEM micrographs of a)1 wt % WC/3%TBCP /EP, b)2 wt % WC/3%TBCP/ EP and c) 3 wt % WC/3%TBCP/EP nanocomposites

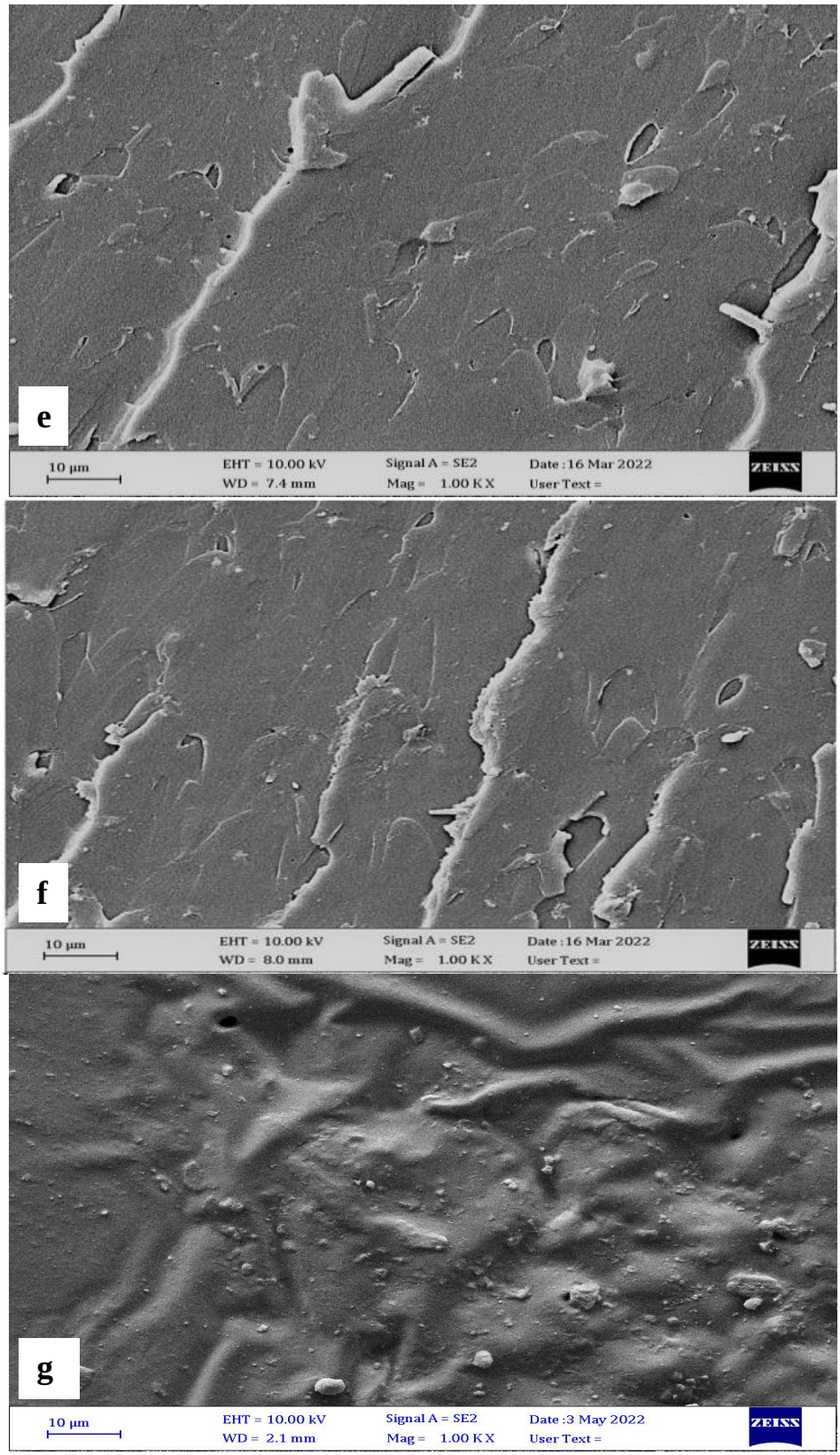

Figure 4.28: FESEM micrographs of e) 1 wt % WC/EP ,f) 2 wt % WC /EP and g) 3 wt % WC /EP nanocomposites.

4.3.3 Thermal test (DSC analyzes)

The T_g values of nanoparticle-filled samples are greater than in epoxy samples see (appendix A/ table 4.14), this may be explained by good interaction between the nanoparticles and matrix as seen in figure 4.29 (a and b) (upper and lower image). In comparison to unmodified epoxy, a temperature rise of 15 °C was recorded for the samples (WC/TBCP/epoxy). The use of block copolymers to stabilize nanoparticle dispersion is a non-covalent modification procedure that does not affect the nanoparticles' electronical structure or mechanical characteristics[253]. Block copolymers can contain a lyophobic portion that is adsorbed on the surface of the nanoparticles and a lyophilic portion that has epoxy affinity, preventing nanoparticle approximation and improving transfer between nanoparticle and matrix [253,254]. It is claimed in the literature that nanoparticles that are stiff might impede the movement of polymer chains and/or alter interactions near the nanoparticles' surfaces in a manner that affects the T_g [255].

The addition of nanoparticles together with TBCP to epoxy matrices resulted in an increase in the T_g, was reported by [256]. As a result, the second phase(TBCP) formation helps to achieve uniform nanoparticle dispersion in the matrix, thereby reducing chain mobility that causes the T_g to rise or at least remain unchanged as compared to neat epoxy[194].

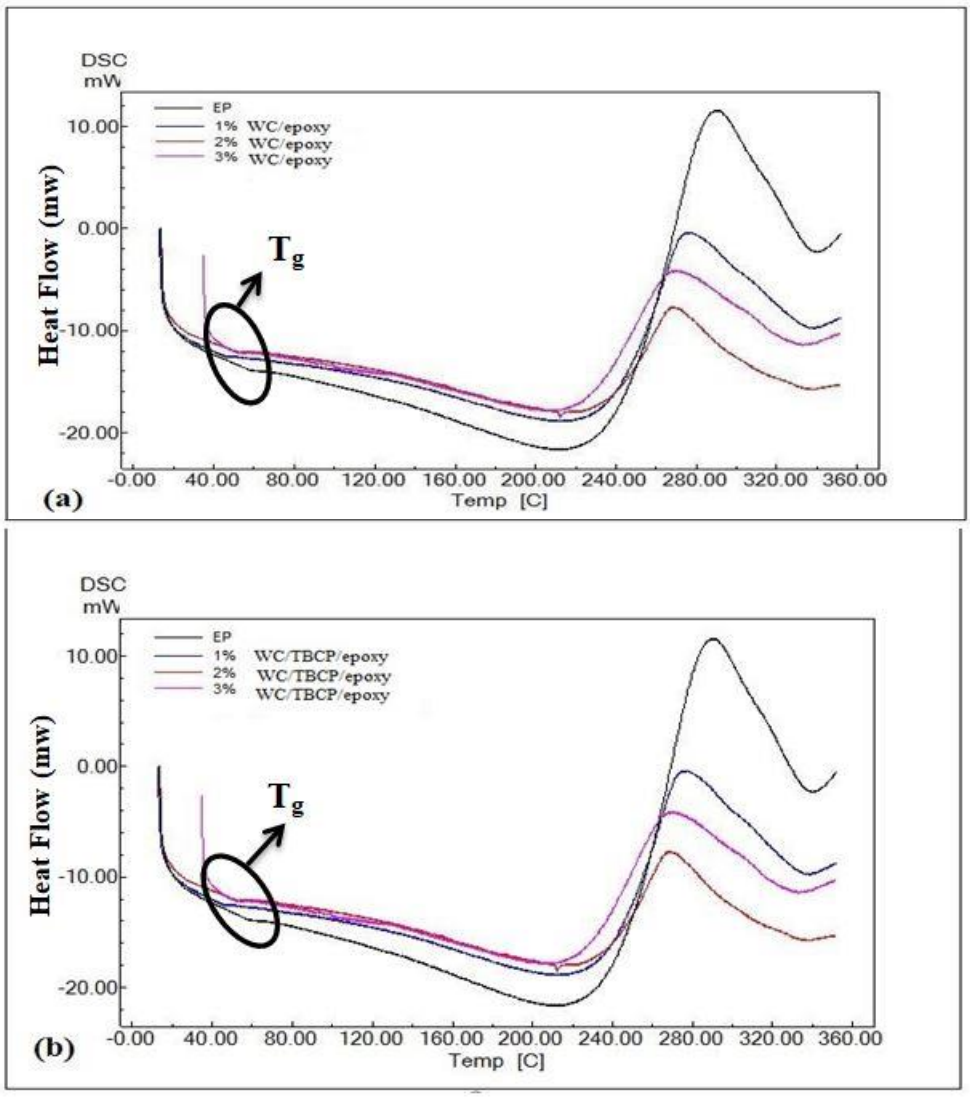

Figure 4.29: Curves of DSC (a) WC /EP Nano composite and (b) WC/TBCP /EP Nano composite

4.3.4 Mechanical test

4.3.4.1 Tensile Properties

Nanocomposite tensile strength is enhanced by adding WC nanoparticles to the epoxy see (figure 4.30(a)). The tensile strength of epoxy nanocomposites increases when particles content increases. At 2% particle weight, nanocomposites have the greatest strength ,enhancement in strength ~55 % see (appendix A/ table 4.15). 2 %wt of WC nanoparticles gives good dispersion of particles, and the load is transferred evenly between the

particles and the matrix, resulting in increased strength. Tensile strength reduces when the WC content is more than 2% wt. It can be explained by the fact that all nanoparticles have a significant propensity to agglomerate in order to reducetheir high surface energy[257,258]. Larger percentages of agglomeration particles create higher stress concentrations at specific places, resulting in a decrease in nanocomposite strength[259].It can conclude from the results of the tensile strength test the bond between WC and epoxy is very good.

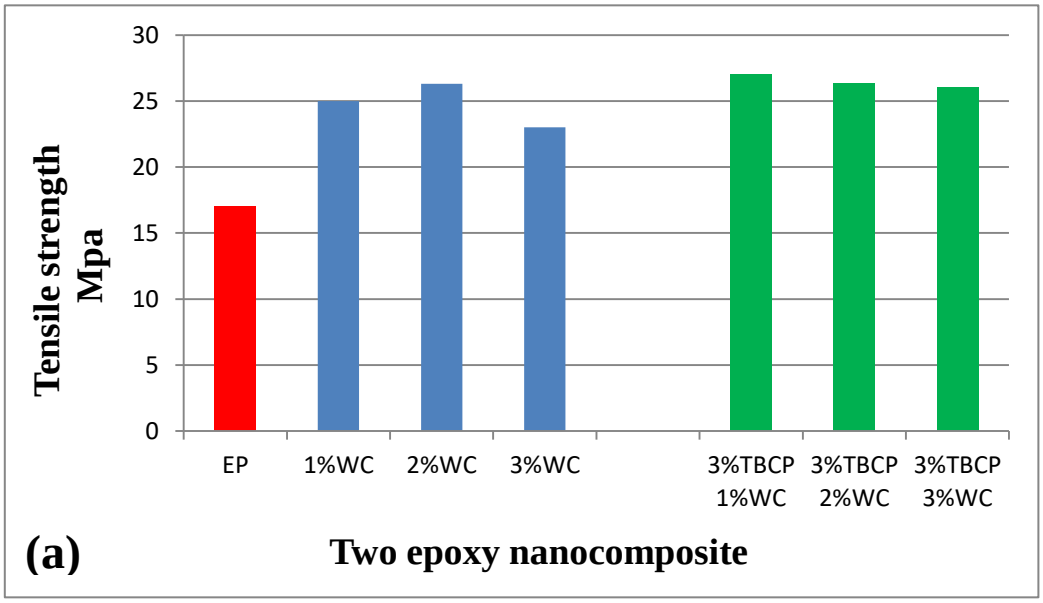

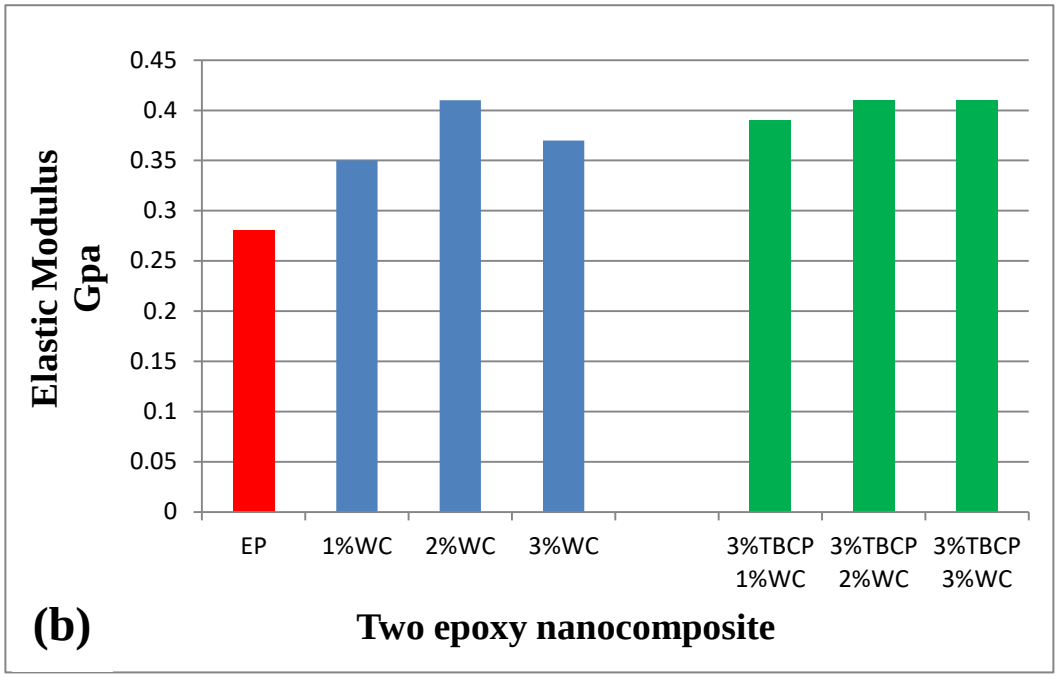

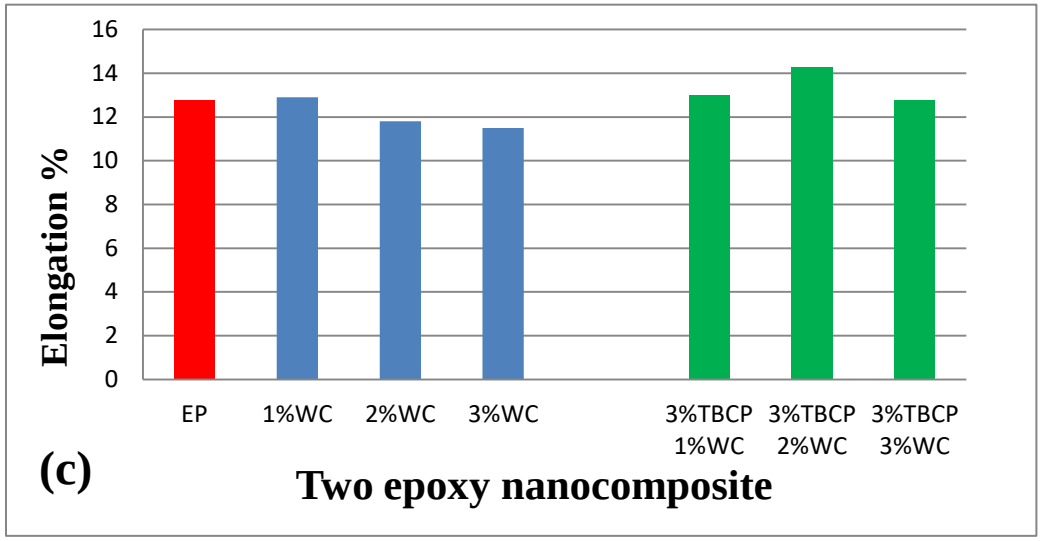

Figure 4.30: Tensile strength (a), Elastic modulus (b), and elongation (c) of WC/EP and WC/(3%TBCP)/EP nanocomposites.

The WC causes a modest reduction in elongation at the break of the nanocomposite, implying that the fillers produce a decrease in matrix deformation owing to the introduction of mechanical limitations see (figure 4.30 (c)). The adhesion of the filler to the epoxy matrix also contributes to the rigidity of the polymer chain and hence resistance to expand when strain is applied. The additional propensity for elongation to diminish at a filler level of around 3% wt, implies that matrix deformation is connected to the dispersion condition of the fillers as well as the interface characteristic.

Figure 4.30 (b) shows that Young's modulus of epoxy nanocomposites including WC is greater than that of unmodified epoxy and progressively increases with filler content, from 0.28 GPa (neat resin) to the maximum value of 0.41 GPa (2 wt. percent of WC) as shown in (appendix A/ table 4.15). Indeed, homogenous dispersion is required for hard particles to acquire stress transfer and hence enhance the young modulus of nanocomposite[255]. This improvement in the modulus of elasticity of the nanocomposite is due to the nature of the hard and high elastic modulus of WC nanoparticles compared to the brittle matrix[249,260,261].

Figure 4.30 (a and b) show that the tensile strength and elastic modulus of WC/ TBCP /epoxy nanocomposites rise as the amount of tungsten carbide nanoparticles in the WC/TBCP/epoxy nanocomposite increases. As it is explained earlier, due to the good compatibility between TBCP and epoxy, the flexible chains of TBCP help the spread and good distribution of WC nanoparticles within the matrix of the nanocomposite. This helps transfer the load from particles to the matrix and reduces the occurrence of positions of stress concentrations within the material, thus increasing the tensile strength and elastic modulus.

In figure 4.30 (c), the elongation at break of WC/TBCP/epoxy nanocomposite remains almost unaffected. This is owing to the tungsten carbide particles not affecting the miscibility of TBCP with the epoxy, as well as the homogenous distribution and excellent interfacial adhesion between particles and matrix.

4.3.4.2 Fracture Toughness and impact strength results

The fracture toughness values of WC/epoxy and WC/TBCP/epoxy nanocomposites are shown in figure 4.31 are summed up in (appendix A/ table 4.16). The results show that when the concentration of WC particles goes up, so does the fracture toughness. This shows that adding WC nanoparticles to epoxy resin makes the composites stronger when they break. In the case of the neat epoxy, the fracture toughness as shown in figure 4.31 , is determined to be 1.2 MPa.√m. The maximum K_{IC} for WC/epoxy nanocomposites was observed to be 5.4 MPa.√m for the sample at 2wt% WC. Various toughening mechanisms, including crack path deflection, crack pinning, and plastic void growth, are responsible for this improvement in fracture characteristics. When WC is dispersed at the nanoscale, the degree of increase in fracture characteristics is greater

because the increase in spacing between the cross-linked chains is smaller agree with[262].

The dispersed nanoparticles cause Vander-Waal bonding between the chains and the particles, which leads to an increase in the amount of constraint between the particles and the polymer chains as well as within the polymer chains themselves[263]. However, the tendency changes with greater filler weight percentage, which may indicate agglomeration of WC particles. These agglomerates lessen the filler's homogeneity and effective volume fraction, which leads to debonding of the particles with the polymeric chain and, ultimately, to cavitation, which in turn lowers the fracture toughness of composites.

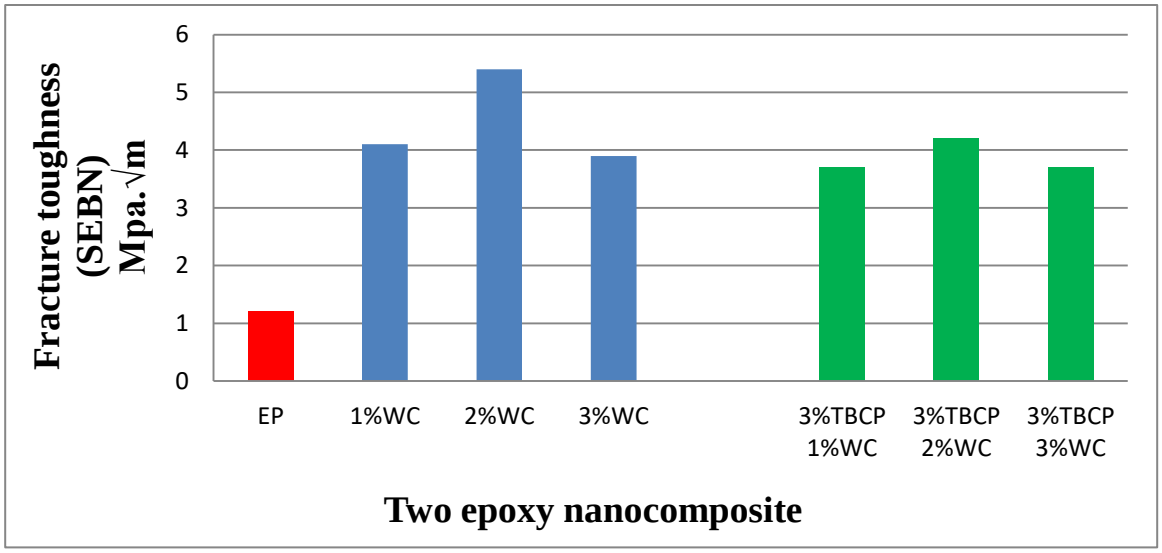

Figure 4.31 : Fracture toughness for WC/EP and WC/(3%TBCP)/EP nanocomposite

In the nanocomposite with the TBCP, the systems with WC are tougher and K_{IC} increases with increasing the WC load content. The largest value obtained is 4.2 MPa.√m at WC percentage (2%wt)compared with neat epoxy with K_{IC} having 1.2 MPa.√m, see (appendix A/ table 4.16) and figure 4.31. Higher deformation zones are likely formed due to the tougher epoxy matrix containing TBCP and WC nanoparticles than epoxy nanocomposites.

Shear, which happens between the particles and makes the samples harder to break, could also explain this zone[264]. TBCP was used to assist in stabilizing WC nanoparticles. This helped keep the dispersion that the sonication process had made, and it also made it easier for the nanoparticles to adhere to the epoxy matrix, which had an effect on the toughening mechanisms. Based on these results, we can say that the TBCP worked to improve the interface and particle/polymer adhesion in the dispersed systems, which made them very tough[255].

The increased critical stress causes and encourages shear bands to develop in the matrix (plastic deformation)as a means of dissipating the fracture energy. [265]. Nanoparticle aggregation in the WC nanocomposites likely reduced the effectiveness of the TBCP at the WC/epoxy interface. Additionally, the action of mechanisms intrinsic to the TBCP itself, rather than the effective interface enhancement, is responsible for the minor increase in toughness of the WC (3wt%)/TBCP, compare with epoxy resin samples[194].

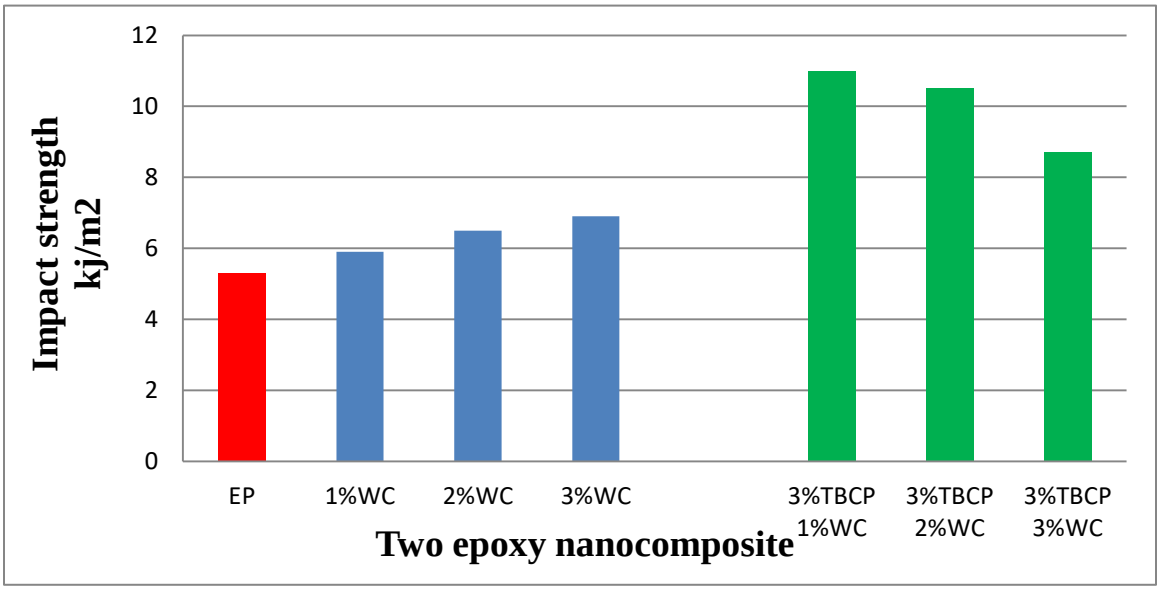

Figure 4.32 : Impact strength of WC/EP and WC /(3%TBCP)/EP nanocomposites

The introduction of WC nanofiller at 3 wt% with epoxy matrix resulted in a considerable improvement of ~30% in impact strength. Impact test results are shown in figure 4.32. When the filler loading is raised from 1% wt to 3% wt, the impact properties significantly improve. Ascribed to the outcomes, improved interfacial contact and hence bonding of nanofiller particles with the epoxy matrix to withstand high impact stress/load.

Internal damage induced by low-velocity impacts on epoxy-based composites may lead to serious safety and reliability difficulties since the resin is very brittle. Since epoxy composites are used in many high-performance applications, it is vital to enhance their ability to resist damage by increasing their impact strength. Using the second phase toughening technique, the modifier may be added as a distinct phase to solve this problem. Depending on the inclusion of an added phase[266]. This describes what has noted the impact resistance grades for nano tungsten carbide and the toughening agent (TBCP) of the composite material. Figure 4.32 show increases impact strength by approximately (107%) at 1% wt WC, and as WC concentration increases, there is a tiny drop in impact property, but it remains greater than pure epoxy. This is associated with particle-matrix adhesion and good distribution with additive TBCP. In addition, TBCP chains have a role in the plastic deformation inside the matrix, thus absorbing more impact energy, and increasing the toughness of the sample to fracture.

4.3.4.3 Hardness Test Results

The hardness of pure epoxy steadily improves with the addition of tungsten carbide content for both epoxy /WC nanocomposite and epoxy / TBCP /WC nanocomposite systems as shown in (appendix A/ table 4.16). This is because WC, as a denser and harder phase than epoxy, improves the hardness of the

composites. However, the stated increase in hardness for EP/WC composites is rather minor, amounting to roughly 5%, see figure 4.33. This enhancement in hardness corresponds to the uniform dispersion of nano WC and better matrix-to-particle interaction with and without TBCP[266,267].

In the hardness test, the indentation force is in action. Thus, the solid tungsten carbide particles and the epoxy matrix phase would be hard-pressed together and will be in contact with each other more firmly.There will be a significant transfer of pressure by the interface, resulting in a further increase in the hardness. Similar results were reported for epoxy matrix composites filled with other nano particles[154,268].

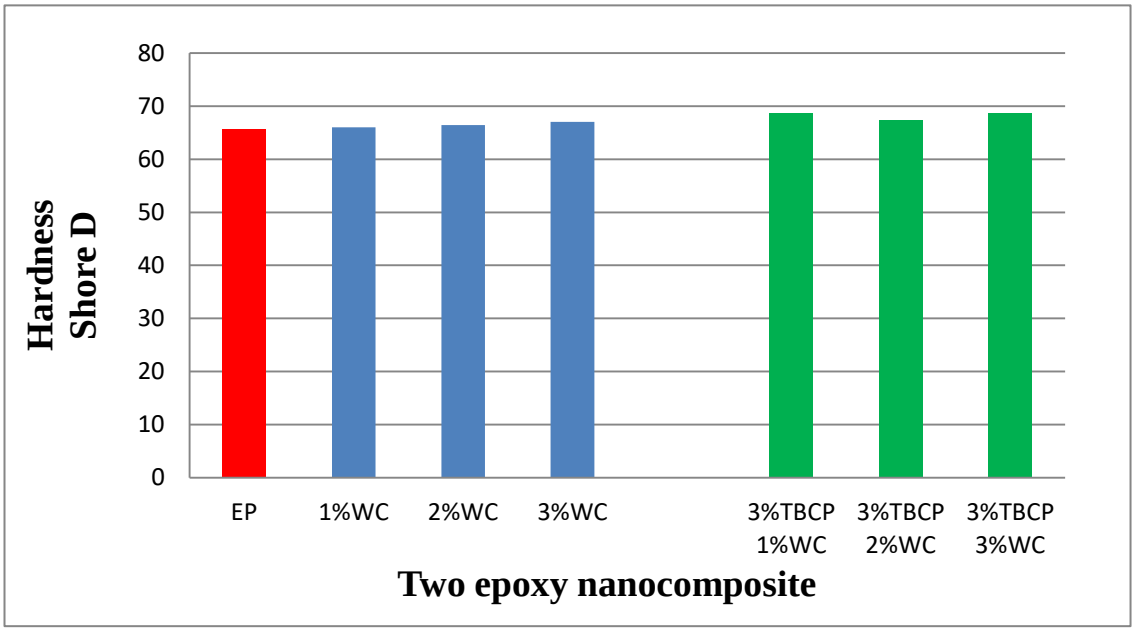

Figure 4.33: Hardness (shore D) value of WC/EP and WC/(3%TBCP)/EP

4.3.4.4 Pull-off Adhesion Result and Discussion

The results of pull off adhesion test of epoxy nanocomposites show that a higher adhesive strength is observed for the WC/EP and WC/TBCP/EP coating, respectively to the metal substrate than that of the neat epoxy coating as shown in figure 4.34 and (appendix A/ table 4.17). The

mechanical properties, chemical structure, and physical properties of the coating, as well as those of the created interface, all have a role in determining the adhesion between the coating and the substrate underneath. It is believed that internal tensions in the film and substrate, in addition to the chemistry and physics of the interface, significantly contribute to the adhesion strength. Cohesive failure, which is dependent on film characteristics, and surface failure, which occurs at the interface between the film and substrate, both contribute to the overall adhesion bond strength,as shown in figure 4.35. Adhesion is the interaction between two materials that results from the sum of their individual interactions at the atomic level (ionic, covalent, polar, and van der Waals)[269].

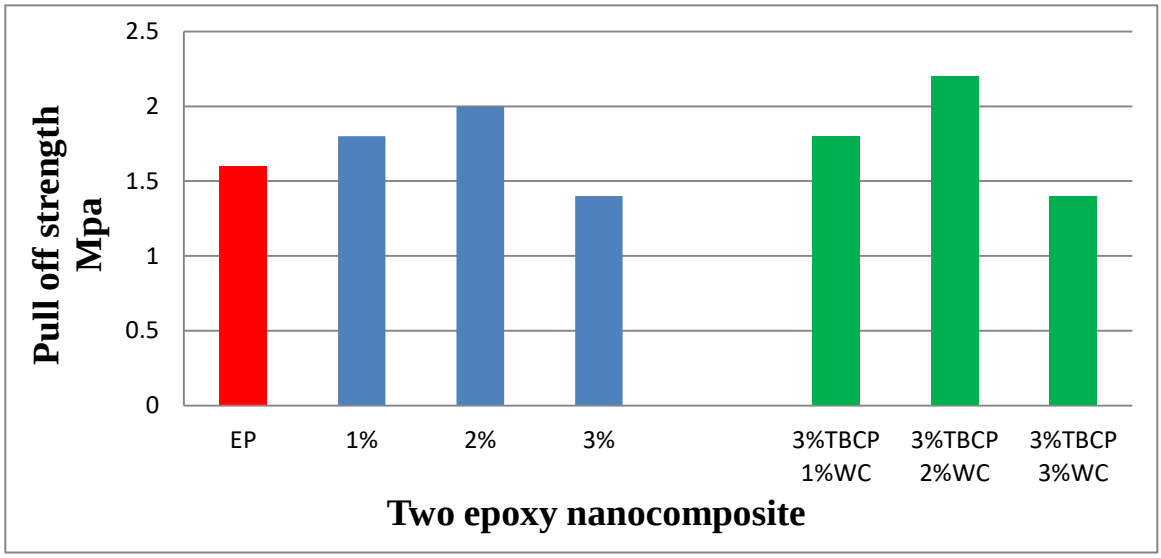

Figure 4.34: Pull off adhesion strength of WC/ EP and WC/(3%TBCP)/EP nanocomposites

The adherence of the coatings changed as the load content of nanoparticles (WC) in the epoxy matrix increased. The coatings maintained their adherence to the substrates due to the uniformly distributed of nano tungsten carbide[270].

Epoxy coating is well known as a polar coating due to the presence of aliphatic hydroxide and ether groups in its structure [271]. The mixture of epoxy resin and curing agent may completely wet the substrate because there are scratches on the substrate surface polished by sandpapers. During the curing process, the substrate surface can be wetted by the curing agent, which increases the bonding areas and improves the bond strength between the coating and substrate[272]. A rough surface has two significant effects on adhesion: it brings a higher density of secondary bonding, namely Van der Waals and hydrogen bonding, at the interface, and at the same time allows mechanical adhesion to occur as the coating liquid can flow into the porous surface of the substrate, creating effective interlocking[273,274].

Additionally, physical bonds can be created between the substrate and polymer through polymer chain penetration into these cavities and pores and thereby make some physical bonds[275]. Another adhesion mechanism involved in the polymer-metal bonding is the dispersion (i.e., van der Waals) forces [276,277].

The epoxide group or oxirane ring of the epoxy resin can also contribute to adhesion by making chemical bonds with the active surficial hydroxyl groups of the substrate. Furthermore, in the case of nonpolar sites of the epoxy, it is the dispersion forces that aid the bonding, but it has less strength compared to hydrogen bonds [238].

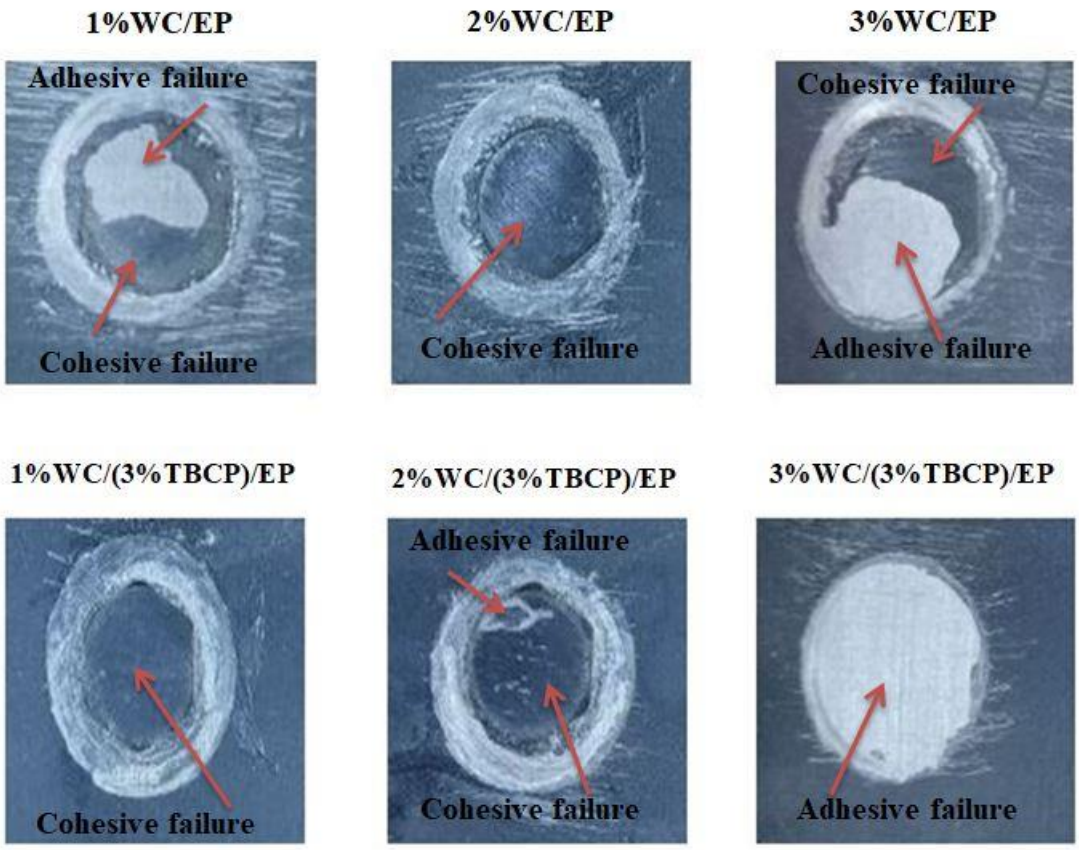

Figure 4.35: Visual inspection of samples WC/EP and WC/(3%TBCP)/EP nanocomposites after pull-off test

The adhesion for epoxy coating may be altered somewhat by the presence of evenly dispersed nanoparticles, which may affect both the adhesive's chemical and physical properties. Because of where they were located in the surface asperities of the steel, they offered more secure anchoring and hence improved adhesion. However, the chemical characteristics of nanoparticles may explain the varying degrees of improvement, as they may affect the chemical properties of the steel and epoxy coating surfaces, generate chemical interactions at the interfaces between the two, and so increase adhesion strength. Nanoparticles here were mediating between the steel and epoxy coated at the molecular level [278,279].

Where note from the results that the addition of TBCP has a role in good dispersing and distributing nanoparticles inside the epoxy matrix, but did not significantly affect the adhesion properties compared to its absence with EP/WC, which is due to the stronger effect of hard tungsten carbide particles and their stiffness in adhesion with the surface of the metal

4.3.4.5 Wear Test Result and Discussion

Pin-on-disc tribological test result for epoxy and nanocomposite samples have been presented in (appendix A/ table 4.18). After analyzing the results, it becomes clear that adding fillers to the epoxy matrix enhances the samples' wear properties. Figure 4.36 demonstrates the effect of the addition of WC nanoparticles on the wear rate of the epoxy resin. This work creates two WC/epoxy nanocomposites, as well as a WC/TBCP/epoxy nanocomposite. It has been shown that adding WC nanoparticles to epoxy reduces wear rates. The wear rate of EP decreases from $6.808*10^{-9}$ g/mm to $2.553*10^{-9}$ g/mm when WC/epoxy nanocomposite was used, while the wear rate of EP decreases considerably from $6.808*10^{-9}$ g/mm to $1.702*10^{-9}$ g/mm when WC /TBCP/EP was used. It is indicating the wear resistance of all samples is increased by employing the tungsten carbide particles. This may be connected to the fact that the hard outer layer protects the surface from intense contact. When the weight percent of WC is increased, the wear rate of the sample is low. This is owing to the epoxy may readily be removed at the contact region (sliding surfaces)but in the composite mode, the WC particles function as a rough condition compared to the counter surface across which they slide. similar with[280,281].

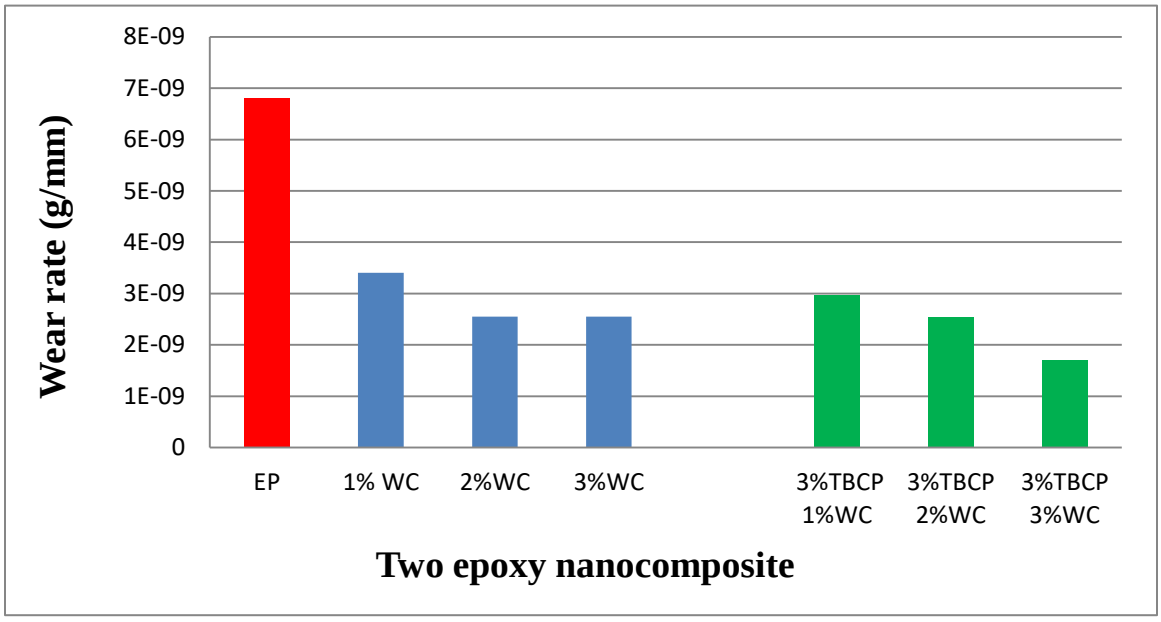

Figure 4.36: Comparison wear rate values between WC/EP and WC/(3%TBCP)/EP nanocomposites.

The inclusion of TBCP with WC particles, as previously discussed, resulted in better particle dispersion within the epoxy matrix and decreased agglomeration at high concentrations. Nanocomposites lose their well-dispersed WC and transfer it to the steel ball-nanocomposites interfacial. To prevent the steel ball from coming into touch with the nanocomposites, WC may function as spacers similar to [282]. The improved wear resistance is related to the polymer's uniform distribution of nanoparticle particles, which assists to protect the polymer[283,284]. As mentioned earlier, the addition of WC particles in the epoxy matrix led to an increase in the hardness values. Increasing the hardness of materials is associated with increased wear resistance. In other words, a material with higher hardness presents higher resistance against sliding. Therefore, increasing surface hardness of epoxy matrix by the inclusion of WC particles can be introduced as a strong reason for observed wear improvement agree with[285].

Chapter Five

Conclusion and Recommendations

Chapter Five

Conclusion and Recommendations

5.1 Conclusion

From the obtained results and their discussion in chapter four, the following conclusions can be drawn:

1.For the FT-IR toughening agent/ epoxy blends results proved, that there is no chemical reaction, and there is only physical interaction between different toughening agents and the polar epoxy polymer.

2.DSC epoxy blends results showed, that there is decreasing in the T_g value, which points to the action of toughening agent on flexibility chains and plasticizer effect

3.In SEM epoxy blends images, TBCP modified epoxy matrix which proves occurred phase separation of immiscible PEO domine on epoxy matrix . PU and LSR modified epoxy matrix which proves occurred phase separation of polyether polyol and liquid silicon rubber inside the epoxy matrix. PVC and PSR modified epoxy matrix proved that there is no phase separation inside an epoxy matrix.

4.The tensile strength and elastic modulus increase for TBCP/epoxy with the increase of TBCP content as compared to pure epoxy and other toughening agents/EP blends.

5.The fracture toughness of (TBCP/EP), (PU/EP), (LSR/EP),(PVC/EP), and (PSR/EP) blends are higher than that of unmodified epoxy polymer.

6.The impact strength of (TBCP/EP), (PU/EP), (LSR/EP),(PVC/EP), and (PSR/EP) blends are higher than that of unmodified epoxy polymer.

7.The hardness results of the toughening agent /epoxy blends showed a slight improvement or preservation of hardness compared to neat epoxy.

8.Pull-off adhesion strength of epoxy blends shows improvement when adding TBCP, PU, and PVC to the epoxy system, but when added LSR and PVC show a drop in pull-off adhesion strength and pull-off adhesion test samples show both adhesion and cohesive failure.

9.FE-SEM images for WC /epoxy and WC/ (3%wt) TBCP/EP nanocomposite showed WC nanoparticle aggregation at high load WC content (3% WC), this gave a reason for the deterioration of the mechanical properties at that ratio

10.DSC results for two WC nano composite proved, that there is increasing in the T_g value, which points to an expected improvement in mechanical properties.

11.Tensile strength and elastic modulus increase with increasing WC content for WC/EP and WC/(3%wt) TBCP /EP nanocomposite

12.Fracture toughness and impact strength for WC/EP and WC/(3%wt)TBCP /EP nanocomposite increase with increasing WC content as compared to neat epoxy.

13.Pull-off adhesion strength shows improvement when adding WC to the epoxy system with present TBCP or not.

14.Wear rate of WC/(3%wt) TBCP/EP nanocomposite lower than WC/EP nanocomposites with the increase in the content of WC nanoparticles

5.2 Recommendations

1. Using binary toughening agent with epoxy matrix

2. Studying other tests such as corrosion resistance of coating epoxy nanocomposites

3. Using another substrate like aluminum.

4. Studying the wear rate in wet conditions for WC/EP and WC/TBCP/EP nanocomposites.

5. Using hybrid nanocomposites like TiC, and SiC with WC nanoparticles

Reference:-

[1] S. A. Bello, J. O. Agunsoye, S. B. Hassan, M. G. Z. Kana, and I. A. Raheem, "Epoxy resin based composites, mechanical and tribological properties: A review," *Tribol. Ind.*, vol. 37, no. 4, pp. 500–524, 2015.

[2] J. Bhadra, A. Alkareem, and N. Al-Thani, "A review of advances in the preparation and application of polyaniline based thermoset blends and composites," *J. Polym. Res.*, vol. 27, no. 5, 2020, doi: 10.1007/s10965-020-02052-1.

[3] D. Gunwant, P. L. Sah, and M. G. H. Zaidi, "Morphology and micromechanics of liquid rubber toughened epoxies," *E-Polymers*, vol. 18, no. 6, pp. 511–527, 2018, doi: 10.1515/epoly-2018-0141.

[4] F. Pakaya, H. Ardhyananta, and S. T. Wicaksono, "Mechanical Properties and Thermal Stability of Epoxy/RTV Silicone Rubber," *IPTEK J. Technol. Sci.*, vol. 28, no. 1, p. 7, 2017, doi: 10.12962/j20882033.v28i1.2216.

[5] H. N. Minh, "Epoxy/Titanate Modified Nanosilica Composites: Morphology, Mechanical Properties and Fracture Toughness," *Vietnam J. Sci. Technol.*, vol. 56, no. 2A, pp. 133–140, 2018, doi: 10.15625/2525-2518/56/2a/12641.

[6] A. J. Hsieh, T. H. , Kinloch, A. C. and Taylor, and S. Sprenger, "The Effect of Silica Nanoparticles and Carbon Nanotubes on the Toughness of a Thermosetting Epoxy Polymer," *J. Appl. Polym. Sci.*, vol. 119, pp. 2135–2142, 2010, doi: 10.1002/app.

[7] Y. Hua, L. Gu, S. Premaraj, and X. Zhang, "Role of interphase in the mechanical behavior of silica/epoxy resin nanocomposites," *Materials (Basel).*, vol. 8, no. 6, pp. 3519–3531, 2015, doi: 10.3390/ma8063519.

[8] H. N. Minh, N. T. Chinh, T. T. T. Van, D. X. Thang, and T. Hoang, "Characteristics and Morphology of Nanosilica Modified with Isopropyl Tri(dioctyl Phosphate) Titanate Coupling Agent," *J. Nanosci. Nanotechnol.*, vol. 18, no. 5, pp. 3624–3630, 2017, doi: 10.1166/jnn.2018.14854.

[9] F. L. Jin, X. Li, and S. J. Park, "Synthesis and application of epoxy resins: A review," *J. Ind. Eng. Chem.*, vol. 29, pp. 1–11, 2015, doi: 10.1016/j.jiec.2015.03.026.

[10] D. Carolan, A. Ivankovic, A. J. Kinloch, S. Sprenger, and A. C.

Taylor, “Toughened carbon fibre-reinforced polymer composites with nanoparticle-modified epoxy matrices,” *J. Mater. Sci.*, vol. 52, no. 3, pp. 1767–1788, 2017, doi: 10.1007/s10853-016-0468-5.

[11] T. J. Gutiérrez, *Reactive and Functional Polymers Volume Four*. Book: Springer, 2020.

[12] H. Münstedt, *Rheological and Morphological Properties of Dispersed Polymeric Materials*. Book: Hanser Publishers, 2016.

[13] G. Luciano, A. Brinkmann, S. Mahanty, and M. Echeverría, “Development and evaluation of an eco-friendly hybrid epoxy-silicon coating for the corrosion protection of aluminium alloys,” *Prog. Org. Coatings*, vol. 110, no. July 2016, pp. 78–85, 2017, doi: 10.1016/j.porgcoat.2017.04.028.

[14] S. Pourhashem, M. R. Vaezi, A. Rashidi, and M. R. Bagherzadeh, “Exploring corrosion protection properties of solvent based epoxy-graphene oxide nanocomposite coatings on mild steel,” *Corros. Sci.*, vol. 115, pp. 78–92, 2017, doi: 10.1016/j.corsci.2016.11.008.

[15] Z. Mahidashti, B. Ramezanzadeh, and G. Bahlakeh, “Screening the effect of chemical treatment of steel substrate by a composite cerium-lanthanum nanofilm on the adhesion and corrosion protection properties of a polyamide-cured epoxy coating; Experimental and molecular dynamic simulations,” *Prog. Org. Coatings*, vol. 114, no. October 2017, pp. 188–200, 2018, doi: 10.1016/j.porgcoat.2017.10.020.

[16] S. J. O. Dagdag , A. El Harfi , A. Essamri, M. El Gouri , S. Chraibi, M. Assouag , B. Benzidia , O. Hamed , H. Lgaz, “Phosphorous-based epoxy resin composition as an effective anticorrosive coating for steel,” *Int. J. Ind. Chem.*, vol. 9, no. 3, pp. 231–240, 2018, doi: 10.1007/s40090-018-0152-5.

[17] C. C. Matthews, “Autonomous Indication of Damage in Epoxy Coatings By,” 2015.

[18] K. K. Muna Ibrahim, O. S. , Hemalatha Parangusan, Shady Eldeib, and R. Z. and K. K. S. Mohammad Ismail, “Enhanced corrosion protection of Epoxy/ZnO-NiO nanocomposite coatings on steel,” *Coatings*, vol. 10, no. 8, 2020, doi: 10.3390/COATINGS10080783.

[19] S. Mohapatra, S. Mantry, and S. K. Singh, “Performance Evaluation of Glass-Epoxy-TiC Hybrid Composites Using Design of Experiment,” *J.*

Compos., vol. 2014, pp. 1–9, 2014, doi: 10.1155/2014/670659.

[20] K. Friedrich and A. K. Schlarb, *Tribology of Polymeric Nanocomposites*. 2008.

[21] A. M. Tomuta, "New and Improved Thermosets Based on Epoxy Resins and Dendritic Polyesters," 2013.

[22] E. J. Barbero, *Introduction to Composite Materials Design*, Third Ed. Taylor & Francis Group, LLC, 2018.

[23] S.-J. P. c Fan-Long Jin , Xiang Li, "Synthesis and application of epoxy resins: A review," *J. Ind. Eng. Chem.*, vol. 29, pp. 1–11, 2015, [Online]. Available: http://dx.doi.org/10.1016/j.jiec.2015.03.026.

[24] S. I. Owuamanam, "Fabrication and Characterization of Bio-Epoxy Eggshell Composites," 2019.

[25] A. B. and B. Wetzel, "Toughening and Mechanical Properties of Epoxy Modified with Block Co-Polymers and Titanium Dioxide Nanoparticles," *ECCM17 - 17th Eur. Conf. Compos. Mater.*, 2016, doi: 10.1016/j.prostr.2016.06.014.

[26] G. Kortaberria and A. Tercjak, *Block Copolymer Nanocomposites*. 2017.

[27] C. A. Gorostiza, "Hyperbranched poly((ethyleneimine) derivatives as modifiers in epoxy networks," 2016.

[28] I. M. McAninch, "Molecular Toughening of Epoxy Networks," 2014.

[29] Y. Tong, "Application of New Materials in Sports Equipment," *IOP Conf. Ser. Mater. Sci. Eng.*, vol. 493, no. 1, 2019, doi: 10.1088/1757-899X/493/1/012112.

[30] T. Vidil, F. Tournilhac, S. Musso, A. Robisson, and L. Leibler, "Control of reactions and network structures of epoxy thermosets," *Prog. Polym. Sci.*, vol. 62, pp. 126–179, 2016, doi: 10.1016/j.progpolymsci.2016.06.003.

[31] G. Poynton, "Multi - component Epoxy Resin Formulation for High Temperature Applications," 2014.

[32] F. Ferdosian, "Synthesis, Characterization and Applications of Lignin-Based Epoxy Resins," 2015.

[33] D. Galpaya, "Synthesis, Characterization and Application of

Graphene-Oxide Polymer Composites," 2015.

[34] D. Haba, "Toughening of epoxy with WS2 nanoparticles," Thesis, 2016.

[35] S. S. Ray, *Processing of Polymer-based Nanocomposites*. Book, 2018.

[36] H. Dodiuk and S. H. Goodman, *Handbook of Thermoset Plastics*, Third Edit. BOOK, 2014.

[37] D. B. Elvers, *Ullmann's Polymers and Plastics*. Book: Wiley-VCH, 2016.

[38] R. R. M. Dornbusch, U. Christ, *Epoxy Resins Fundamentals and Applications*. Book, 2016.

[39] A. Gergely, T. Bertoti, Imre, Torok, and E. Pfeifer, Eva, Kalman, "Corrosion protection with zinc-rich epoxy paint coatings embedded with various amounts of highly dispersed polypyrrole-deposited alumina monohydrate particles," *Prog. Org. Coatings*, vol. 76, no. 1, pp. 17–32, 2013, doi: https://doi.org/10.1016/j.porgcoat.2012.08.005.

[40] M. N. Katariya, A. K. Jana, and P. A. Parikh, "Corrosion inhibition effectiveness of zeolite ZSM-5 coating on mild steel against various organic acids and its antimicrobial activity," *J. Ind. Eng. Chem.*, vol. 19, no. 1, pp. 286–291, 2013, doi: 10.1016/j.jiec.2012.08.013.

[41] Y. Hao, F. Liu, and E. H. Han, "Protection of epoxy coatings containing polyaniline modified ultra-short glass fibers," *Prog. Org. Coatings*, vol. 76, no. 4, pp. 571–580, 2013, doi: 10.1016/j.porgcoat.2012.11.012.

[42] Z. Ahmadi, "Nanostructured epoxy adhesives: A review," *Prog. Org. Coatings*, vol. 135, no. March, pp. 449–453, 2019, doi: 10.1016/j.porgcoat.2019.06.028.

[43] H. Jin *et al.*, "Fracture behavior of a self-healing, toughened epoxy adhesive," *Int. J. Adhes. Adhes.*, vol. 44, pp. 157–165, 2013, doi: 10.1016/j.ijadhadh.2013.02.015.

[44] A. Kaboorani and B. Riedl, "Nano-aluminum oxide as a reinforcing material for thermoplastic adhesives," *J. Ind. Eng. Chem.*, vol. 18, no. 3, pp. 1076–1081, 2012, doi: 10.1016/j.jiec.2011.12.001.

[45] Y. Liu, G. Yang, H. M. Xiao, Q. P. Feng, and S. Y. Fu, "Mechanical properties of cryogenic epoxy adhesives: Effects of mixed curing agent

content," *Int. J. Adhes. Adhes.*, vol. 41, pp. 113–118, 2013, doi: 10.1016/j.ijadhadh.2012.10.006.

[46] H. V. Nguyen, E. Andreassen, H. Kristiansen, R. Johannessen, N. Hoivik, and K. E. Aasmundtveit, "Rheological characterization of a novel isotropic conductive adhesive - Epoxy filled with metal-coated polymer spheres," *Mater. Des.*, vol. 46, pp. 784–793, 2013, doi: 10.1016/j.matdes.2012.11.036.

[47] C. H. Park, S. W. Lee, J. W. Park, and H. J. Kim, "React," *Funct. Polym*, vol. 73, pp. 641–646, 2013.

[48] S. M. Ali, "Ultrasonic and thermo- kinetic characterization of curing epoxy resin .," 2013.

[49] P. Ghosh, *Polymer Science and Technology Plastics, Rubbers, Blends and Composites*, Third Edit. 2011.

[50] Y. G. S. Thomas and and P. Jyotishkumar, *Characterization of Polymer Blends*, First Edit., vol. 9783527331. Wiley-VCH Verlag GmbH & Co. KGaA., 2015.

[51] L. A. Utracki, "Introduction to polymer blends," *Polym. blends Handb.*, p. 1, 2003.

[52] J. L. White and S. H. Bumm, "Polymer blend compounding and processing," *Encycl. Polym. blends*, vol. 2, pp. 1–26, 2011.

[53] J. R. Fried, *Polymer Science and Technology*, Third Edit. 2014.

[54] B. Crist, "Yield processes in glassy polymers," in *The physics of glassy polymers*, Springer, 1997, pp. 155–212.

[55] A. Bajpai, "Modification of Epoxy Systems for Mechanical Performance Improvement," no. December, p. 28, 2017.

[56] R. Wazalwar, M. Sahu, and A. M. Raichur, "Mechanical properties of aerospace epoxy composites reinforced with 2D nano-fillers: current status and road to industrialization," *Nanoscale Adv.*, vol. 3, no. 10, pp. 2741–2776, 2021, doi: 10.1039/d1na00050k.

[57] A. Zotti, S. Zuppolini, A. Borriello, and M. Zarrelli, "Thermal properties and fracture toughness of epoxy nanocomposites loaded with hyperbranched-polymers-based core/shell nanoparticles," *Nanomaterials*, vol. 9, no. 3, 2019, doi: 10.3390/nano9030418.

[58] N. K. Aparna Thankappan, S. Thomas, and A. Padinjakkara, *Polymeric and Nanostructured Materials*. 2019.

[59] G. Giannakopoulos, K. Masania, and A. C. Taylor, "Toughening of epoxy using core-shell particles," *J. Mater. Sci.*, vol. 46, no. 2, pp. 327–338, 2011, doi: 10.1007/s10853-010-4816-6.

[60] J. Parameswaranpillai, N. Hameed, J. Pionteck, and E. M. Woo, *Handbook of epoxy blends*. 2017.

[61] M. Mehrabi-Kooshki and A. Jalali-Arani, "Preparation of binary and hybrid epoxy nanocomposites containing graphene oxide and rubber nanoparticles: Fracture toughness and mechanical properties," *J. Appl. Polym. Sci.*, vol. 136, no. 4, pp. 1–9, 2018, doi: 10.1002/app.46988.

[62] B. B. Johnsen, A. J. Kinloch, R. D. Mohammed, A. C. Taylor, and S. Sprenger, "Toughening mechanisms of nanoparticle-modified epoxy polymers," *Polymer (Guildf).*, vol. 48, no. 2, pp. 530–541, 2007, doi: 10.1016/j.polymer.2006.11.038.

[63] M. J. Mullins, D. Liu, and H. J. Sue, *Mechanical properties of thermosets*, 2nd ed. Elsevier Ltd., 2018.

[64] M. Kutz, *Handbook of Measurement in Science and Engineering*, Volume 2. Hoboken, New Jersey Published: John Wiley & Sons, Inc., 2013.

[65] T. S. Velayutham, "Physical Characterization of Oleic Acid Polyol Based Polyurethane Coatings," 2009.

[66] J. Karl Fink, *Reactive Polymers Fundamentals and Applications*, Third edit. Elsevier Inc., 2018.

[67] S. Rattanapan, "Preparation and Properties of Bio-Based Polyurethane Foam Prepared from Modified Natural Rubber and Preparation and Properties of Bio-Based Polyurethane Foam Prepared from Modified Natural Rubber and Poly(ϵ-caprolactone) from Modified Natural Rubber and P," 2016.

[68] A. B. B. Saleh, Z. A. M. Ishak, A. S. Hashim, W. A. Kamil, and U. S. Ishiaku, "Synthesis and characterization of liquid natural rubber as impact modifier for epoxy resin," *Phys. Procedia*, vol. 55, pp. 129–137, 2014, doi: 10.1016/j.phpro.2014.07.019.

[69] S. T. R. Thomas, A. Boudenne, L. Ibos, Y. Candau, "Thermophysical

Properties of CTBN and HTPB Liquid Rubber Modified Epoxy Blends," *J. Appl. Polym. Sci.*, vol. 116, no. 5, pp. 3232–3241, 2010, doi: 10.1002/app.

[70] S. Xu, *Handbook of Epoxy Blends "Miscibility and Phase Separation of Epoxy/ Rubber Blends."* DOI 10.1007/978-3-319-18158-5_3-1: Book, 2015.

[71] P. P. Vijayan, D. Puglia, P. Jyotishkumar, J. M. Kenny, and S. Thomas, "Effect of nanoclay and carboxyl-terminated (butadiene-coacrylonitrile) (CTBN) rubber on the reaction induced phase separation and cure kinetics of an epoxy/cyclic anhydride system," *J. Mater. Sci.*, vol. 47, no. 13, pp. 5241–5253, 2012, doi: 10.1007/s10853-012-6409-z.

[72] W. Chonkaew, N. Sombatsompop, and W. Brostow, "High impact strength and low wear of epoxy modified by a combination of liquid carboxyl terminated poly(butadiene-co-acrylonitrile) rubber and organoclay," *Eur. Polym. J.*, vol. 49, no. 6, pp. 1461–1470, 2013, doi: 10.1016/j.eurpolymj.2013.03.022.

[73] R. Thomas, J. Abraham, S. Thomas P, and S. Thomas, "Influence of carboxyl-terminated (butadiene-co-acrylonitrile) loading on the mechanical and thermal properties of cured epoxy blends," *J. Polym. Sci. Part B Polym. Phys.*, vol. 42, no. 13, pp. 2531–2544, 2004, doi: 10.1002/polb.20115.

[74] S. Xu, X. Song, and Y. Cai, "Mechanical properties and morphologies of carboxyl-terminated butadiene acrylonitrile liquid rubber/epoxy blends compatibilized by pre-crosslinking," *Materials (Basel).*, vol. 9, no. 8, 2016, doi: 10.3390/ma9080640.

[75] A. B. Cherian, L. A. Varghese, and E. T. Thachil, "Epoxy-modified, unsaturated polyester hybrid networks," *Eur. Polym. J.*, vol. 43, no. 4, pp. 1460–1469, 2007, doi: 10.1016/j.eurpolymj.2006.12.041.

[76] S. Thomas, C. Sinturel, and R. Thomas, *Micro- and Nanostructured Epoxy/Rubber Blends*. 2014.

[77] S. Bietto, "Nano-fifilled Epoxy: Mechanical and Fire Behavior and Modeling of Nanocomposite Columns Under Fire," 2007.

[78] M. Rahmandoust and M. R. Ayatollahi, *Erratum to: Characterization of Carbon Nanotube-Based Composites Under Consideration of Defects*. 2016.

[79] I. S. Pramendra K. Bajpai, *Reinforced Polymer Composites*, vol. 53, no. 9. Wiley-VCH, 2020.

[80] A. Bhat *et al.*, "Review on nanocomposites based on aerospace applications," *Nanotechnol. Rev.*, vol. 10, no. 1, pp. 237–253, 2021, doi: 10.1515/ntrev-2021-0018.

[81] R. Konnola, "Toughened Epoxy Nano composites Based on Surface Engineered Department of Chemistry," 2016.

[82] M. V. de V. Elisabeth Mansfiel, Debra L. Kaiser, Daisuke Fujita, *Metrology and Standardization for Nanotechnology*. Wiley-VCH, 2017.

[83] V. Mittal, *Polymer Nanocomposite Coatings*. Taylor & Francis Group, LLC, 2014.

[84] A. S. Thakur, N. Sharma, S. Kango, and S. Sharma, "Effect of nanoparticles on epoxy based composites: A short review," *Mater. Today Proc.*, vol. 44, pp. 4640–4642, 2021, doi: 10.1016/j.matpr.2020.10.924.

[85] A. J. Vivek T. Rathod, Jayanth S. Kumar, "Polymer and ceramic nanocomposites for aerospace applications," *Appl. Nanosci.*, vol. 7, no. 8, pp. 519–548, 2017, doi: 10.1007/s13204-017-0592-9.

[86] M. Z. Rong, M. Q. Zhang, and W. H. Ruan, "Surface modification of nanoscale fillers for improving properties of polymer nanocomposites: A review," *Mater. Sci. Technol.*, vol. 22, no. 7, pp. 787–796, 2006, doi: 10.1179/174328406X101247.

[87] Faisal Aldawsari, "Influence of interface on the electrical properties of silicone nanocomposites," 2018.

[88] Chunxia Sun, "Controlling the rheology of polymer / silica nanocomposites," 2010.

[89] Jiongxin Lu, "High Dielectric Constant Polymer Nanocomposites for Embedded Capacitor Applications," *Mater. Sci.*, no. December, 2008.

[90] P. M. Ajayan, L. S. Schadler, and P. V Braun, *Nanocomposite Science and Technology*. 2003.

[91] C. F. Jasso-Gastinel and J. M. Kenny, *Modification of Polymer Properties*. 2017.

[92] E. V. Polyakov, V. N. Krasil'nikov, A. P. Tyutyunnik, N. A. Khlebnikov, and G. P. Shveikin, "Precursor-based synthesis of nanosized tungsten carbide WC and WC:nCo nanocomposites," *Dokl. Phys. Chem.*, vol. 457, no. 1, pp. 104–107, 2014, doi: 10.1134/S0012501614070033.

[93] K. K. Chawla, *Composite Materials*, Third Edit., vol. 263. 2013.

[94] J. Townsend, "Fabrication and Characterization of Silicon Carbide Epoxy Composites," 2017.

[95] A. Dasari and J. Njuguna, *Functional and Physical Properties of Polymer Nanocomposites*. 2016.

[96] J. H. Koo, *Polymer nanocomposite processing, characterization, and applications*. The McGraw-Hill Companies, 2006.

[97] B. J. P. Dewangan and M. N. Yenkie, *Novel Applications in Polymers and Waste Management*. 2018.

[98] L. Z. Xiao-Su Yi, Shanyi Du, *Composite Materials Engineering, Volume 2*, vol. 2. 2018.

[99] H. Gu *et al.*, "An overview of multifunctional epoxy nanocomposites," *J. Mater. Chem. C*, vol. 4, no. 25, pp. 5890–5906, 2016, doi: 10.1039/c6tc01210h.

[100] S. A. O. Visakh P.M, *High Performance Polymers and Their Nanocomposites*. 2019.

[101] A. Chatterjee and M. S. Islam, "Fabrication and characterization of TiO2-epoxy nanocomposite," *Mater. Sci. Eng. A*, vol. 487, no. 1–2, pp. 574–585, 2008, doi: 10.1016/j.msea.2007.11.052.

[102] A. T. Maider Larran˜ aga, Elena Serrano, Maria Dolores Martin, C. C. R. and Galder Kortaberria, Koro de la Caba, and I. aki Mondragon, "Mechanical properties–morphology relationships in nano-/microstructured epoxy matrices modified with PEO–PPO–PEO block copolymers," *Polym Int*, vol. 56, no. April, pp. 1392–1403, 2007, doi: 10.1002/pi.

[103] A. K. N. Arundhati, Reena Singhal, "Effect of polysulfide modifier on mechanical and morphological properties of epoxy / phthalic anhydride system," vol. 13, no. January, pp. 193–204, 2010.

[104] W. Zhou and J. Cai, "Mechanical and Dielectric Properties of Epoxy

Resin Modified Using Reactive Liquid Rubber (HTPB)," *J. Appl. Polym. Sci.*, vol. 124, pp. 4346–4351, 2011, doi: 10.1002/app.

[105] S. Rahman, Muhammad M., Hosur, Mahesh, Ludwick, Adriane G., Zainuddin, Shaik, Kumar, Ashok, Trovillion, Jonathan, Jeelani, "Thermo-mechanical behavior of epoxy composites modified with reactive polyol diluent and randomly-oriented amino-functionalized multi-walled carbon nanotubes," *Polym. Test.*, vol. 31, no. 6, pp. 777–784, 2012, doi: 10.1016/j.polymertesting.2012.05.006.

[106] H. Lützen, P. Bitomsky, K. Rezwan, and A. Hartwig, "Partially crystalline polyols lead to morphology changes and improved mechanical properties of cationically polymerized epoxy resins," *Eur. Polym. J.*, vol. 49, no. 1, pp. 167–176, 2013, doi: 10.1016/j.eurpolymj.2012.10.015.

[107] S. M. George, D. Puglia, J. M. Kenny, J. Parameswaranpillai, and S. Thomas, "Reaction-induced phase separation and thermomechanical properties in epoxidized Styrene- block -butadiene- block -styrene triblock copolymer modified epoxy/DDM system," *Ind. Eng. Chem. Res.*, vol. 53, no. 17, pp. 6941–6950, 2014, doi: 10.1021/ie404124b.

[108] K. C. Jajam, M. M. Rahman, M. V. Hosur, and H. V. Tippur, "Fracture behavior of epoxy nanocomposites modified with polyol diluent and amino-functionalized multi-walled carbon nanotubes: A loading rate study," *Compos. Part A Appl. Sci. Manuf.*, vol. 59, pp. 57–69, 2014, doi: 10.1016/j.compositesa.2013.12.014.

[109] J. Abenojar, J. Tutor, Y. Ballesteros, J. C. Real, and M. A. Martínez, "Wear and cavitation effect in an epoxy filled with boron and silicon nanocarbides," *Int. J. Fract. Fatigue Wear*, vol. 3, pp. 167–173, 2015.

[110] F. Wang, L. T. Drzal, Y. Qin, and Z. Huang, "Enhancement of fracture toughness, mechanical and thermal properties of rubber/epoxy composites by incorporation of graphene nanoplatelets," *Compos. Part A Appl. Sci. Manuf.*, vol. 87, pp. 10–22, 2016, doi: 10.1016/j.compositesa.2016.04.009.

[111] M. N. G. Chanshetti and M. A. S. Pol, "Wear Behavior of TiO 2 and WC Reinforced Epoxy Resin Composites," pp. 2342–2346, 2016.

[112] W. Dong, Lina, Zhou, Z. Sui, Xuezhen, Wang, and X. Wu, Peng, Zuo, Jing, Cai, Huiwu, Liu, "Thermal, mechanical, and dielectric properties of epoxy resin modified using carboxyl-terminated polybutadiene

liquid rubber," *J. Elastomers Plast.*, vol. 49, no. 4, pp. 281–297, 2017, doi: 10.1177/0095244316653261.

[113] M. T. Mohamed, "Toughening of Epoxy Polysulfide Binary Blend Composite," vol. 11, no. 2, pp. 79–83, 2018, doi: 10.26367/DJES/VOL.11/NO.2/11.

[114] Y. Sun, Zeyu, Xu, Lei, Chen, Zhengguo, Wang, Yuhao, Tusiime, Rogers, Cheng, Chao, Zhou, Shuai, Liu and H. Yu, Muhuo, Zhang, "Enhancing the mechanical and thermal properties of epoxy resin via blending with thermoplastic polysulfone," *Polymers (Basel).*, vol. 11, no. 3, 2019, doi: 10.3390/polym11030461.

[115] A. J. Farhan and H. I. Jaffer, "Effect of RTV Silicon Rubber on Some Mechanical Properties of Epoxy/Polyester Polymer Blends," *IOP Conf. Ser. Mater. Sci. Eng.*, vol. 757, no. 1, 2020, doi: 10.1088/1757-899X/757/1/012037.

[116] M. K. Reddy, V. S. Babu, and K. V. S. Srinadh, "Micro hardness and erosive wear behavior of tungsten carbide filled epoxy polymer nano composites," *Int. J. Math. Eng. Manag. Sci.*, vol. 5, no. 3, pp. 405–415, 2020, doi: 10.33889/IJMEMS.2020.5.3.034.

[117] V. Gavrish, T. Chayka, A. Oleynik, and O. Gavrish, "Tungsten Carbide Nanopowder Influence Study on Tensile Strength of GRP Specimens Made of Lavesan Glass Fabric and EPR 320 Momentive Epoxy," *J. Phys. Conf. Ser.*, vol. 1891, no. 1, 2021, doi: 10.1088/1742-6596/1891/1/012031.

[118] Company data sheet, "Epoxy Sikadur 52 (TR Produced),." .

[119] D. Chemicals, "The Material Science Company." [Online]. Available: https://www.dow.com/en-us.

[120] Sigma Aldrich Company, "'Sigma Aldrich, UK ." [Online]. Available:, [Online]. Available: www.sigmaaldrich.com/United-Kingdom.

[121] Zoalfokkar Kareem Mezaal Al-obad, "Designing PU Resins for Fibre Composite Applications," 2017.

[122] L. Shenzhen Hong Ye Jie Technology Co., "YE Jie - hong." Shenzhen,China.", [Online]. Available: www.szrl.net/index.html.

[123] Annual Book of ASTM Standard, "Standard Practice for General

techniques for Obtaining Infrared Spectra for Qualitative Analysis." E 1252-98, PP.(1-11), 2002.

[124] Annual Book of ASTM Standard, "Standard Test Method for Transition Temperatures of Polymers by Differential Scanning Calorimetry." D 3418-03, PP. (1-6), (2003).

[125] P. B. Raja, K. R. Munusamy, V. Perumal, and M. N. M. Ibrahim, "Characterization of nanomaterial used in nanobioremediation:in Nano-Bioremediation : Fundamentals and Applications," *Nano-Bioremediation: Fundamentals and Applications*. pp. 57–83, 2022, doi: 10.1016/B978-0-12-823962-9.00037-4.

[126] Annual Book of ASTM Standard, "ASTM D638: Standard Test Method for Tensile Properties of Plastics," *ASTM Stand.*, no. January, pp. 1–15, 2003.

[127] Annual Book of ISO Standard, "Iso 179-2," vol. 1997, 1997.

[128] M. N. O. Ashoor, "Characterization of Biomaterials and Structural Analysis of a Knee Joint Replacement Applications," 2020.

[129] S. M. Hashim and W. B. Salih, "Study of effect reinforcement by coconut fiber on some mechanical and physical properties of thermoset polymer," *IOP Conf. Ser. Mater. Sci. Eng.*, vol. 757, no. 1, 2020, doi: 10.1088/1757-899X/757/1/012020.

[130] Annual Book of ASTM Standard, "Rubber Property—Durometer HardnesMaterials, E. I., Manufacturing, C. B., Hardness, D., & Laboratories, C. (2017). Rubber Property—Durometer Hardness 1Methods, S. T. (2008). Standard Test Methods for Rubber Property — Compression Set 1, i(Reapproved), 1–6.," *Astm D 2240*, pp. 1–13, 2015, doi: 10.1520/D2240-15.2.

[131] Annual Book of ASTM Standard, "Standard Test Methods for Plane-Strain Fracture Toughness and Strain Energy Release Rate of Plastic Materials," *Annu. B. ASTM Stand.*, vol. 99, no. Reapproved, pp. 1–9, 2014, doi: 10.1520/D5045-99R07E01.2.

[132] Annual Book of ASTM Standard, "D4541-09: Standard Test Method for Pull-Off Strength of Coatings Using Portable Adhesion," *ASTM Int.*, pp. 1–16, 2009, doi: 10.1520/D4541-09E01.2.

[133] Annual Book of ASTM Standard, "ASTM G99-17, Standard Test Method for Wear Testing with a Pin-on-Disk Apparatus," *Annu. B.*

ASTM Stand., vol. 05, no. 2016, pp. 1–6, 2020, doi: 10.1520/G0099-17.Copyright.

[134] D. Dowson, "The History of Tribology." Longman, London, 1978.

[135] H. M. Sadiq, "Preparation of Hybrid Composite from Polymer Blends and Natural Nanoparticles Used in Dentures Fabrication," 2020.

[136] H. Shinzawa, T. Uchimaru, J. Mizukado, and S. G. Kazarian, "Non-equilibrium behavior of polyethylene glycol (PEG)/polypropylene glycol (PPG) mixture studied by Fourier transform infrared (FTIR) spectroscopy," *Vib. Spectrosc.*, vol. 88, pp. 49–55, 2017, doi: 10.1016/j.vibspec.2016.11.001.

[137] C. V. Teixeira, Y. Alencar Marques, M. Carvalho de Abreu Fantini, D. da Rocha Santos Bittencourt, and C. L. Pinto Oliveira, "Structural Investigation of Diol and Triol Poly(oxypropylene)-Poly(oxyethylene) Block Copolymers Micelles: Composition Dependence, Temperature Response and Clouding Behavior," *J. Surfactants Deterg.*, vol. 24, no. 5, pp. 783–800, 2021, doi: 10.1002/jsde.12494.

[138] M. A. Alaa, K. Yusoh, and S. F. Hasany, "Synthesis and characterization of polyurethane–organoclay nanocomposites based on renewable castor oil polyols," *Polym. Bull.*, vol. 72, no. 1, pp. 1–17, 2015, doi: 10.1007/s00289-014-1255-6.

[139] J. Datta, P. Kosiorek, and M. Włoch, "Synthesis, structure and properties of poly(ether-urethane)s synthesized using a tri-functional oxypropylated glycerol as a polyol," *J. Therm. Anal. Calorim.*, vol. 128, no. 1, pp. 155–167, 2017, doi: 10.1007/s10973-016-5928-2.

[140] M. Fuensanta and J. M. Martín-Martínez, "Viscoelastic and Adhesion Properties of New Poly(Ether-Urethane) Pressure-Sensitive Adhesives," *Front. Mech. Eng.*, vol. 6, no. June, pp. 1–10, 2020, doi: 10.3389/fmech.2020.00034.

[141] C. M. Patel, A. A. Barot, and V. Kumar Sinha, "Sequential liquefaction of Nicotiana tabacum stems biomass by crude polyhydric alcohols for the production of polyols and rigid polyurethane foams," *J. Appl. Polym. Sci.*, vol. 133, no. 38, 2016, doi: 10.1002/app.43974.

[142] S. Hassanajili and M. T. Sajedi, "Fumed silica/polyurethane nanocomposites: effect of silica concentration and its surface modification on rheology and mechanical properties," *Iran. Polym. J. (English Ed.*, vol. 25, no. 8, pp. 697–710, 2016, doi: 10.1007/s13726-

016-0458-0.

[143] X. Wu, Y. Liu, Q. Yang, S. Wang, G. Hu, and C. Xiong, "Properties of gel polymer electrolytes based on poly(butyl acrylate) semi-interpenetrating polymeric networks toward Li-ion batteries," *Ionics (Kiel).*, vol. 23, no. 9, pp. 2319–2325, 2017, doi: 10.1007/s11581-017-2083-0.

[144] H. Jia and S. Y. Gu, "Remote and efficient infrared induced self-healable stretchable substrate for wearable electronics," *Eur. Polym. J.*, vol. 126, no. December 2019, p. 109542, 2020, doi: 10.1016/j.eurpolymj.2020.109542.

[145] X. Jin, N. Guo, Z. You, and Y. Tan, "Design and performance of polyurethane elastomers composed with different soft segments," *Materials (Basel).*, vol. 13, no. 21, pp. 1–26, 2020, doi: 10.3390/ma13214991.

[146] Y. Gao, J. Wang, X. Liang, Z. Yan, Y. Liu, and Y. Cai, "Investigation on permeation properties of liquids into HTV silicone rubber materials," *IEEE Trans. Dielectr. Electr. Insul.*, vol. 21, no. 6, pp. 2428–2437, 2014, doi: 10.1109/TDEI.2014.004476.

[147] W. L. Wu and Z. Chen, "A silicone rubber based composites using n-octadecane/poly (styrene-methyl methacrylate) microcapsules as energy storage particle," *Results Phys.*, vol. 7, pp. 2445–2450, 2017, doi: 10.1016/j.rinp.2017.07.020.

[148] A. Kassu, K. Powers, W. Petway, and A. Sharma, "Journal home page Fourier Transform Infrared Characterization of Construction Joint Sealants epartment of Mechani cal , Ci vil E ngi neering and C onstruction Managem ent," *J. Civ. Eng. Mater. Appl. is Publ. by Pendar Pub*, vol. 4, no. 3, pp. 155–160, 2020, doi: 10.22034/jcema.2020.237399.1029.

[149] N. Seeponkai, J. Wootthikanokkhan, and C. Thanachayanont, "Synthesis and characterization of fullerene functionalized poly(vinyl chloride) (PVC) and dehydrochlorinated PVC using atom transfer radical addition and AIBN based fullerenation," *J. Appl. Polym. Sci.*, vol. 130, no. 4, pp. 2410–2421, 2013, doi: 10.1002/app.39443.

[150] J. J. Hermosillo-Nevárez, V. Bustos-Terrones, Y. A. Bustos-Terrones, P. M. Uriarte-Aceves, and J. G. Rangel-Peraza, "Feasibility study on the use of recycled polymers for malathion adsorption: Isotherms and

kinetic modeling," *Materials (Basel).*, vol. 13, no. 8, 2020, doi: 10.3390/MA13081824.

[151] M. Pandey, G. M. Joshi, A. Mukherjee, and P. Thomas, "Electrical properties and thermal degradation of poly(vinyl chloride)/polyvinylidene fluoride/ZnO polymer nanocomposites," *Polym. Int.*, vol. 65, no. 9, pp. 1098–1106, 2016, doi: 10.1002/pi.5161.

[152] H. Xia, M. Takasaki, and T. Hirai, "Actuation mechanism of plasticized PVC by electric field," *Sensors Actuators, A Phys.*, vol. 157, no. 2, pp. 307–312, 2010, doi: 10.1016/j.sna.2009.11.028.

[153] T. Hwang, Z. Frank, J. Neubauer, and K. J. Kim, "High-performance polyvinyl chloride gel artificial muscle actuator with graphene oxide and plasticizer," *Sci. Rep.*, vol. 9, no. 1, pp. 2–10, 2019, doi: 10.1038/s41598-019-46147-2.

[154] S. Bhatia, S. Khan, and S. Angra, "Effect of the content of silane-functionalized boron carbide on the mechanical and wear performance of B4C reinforced epoxy composites," *High Perform. Polym.*, vol. 33, no. 10, pp. 1165–1180, 2021, doi: 10.1177/09540083211031129.

[155] I. J. Fernandesa, R. V. Santos, E. C. A. Dos Santos, T. L. A. C. Rocha, N. S. D. Junior, and C. A. M. Moraes, "Replacement of commercial silica by rice husk ash in epoxy composites: A comparative analysis," *Mater. Res.*, vol. 21, no. 3, 2018, doi: 10.1590/1980-5373-MR-2016-0562.

[156] B. W. Chieng, N. A. Ibrahim, W. M. Z. W. Yunus, and M. Z. Hussein, "Poly(lactic acid)/poly(ethylene glycol) polymer nanocomposites: Effects of graphene nanoplatelets," *Polymers (Basel).*, vol. 6, no. 1, pp. 93–104, 2014, doi: 10.3390/polym6010093.

[157] J. Harikrishnan Pulikkalparambila, Sandhya Alice Vargheseb, Suchart Siengchin a, 11, and Parameswaranpillaib, "Thermally mendable and improved hydrophilic bioepoxy/PEG-PPG-PEG blends for coating application," 2018.

[158] S. Parameswaranpillai, Jyotishkumar, Sidhardhan, Sisanth Krishnan, Harikrishnan, P., Pionteck, Jürgen, Siengchin and S. Unni, Aparna Beena, Magueresse, Anthony, Grohens, Yves, Hameed, Nishar, Jose, "Morphology, thermo-mechanical properties and surface hydrophobicity of nanostructured epoxy thermosets modified with PEO-PPO-PEO triblock copolymer," *Polym. Test.*, vol. 59, pp. 168–

176, 2017, doi: 10.1016/j.polymertesting.2017.01.029.

[159] W. C. Chu, W. S. Lin, and S. W. Kuo, “Flexible epoxy resin formed upon blending with a triblock copolymer through reaction-induced microphase separation,” *Materials (Basel).*, vol. 9, no. 6, 2016, doi: 10.3390/ma9060449.

[160] M. Kostrzewa, M. Bakar, A. Białkowska, J. Szymańska, and W. Kucharczyk, “Structure and properties evaluation of epoxy resin modified with polyurethane based on polymeric MDI and different polyols,” *Polym. Polym. Compos.*, vol. 27, no. 2, pp. 35–42, 2019, doi: 10.1177/0967391118814595.

[161] N. Parameswaranpillai, Jyotishkumar, Krishnan Sidhardhan, Sisanth, Jose, Seno, Siengchin, Suchart, Pionteck, Jürgen, Magueresse, Anthony, Grohens, Yves, Hameed, “Reaction-induced phase separation and resulting thermomechanical and surface properties of epoxy resin/poly(ethylene oxide)–poly(propylene oxide)–poly(ethylene oxide) blends cured with 4,4′-diaminodiphenylsulfone,” *J. Appl. Polym. Sci.*, vol. 134, no. 4, pp. 1–8, 2017, doi: 10.1002/app.44406.

[162] S. Ahmad, A. P. Gupta, E. Sharmin, M. Alam, and S. K. Pandey, “Synthesis, characterization and development of high performance siloxane-modified epoxy paints,” *Prog. Org. Coatings*, vol. 54, no. 3, pp. 248–255, 2005, doi: 10.1016/j.porgcoat.2005.06.013.

[163] S. J. Park, F. L. Jin, and J. R. Lee, “Effect of biodegradable epoxidized castor oil on physicochemical and mechanical properties of epoxy resins,” *Macromol. Chem. Phys.*, vol. 205, no. 15, pp. 2048–2054, 2004, doi: 10.1002/macp.200400214.

[164] Z. Heng, Z. Zeng, Y. Chen, H. Zou, and M. Liang, “Silicone modified epoxy resins with good toughness, damping properties and high thermal residual weight,” *J. Polym. Res.*, vol. 22, no. 11, 2015, doi: 10.1007/s10965-015-0852-x.

[165] S. P. Khatiwada, S. Thomas, J. M. Saiter, R. Lach, and R. Adhikari, “Mechanical and thermal properties of triblock copolymer modified epoxy resins,” *Bibechana*, vol. 16, pp. 196–203, 2018, doi: 10.3126/bibechana.v16i0.21651.

[166] Arundhati, R. Singhal, and A. K. Nagpal, “Thermal and chemical resistance behavior of cured epoxy based on diglycidyl ether of

bisphenol-A and thiol treated liquid polysulfide blends," *Adv. Mater. Lett.*, vol. 1, no. 3, pp. 238–245, 2010, doi: 10.5185/amlett.2010.10172.

[167] M. Abdouss, T. Farajpour, and M. Derakhshani, "Investigating of polysulfide and epoxy-polysulfide copolymer curing," *Materwiss. Werksttech.*, vol. 41, no. 10, pp. 884–888, 2010, doi: 10.1002/mawe.201000680.

[168] Masoud Sobani December, "Smart Flexible Anticorrosion Coating," 2018.

[169] R. M. Lin and C. Lu, "Modeling of interfacial friction damping of carbon nanotube-based nanocomposites," *Mech. Syst. Signal Process.*, vol. 24, no. 8, pp. 2996–3012, 2010, doi: 10.1016/j.ymssp.2010.06.003.

[170] M. T. Mohamed, "Toughening of Epoxy Polysulfide Binary Blend Composite," *Diyala J. Eng. Sci.*, vol. 11, no. 2, pp. 79–83, 2018, doi: 10.24237/djes.2018.11211.

[171] F. N. Alhabill, R. Ayoob, T. Andritsch, and A. S. Vaughan, "Influence of filler/matrix interactions on resin/hardener stoichiometry, molecular dynamics, and particle dispersion of silicon nitride/epoxy nanocomposites," *J. Mater. Sci.*, vol. 53, no. 6, pp. 4144–4158, 2018, doi: 10.1007/s10853-017-1831-x.

[172] V. Nguyen, A. Vaughan, P. Lewin, and A. Krivda, "The effect of resin stoichiometry and nanoparticle addition on epoxy/silica nanodielectrics," *IEEE Trans. Dielectr. Electr. Insul.*, vol. 22, no. 2, pp. 895–905, 2015, doi: 10.1109/TDEI.2015.7076790.

[173] A. Lavoratti, A. J. Zattera, and S. C. Amico, "Effect of carbonaceous nanofillers and triblock copolymers on the toughness of epoxy resin," *Polym. Bull.*, vol. 78, no. 10, pp. 5467–5480, 2021, doi: 10.1007/s00289-020-03375-1.

[174] M. Martin-Gallego, R. Verdejo, A. Gestos, M. A. Lopez-Manchado, and Q. Guo, "Morphology and mechanical properties of nanostructured thermoset/block copolymer blends with carbon nanoparticles," *Compos. Part A Appl. Sci. Manuf.*, vol. 71, pp. 136–143, 2015, doi: 10.1016/j.compositesa.2015.01.010.

[175] L. Cano, D. H. Builes, and A. Tercjak, "Morphological and mechanical study of nanostructured epoxy systems modified with

amphiphilic poly(ethylene oxide-b-propylene oxide-b-ethylene oxide)triblock copolymer," *Polymer (Guildf).*, vol. 55, no. 3, pp. 738–745, 2014, doi: 10.1016/j.polymer.2014.01.005.

[176] M. E. Islam, M. M. Rahman, M. Hosur, and S. Jeelani, "Thermal stability and kinetics analysis of epoxy composites modified with reactive polyol diluent and multiwalled carbon nanotubes," *J. Appl. Polym. Sci.*, vol. 132, no. 9, pp. 1–11, 2015, doi: 10.1002/app.41558.

[177] M. M. Rahman, M. Hosur, S. Zainuddin, K. C. Jajam, H. V. Tippur, and S. Jeelani, "Mechanical characterization of epoxy composites modified with reactive polyol diluent and randomly-oriented amino-functionalized MWCNTs," *Polym. Test.*, vol. 31, no. 8, pp. 1083–1093, 2012, doi: 10.1016/j.polymertesting.2012.08.010.

[178] F. Pakaya, H. Ardhyananta, and S. T. Wicaksono, "Mechanical Properties and Thermal Stability of Epoxy/RTV Silicone Rubber," *IPTEK J. Technol. Sci.*, vol. 28, no. 1, p. 7, 2017, doi: 10.12962/j20882033.v28i1.2216.

[179] C. Wang, Q. Sun, K. Lei, C. Chen, L. Yao, and Z. Peng, "Effect of toughening with different liquid rubber on dielectric relaxation properties of epoxy resin," *Polymers (Basel).*, vol. 12, no. 2, 2020, doi: 10.3390/polym12020433.

[180] K. Leelachai, P. Kongkachuichay, and P. Dittanet, "Toughening of epoxy hybrid nanocomposites modified with silica nanoparticles and epoxidized natural rubber," *J. Polym. Res.*, vol. 24, no. 3, 2017, doi: 10.1007/s10965-017-1202-y.

[181] J. Huang and X. Nie, "A simple and novel method to design flexible and transparent epoxy resin with tunable mechanical properties," *Polym. Int.*, vol. 65, no. 7, pp. 835–840, 2016, doi: 10.1002/pi.5144.

[182] X. L. Lijuan Luo, Yan Meng, Teng Qiu, Zhuoxin Li, Jing Yang, Xingzhong Cao, "Dielectric and Mechanical Properties of Diglycidyl Ether of Bisphenol A Modified by a New Fluoro-terminated Hyperbranched Poly(phenylene oxide)," vol. 16, no. 2, pp. 101–113, 2013, doi: 10.1002/pc.

[183] L. Xiao *et al.*, "A renewable tung oil-derived nitrile rubber and its potential use in epoxy-toughening modifiers," *RSC Adv.*, vol. 9, no. 44, pp. 25880–25889, 2019, doi: 10.1039/c9ra01918a.

[184] S. Ren, M. Cui, H. Zhao, and L. Wang, "Effect of nitrogen-doped

carbon dots on the anticorrosion properties of waterborne epoxy coatings," *Surf. Topogr. Metrol. Prop.*, vol. 6, no. 2, 2018, doi: 10.1088/2051-672X/aab588.

[185] H. A. Shnawa, M. N. Khalaf, and Y. Jahani, "Thermal degradation, dynamic mechanical and morphological properties of PVC stabilized with natural polyphenol-based epoxy resin," *Polym. Bull.*, vol. 75, no. 8, pp. 3473–3498, 2018, doi: 10.1007/s00289-017-2220-y.

[186] A. S. Ismail, M. Jawaid, N. H. Hamid, R. Yahaya, and A. Hassan, "Mechanical and morphological properties of bio-phenolic/epoxy polymer blends," *Molecules*, vol. 26, no. 4, pp. 1–11, 2021, doi: 10.3390/molecules26040773.

[187] J. Parameswaranpillai *et al.*, "Shape Memory Properties of Epoxy/PPO-PEO-PPO Triblock Copolymer Blends with Tunable Thermal Transitions and Mechanical Characteristics," *Ind. Eng. Chem. Res.*, vol. 56, no. 47, pp. 14069–14077, 2017, doi: 10.1021/acs.iecr.7b03676.

[188] Y. Qin, Y. Wang, Y. Wu, Y. Zhang, H. Li, and M. Yuan, "Effect of Hexadecyl Lactate as Plasticizer on the Properties of Poly(l-lactide) Films for Food Packaging Applications," *J. Polym. Environ.*, vol. 23, no. 3, pp. 374–382, 2015, doi: 10.1007/s10924-014-0702-7.

[189] J. Szymańska, M. Bakar, M. Kostrzewa, and M. Lavorgna, "Preparation and characterization of reactive liquid rubbers toughened epoxy-clay hybrid nanocomposites," *J. Polym. Eng.*, vol. 36, no. 1, pp. 43–52, 2016, doi: 10.1515/polyeng-2014-0393.

[190] S. T. Sajeev Martin George, Debora Puglia, Jose` M. Kenny, P. Jyotishkumar, "Cure Kinetics and Thermal Stability of Micro and Nanostructured Thermosetting Blends of Epoxy Resin and Epoxidized Styrene-Block-Butadiene-Block-Styrene Triblock Copolymer Systems," *Society*, pp. 1–10, 2012, doi: 10.1002/pen.

[191] Q. G. Mario Martin-Gallego, Raquel Verdejo, Adrian Gestos, Miguel A. Lopez- Manchado, Manchado, "Morphology and Mechanical Properties of Nanostructured Thermoset/Bloc Copolymer Blends with Carbon Nanoparticles," vol. 15, no. 2, pp. 1–23, 2015.

[192] L. Ruiz-Pérez, G. J. Royston, J. P. A. Fairclough, and A. J. Ryan, "Toughening by nanostructure," *Polymer (Guildf).*, vol. 49, no. 21, pp. 4475–4488, 2008, doi: 10.1016/j.polymer.2008.07.048.

[193] Z. Wang, Jing, Xue and X. Li, Yichao, Li, Gang, Wang, Yu, Zhong, Wei Hong, Yang, "Synergistically effects of copolymer and core-shell particles for toughening epoxy," *Polymer (Guildf).*, vol. 140, pp. 39–46, 2018, doi: 10.1016/j.polymer.2018.02.031.

[194] M. B. Schuster, I. K. de Abreu, D. Becker, and L. A. F. Coelho, "Effects of adding different concentrations of block copolymers in epoxy matrix nanocomposites with carbon allotropic nanoparticles," *Polym. Compos.*, vol. 42, no. 2, pp. 995–1007, 2021, doi: 10.1002/pc.25881.

[195] L. Tao, Z. Sun, W. Min, H. Ou, L. Qi, and M. Yu, "Improving the toughness of thermosetting epoxy resins: Via blending triblock copolymers," *RSC Adv.*, vol. 10, no. 3, pp. 1603–1612, 2020, doi: 10.1039/c9ra09183a.

[196] R. Januszewski, M. Dutkiewicz, M. Nowicki, M. Szołyga, and I. Kownacki, "Synthesis and Properties of Epoxy Resin Modified with Novel Reactive Liquid Rubber-Based Systems," *Ind. Eng. Chem. Res.*, vol. 60, no. 5, pp. 2178–2186, 2021, doi: 10.1021/acs.iecr.0c05781.

[197] C. Wang, Q. Sun, K. Lei, C. Chen, L. Yao, and Z. Peng, "Effect of toughening with different liquid rubber on dielectric relaxation properties of epoxy resin," *Polymers (Basel).*, vol. 12, no. 2, 2020, doi: 10.3390/polym12020433.

[198] A. B. S. D.Hussinaiah, M.Prasad, K.Mohanaraju, "Synthesis and Characterization of Silicone epoxy resin /poly (methyl methacrylate) Interpenetrating Polymer Networks," vol. 3, no. 9, pp. 9–19, 2014.

[199] S. H. Mahdi, W. H. Jassim, I. A. Hamad, and K. A. Jasima, "Epoxy/Silicone Rubber Blends for Voltage Insulators and Capacitors Applications," *Energy Procedia*, vol. 119, pp. 501–506, 2017, doi: 10.1016/j.egypro.2017.07.059.

[200] I. M. Kalogeras, "Glass-Transition Phenomena in Polymer Blends," *Encycl. Polym. Blends*, vol. 3, pp. 1–134, 2016, doi: 10.1002/9783527653966.ch1.

[201] J. Mijović, "Cure kinetics of neat versus reinforced epoxies," *J. Appl. Polym. Sci.*, vol. 31, no. 5, pp. 1177–1187, 1986, doi: 10.1002/app.1986.070310503.

[202] Y. Grohens, B. George, F. Touyeras, J. Vebrel, and B. Laude, "Experimental design as a route for improving the performances of

formulated epoxy adhesives," *Polym. Test.*, vol. 16, no. 5, pp. 417–427, 1997, doi: 10.1016/S0142-9418(97)00002-0.

[203] M. T. Rodríguez, S. J. García, R. Cabello, J. J. Suay, and J. J. Gracenea, "Effect of plasticizer on the thermal, mechanical, and anticorrosion properties of an epoxy primer," *J. Coatings Technol. Res.*, vol. 2, no. 7, pp. 557–564, 2005, doi: 10.1007/s11998-005-0015-9.

[204] E. Kerdawy, I. Ramzia, E. Bag, and A. Othm, "Development and validation of a stability-indicating RP-LC method for the simultaneous determination of otilonium bromide and its expected degradation product in bulk drug and pharmaceutical preparation.," *Eur. J. Chem.*, vol. 7, no. 1, pp. 97–101, 2016, doi: 10.5155/e.

[205] T. Farajpour, Y. Bayat, M. Keshavarz, and E. Zanjirian, "Viscoelastic and thermal properties of polysulfide modified epoxy resin: The effect of modifier molecular weight," *Materwiss. Werksttech.*, vol. 44, no. 12, pp. 991–996, 2013, doi: 10.1002/mawe.201300110.

[206] A. Pirayesh, M. Salami-Kalajahi, H. Roghani-Mamaqani, and M. Mazloomi-Rezvani, "Synthesis and characterization of bis(oxiranylmethyl)sulfanes as new epoxide-terminated polysulfide prepolymers and their use in synthesis of new amine-cured polysulfide polymers," *Adv. Polym. Technol.*, vol. 37, no. 8, pp. 3325–3334, 2018, doi: 10.1002/adv.22117.

[207] A. Wilford, T. C. P. Lee, and T. J. Kemp, "Phase separation of polysulphide polymers in epoxy adhesives," *Int. J. Adhes. Adhes.*, vol. 12, no. 3, pp. 171–177, 1992, doi: 10.1016/0143-7496(92)90050-6.

[208] A. Pirayesh, M. Salami-Kalajahi, H. Roghani-Mamaqani, and F. Najafi, "Polysulfide Polymers: Synthesis, Blending, Nanocomposites, and Applications," *Polym. Rev.*, vol. 59, no. 1, pp. 124–148, 2019, doi: 10.1080/15583724.2018.1492616.

[209] M. Bakar, R. Duk, M. PrzybyÅek, and M. Kostrzewa, "Mechanical and thermal properties of epoxy resin modified with polyurethane," *J. Reinf. Plast. Compos.*, vol. 28, no. 17, pp. 2107–2118, 2009, doi: 10.1177/0731684408091703.

[210] Y. Zhao, Z. K. Chen, Y. Liu, H. M. Xiao, Q. P. Feng, and S. Y. Fu, "Simultaneously enhanced cryogenic tensile strength and fracture toughness of epoxy resins by carboxylic nitrile-butadiene nano-

rubber," *Compos. Part A Appl. Sci. Manuf.*, vol. 55, pp. 178–187, 2013, doi: 10.1016/j.compositesa.2013.09.005.

[211] K. Zhao, X. X. Song, C. S. Liang, J. Wang, and S. A. Xu, "Morphology and properties of nanostructured epoxy blends toughened with epoxidized carboxyl-terminated liquid rubber," *Iran. Polym. J. (English Ed.*, vol. 24, no. 5, pp. 425–435, 2015, doi: 10.1007/s13726-015-0334-3.

[212] D. Carolan, A. Ivankovic, A. J. Kinloch, S. Sprenger, and A. C. Taylor, "Toughening of epoxy-based hybrid nanocomposites," *Polymer (Guildf).*, vol. 97, pp. 179–190, 2016, doi: 10.1016/j.polymer.2016.05.007.

[213] Y. Zhang, P. Song, S. Fu, and F. Chen, "Morphological structure and mechanical properties of epoxy/polysulfone/cellulose nanofiber ternary nanocomposites," *Compos. Sci. Technol.*, vol. 115, pp. 66–71, 2015, doi: 10.1016/j.compscitech.2015.05.003.

[214] D. Kiatiporntipthak, Krittameth, Thajai, Nanthicha, Kanthiya, Thidarat, Rachtanapun, Pornchai, Leksawasdi, Noppol, Phimolsiripol, Yuthana Rohindra, W. Ruksiriwanich, S. R. Sommano, and K. Jantanasakulwong, "Reaction mechanism and mechanical property improvement of poly(lactic acid) reactive blending with epoxy resin," *Polymers (Basel).*, vol. 13, no. 15, 2021, doi: 10.3390/polym13152429.

[215] R. He, X. Zhan, Q. Zhang, G. Zhang, and F. Chen, "Control of inclusion size and toughness by reactivity of multiblock copolymer in epoxy composites," *Polymer (Guildf).*, vol. 92, pp. 222–230, 2016, doi: 10.1016/j.polymer.2016.04.003.

[216] R. He, X. Zhan, Q. Zhang, and F. Chen, "Toughening of polyamide-6 with little loss in modulus by block copolymer containing poly(styrene-alt-maleic acid) segment," *J. Appl. Polym. Sci.*, vol. 134, no. 27, pp. 1–7, 2017, doi: 10.1002/app.44849.

[217] J. M. Misasi, Q. Jin, K. M. Knauer, S. E. Morgan, and J. S. Wiggins, "Hybrid POSS-Hyperbranched polymer additives for simultaneous reinforcement and toughness improvements in epoxy networks," *Polymer (Guildf).*, vol. 117, pp. 54–63, 2017, doi: 10.1016/j.polymer.2017.04.007.

[218] P. M. Mohammad T. Bashar1, Uttandaraman Sundararaj2,

"Morphology and Mechanical Properties of Nanostructured Acrylic Tri-Block-Copolymer Modified Epoxy," *Soc. Plast. Eng.*, pp. 1–10, 2013, doi: 10.1002/pen.23648.

[219] M. Demleitner, Martin, Schönl, Florian, Angermann, Jörg, Fässler, Pascal, Lamparth, Iris, Rist, Kai, Schnur, Thomas, Catel, Yohann, Rosenfeldt, Sabine, Retsch, "Influence of Block Copolymer Concentration and Resin Crosslink Density on the Properties of UV-Curable Methacrylate Resin Systems," vol. 2200320, pp. 1–13, 2022, doi: 10.1002/mame.202200320.

[220] H. Yi, T. Wei, H. Lin, and J. Zhou, "Preparation and properties of hybrid epoxy/hydro-terminated polybutadiene/modified MMT nanocomposites," *J. Coatings Technol. Res.*, vol. 15, no. 6, pp. 1413–1422, 2018, doi: 10.1007/s11998-018-0093-0.

[221] M. Bakar and F. Djaider, "Effect of plasticizers content on the mechanical properties of unsaturated polyester resin," *J. Thermoplast. Compos. Mater.*, vol. 20, no. 1, pp. 53–64, 2007, doi: 10.1177/0892705707068820.

[222] X. Yang, Jiayao, He, Xingwei, Wang, Hengxu, Liu, S. Lin, Peng, Yang, and S. Fu, "High-toughness, environment-friendly solid epoxy resins: Preparation, mechanical performance, curing behavior, and thermal properties," *J. Appl. Polym. Sci.*, vol. 137, no. 17, pp. 27–30, 2020, doi: 10.1002/app.48596.

[223] Y. Xu, X. Fu, G. Liao, H. Zhou, and X. Jian, "Preparation, morphology and thermo-mechanical properties of epoxy resins modified by co-poly (phthalazinone ether sulfone)," *High Perform. Polym.*, vol. 23, no. 3, pp. 248–254, 2011, doi: 10.1177/0954008310389839.

[224] R. D. Brooker, A. J. Kinloch, and A. C. Taylor, "The morphology and fracture properties of thermoplastic-toughened epoxy polymers," *J. Adhes.*, vol. 86, no. 7, pp. 726–741, 2010, doi: 10.1080/00218464.2010.482415.

[225] M. Saitoo, O. Watanabe, M. Takezawa, and T. Yoshiki, "Fracture behaviour of thermoplastic modified epoxy resins," *J. Adhes.*, vol. 39, no. 4, pp. 227–242, 1992, doi: 10.1080/00218469208030464.

[226] J. X. Wang J, Liu R, "Introduction to Epoxy/Thermoplastic Blends. In: Parameswaranpillai J, Hameed N, Pionteck J, Woo EM, eds.

Handbook of Epoxy Blends." Springer International Publishing, pp. 1–29, 2017.

[227] L. Karthikeyan, D. Mathew, and T. M. Robert, "Poly(ether ether ketone)-bischromenes: Synthesis, characterization, and influence on thermal, mechanical, and thermo mechanical properties of epoxy resin," *Polym. Adv. Technol.*, vol. 30, no. 4, pp. 1061–1071, 2019, doi: 10.1002/pat.4539.

[228] W. J. Kim, Y. J. Heo, J. H. Lee, K. Y. Rhee, and S. J. Park, "Effect of Atmospheric-Pressure Plasma Treatments on Fracture Toughness of Carbon Fibers-Reinforced Composites," *Molecules*, vol. 26, no. 12, pp. 1–13, 2021, doi: 10.3390/molecules26123698.

[229] S. Y. Lee, M. J. Kang, S. H. Kim, K. Y. Rhee, J. H. Lee, and S. J. Park, "Roles of small polyetherimide moieties on thermal stability and fracture toughness of epoxy blends," *Polymers (Basel).*, vol. 13, no. 19, pp. 1–10, 2021, doi: 10.3390/polym13193310.

[230] X. Cheng, Q. Wu, S. E. Morgan, and J. S. Wiggins, "Morphologies and mechanical properties of polyethersulfone modified epoxy blends through multifunctional epoxy composition," *J. Appl. Polym. Sci.*, vol. 134, no. 18, pp. 1–10, 2017, doi: 10.1002/app.44775.

[231] T. Farajpour, Y. Bayat, M. H. Keshavarz, and E. Zanjirian, "Investigating the effect of modifier chain length on insulation properties of polysulfide modified epoxy resin," *Iran. J. Chem. Chem. Eng.*, vol. 33, no. 1, pp. 37–44, 2014.

[232] I. A. Mahmood and M. Ziyara Shamukh, "Characteristics and Properties of Epoxy/Polysulfide Blend Matrix Reinforced by Short Carbon and Glass Fibers," *J. Eng. Sci.*, vol. 20, no. 1, pp. 80–87, 2017.

[233] M. M. Shalaan, A. H. M. Al-Falahi, and B. M. Al-Dabagh, "Study of Mechanical Properties and Thermal Conductivity of Polymeric Blend [Epoxy and polysulfide rubber (EP + PSR)] Reinforced by Nano Ceramic Powder ZrO2," *J. Phys. Conf. Ser.*, vol. 1829, no. 1, 2021, doi: 10.1088/1742-6596/1829/1/012013.

[234] X. Wang, S. Peng, H. Chen, X. Yu, and X. Zhao, "Mechanical properties, rheological behaviors, and phase morphologies of high-toughness PLA/PBAT blends by in-situ reactive compatibilization," *Compos. Part B Eng.*, vol. 173, no. May, p. 107028, 2019, doi: 10.1016/j.compositesb.2019.107028.

[235] R. H. Bello, L. Antonio, and F. Coelho, "Role of Triblock Copolymers in the Properties of Epoxy Matrices Role of Triblock Copolymers in the Properties of Epoxy Matrices With Carbon Nanoparticles," no. January, 2019.

[236] J. R. Xavier, "Enhanced Adhesion and Corrosion Protection Properties of Surface Modified Sb2O3–Epoxy Nanocomposite Coatings on Mild Steel," *J. Fail. Anal. Prev.*, vol. 20, no. 2, pp. 523–531, 2020, doi: 10.1007/s11668-020-00847-4.

[237] D. E. Packham, *Handbook of Adhesion*, 2nd Editio., vol. 1. Book: Handbook of Adhesion Promoters, 2005.

[238] M. T. Majd, T. Shahrabi, and B. Ramezanzadeh, "The role of neodymium based thin film on the epoxy/steel interfacial adhesion and corrosion protection promotion," *Appl. Surf. Sci.*, vol. 464, no. August 2018, pp. 516–533, 2019, doi: 10.1016/j.apsusc.2018.09.109.

[239] M. Ramezanzadeh, Z. Sanaei, and B. Ramezanzadeh, "The influence of steel surface treatment by a novel eco-friendly praseodymium oxide nanofilm on the adhesion and corrosion protection properties of a fusion-bonded epoxy powder coating," *J. Ind. Eng. Chem.*, vol. 62, pp. 427–435, 2018, doi: 10.1016/j.jiec.2018.01.026.

[240] N. Rezaee, M. M. Attar, and B. Ramezanzadeh, "Studying corrosion performance, microstructure and adhesion properties of a room temperature zinc phosphate conversion coating containing Mn2+ on mild steel," *Surf. Coatings Technol.*, vol. 236, pp. 361–367, 2013, doi: 10.1016/j.surfcoat.2013.10.014.

[241] P. Riazaty, R. Naderi, and B. Ramezanzadeh, "Enhancement of the Epoxy Coating Corrosion/Cathodic Delamination Resistances on Steel by a Samarium Based Conversion Coating," *J. Electrochem. Soc.*, vol. 166, no. 13, pp. C353–C364, 2019, doi: 10.1149/2.0151913jes.

[242] Y. He, Dongjing, Cheng, Gang, Tang, Ling, Chen, Lie, Li, Shiyao, Gu, Ping, Zhao, "Research on adhesive properties of polydimethylsiloxane-carbon fiber composite material," *Int. J. Adhes. Adhes.*, vol. 86, pp. 35–39, 2018, doi: 10.1016/j.ijadhadh.2018.08.004.

[243] S. Verma, S. Das, S. Mohanty, and S. K. Nayak, "A facile preparation of epoxy-polydimethylsiloxane (EP-PDMS) polymer coatings for marine applications," *J. Mater. Res.*, vol. 34, no. 16, pp. 2881–2894, 2019, doi: 10.1557/jmr.2019.235.

[244] N. Parhizkar, T. Shahrabi, and B. Ramezanzadeh, "A new approach for enhancement of the corrosion protection properties and interfacial adhesion bonds between the epoxy coating and steel substrate through surface treatment by covalently modified amino functionalized graphene oxide film," *Corros. Sci.*, vol. 123, pp. 55–75, 2017, doi: 10.1016/j.corsci.2017.04.011.

[245] H. Bahramnia, H. M. Semnani, A. Habibolahzadeh, and H. Abdoos, "Epoxy/polyurethane hybrid nanocomposite coatings reinforced with MWCNTs and SiO2 nanoparticles: Processing, mechanical properties and wear behavior," *Surf. Coatings Technol.*, vol. 415, no. January, p. 127121, 2021, doi: 10.1016/j.surfcoat.2021.127121.

[246] F. Bahremand, T. Shahrabi, and B. Ramezanzadeh, "Epoxy coating anti-corrosion properties enhancement via the steel surface treatment by nanostructured samarium oxide-poly-dopamine film," *J. Hazard. Mater.*, vol. 403, no. August 2020, p. 123722, 2021, doi: 10.1016/j.jhazmat.2020.123722.

[247] H. Rombouts, Marleen, Persoons, Rosita, Geerinckx, Eric, Kemps, Raymond, Mertens, Myrjam, Hendrix, Willy, Chen, "Development and characterization of nickel based tungsten carbide laser cladded coatings," *Phys. Procedia*, vol. 5, no. PART 1, pp. 333–339, 2010, doi: 10.1016/j.phpro.2010.08.154.

[248] D. Fan, Xiaoqin, He and Z. Wang, Pei, Li, Dong, Liu, Yinjuan, Ma, Dejiang, Du, Yanchun, Gao, Shangpan, Kou, "High pressure infiltration sintering behavior of WC-Co alloys," *High Press. Res.*, vol. 36, no. 4, pp. 585–594, 2016, doi: 10.1080/08957959.2016.1221950.

[249] P. Hoffmann, H. Galindo, G. Zambrano, C. Rincón, and P. Prieto, "FTIR studies of tungsten carbide in bulk material and thin film samples," *Mater. Charact.*, vol. 50, no. 4–5, pp. 255–259, 2003, doi: 10.1016/S1044-5803(03)00100-1.

[250] Z. Yan, M. Cai, and P. K. Shen, "Nanosized tungsten carbide synthesized by a novel route at low temperature for high performance electrocatalysis," *Sci. Rep.*, vol. 3, pp. 1–7, 2013, doi: 10.1038/srep01646.

[251] G. Singla, K. Singh, and O. P. Pandey, "Structural and thermal analysis of in situ synthesized C-WC nanocomposites," *Ceram. Int.*, vol. 40, no. 4, pp. 5157–5164, 2014, doi: 10.1016/j.ceramint.2013.10.067.

[252] S. Sagadevan, I. Das, P. Singh, and J. Podder, "Synthesis of tungsten carbide nanoparticles by hydrothermal method and its Characterization," *J. Mater. Sci. Mater. Electron.*, vol. 28, no. 1, pp. 1136–1141, 2017, doi: 10.1007/s10854-016-5638-3.

[253] L. Peponi, D. Puglia, L. Torre, L. Valentini, and J. M. Kenny, "Processing of nanostructured polymers and advanced polymeric based nanocomposites," *Mater. Sci. Eng. R Reports*, vol. 85, no. 1, pp. 1–46, 2014, doi: 10.1016/j.mser.2014.08.002.

[254] T. Li, M. J. Heinzer, E. M. Redline, F. Zuo, F. S. Bates, and L. F. Francis, "Microstructure and performance of block copolymer modified epoxy coatings," *Prog. Org. Coatings*, vol. 77, no. 7, pp. 1145–1154, 2014, doi: 10.1016/j.porgcoat.2014.03.015.

[255] M. B. Schuster, C. V. Opelt, D. Becker, and L. A. F. Coelho, "Role and sinergy of block copolymer and carbon nanoparticles on toughness in epoxy matrix," *Polym. Compos.*, vol. 39, pp. E2262–E2273, 2018, doi: 10.1002/pc.24599.

[256] Z. Yang, K. McElrath, J. Bahr, and N. A. D'Souza, "Effect of matrix glass transition on reinforcement efficiency of epoxy-matrix composites with single walled carbon nanotubes, multi-walled carbon nanotubes, carbon nanofibers and graphite," *Compos. Part B Eng.*, vol. 43, no. 4, pp. 2079–2086, 2012, doi: 10.1016/j.compositesb.2012.01.049.

[257] Y. Zare, "Modeling the yield strength of polymer nanocomposites based upon nanoparticle agglomeration and polymer-filler interphase," *J. Colloid Interface Sci.*, vol. 467, pp. 165–169, 2016, doi: 10.1016/j.jcis.2016.01.022.

[258] H. Machrafi, G. Lebon, and C. S. Iorio, "Effect of volume-fraction dependent agglomeration of nanoparticles on the thermal conductivity of nanocomposites: Applications to epoxy resins, filled by SiO2, AlN and MgO nanoparticles," *Compos. Sci. Technol.*, vol. 130, pp. 78–87, 2016, doi: 10.1016/j.compscitech.2016.05.003.

[259] M. Kameswara Reddy, V. Suresh Babu, K. V. Sai Srinadh, and M. Bhargav, "Mechanical properties of tungsten carbide nanoparticles filled epoxy polymer nano composites," *Mater. Today Proc.*, vol. 26, no. xxxx, pp. 2711–2713, 2019, doi: 10.1016/j.matpr.2020.02.569.

[260] P. Schmittinger, "CRC Materials Science and Engineering

Handbook.Fourth Edition," *Chlorine Princ. Ind. Pract.*, vol. 1, pp. 3–9, 2015, doi: 10.1002/9783527613380.ch2.

[261] E. J. F. Shackelford and W. Alexander, "CRC Materials Science and Engineering Handbook.," 2001.

[262] S. K. Singh, S. Singh, A. Kumar, and A. Jain, "Thermo-mechanical behavior of TiO2 dispersed epoxy composites," *Eng. Fract. Mech.*, vol. 184, pp. 241–248, 2017, doi: 10.1016/j.engfracmech.2017.09.005.

[263] I. a Al-ajaj, M. M. Abd, H. I. Jaffer, and A. Materials, "Mechanical Properties of Micro and Nano TiO 2 / Epoxy Composites," *Int. J. Mining, Metall. Mech. Eng.*, vol. 1, no. 2, pp. 2–6, 2013, doi: 10.13140/RG.2.2.30316.31360.

[264] S. Chandrasekaran, N. Sato, F. Tölle, R. Mülhaupt, B. Fiedler, and K. Schulte, "Fracture toughness and failure mechanism of graphene based epoxy composites," *Compos. Sci. Technol.*, vol. 97, pp. 90–99, 2014, doi: 10.1016/j.compscitech.2014.03.014.

[265] K. Wang, L. Chen, J. Wu, M. L. Toh, C. He, and A. F. Yee, "Epoxy nanocomposites with highly exfoliated clay: Mechanical properties and fracture mechanisms," *Macromolecules*, vol. 38, no. 3, pp. 788–800, 2005, doi: 10.1021/ma048465n.

[266] N. Narmadadevi, V. Velmurugan, R. Prabhakaran, and R. Venkatakrishnan, "Effect of Filler Content on the Performance of Epoxy/Haritaki Powder Composite," *Lect. Notes Mech. Eng.*, vol. 2014, pp. 277–283, 2022, doi: 10.1007/978-981-16-4222-7_33.

[267] R. Khan, M. R. Azhar, A. Anis, M. A. Alam, M. Boumaza, and S. M. Al-Zahrani, "Facile synthesis of epoxy nanocomposite coatings using inorganic nanoparticles for enhanced thermo-mechanical properties: a comparative study," *J. Coatings Technol. Res.*, vol. 13, no. 1, pp. 159–169, 2016, doi: 10.1007/s11998-015-9736-6.

[268] M. Sudheer, R. Prabhu, K. Raju, and T. Bhat, "Effect of filler content on the performance of epoxy/PTW composites," *Adv. Mater. Sci. Eng.*, vol. 2014, 2014, doi: 10.1155/2014/970468.

[269] S. M. Ibraheim and S. I. Hussein, "Study on the contact angle, adhesion strength, and antibacterial activity of polymer/cement composites for waterproof coating," *Iraqi J. Sci.*, vol. 61, no. 8, pp. 1971–1977, 2020, doi: 10.24996/ijs.2020.61.8.14.

[270] D. Jafari, M. Shishesaz, D. Zaarei, and I. Danaee, "Nanocomposite Coating Based on Thermoplastic Acrylic Resin and Montmorillonite Clay : Preparation and Corrosion Prevention Properties," *Iran. J. Oil Gas Sci. Technol.*, vol. 6, no. 1, pp. 63–76, 2017.

[271] H. Eivaz Mohammadloo, A. A. Sarabi, R. Mohammad Hosseini, M. Sarayloo, H. Sameie, and R. Salimi, "A comprehensive study of the green hexafluorozirconic acid-based conversion coating," *Prog. Org. Coatings*, vol. 77, no. 2, pp. 322–330, 2014, doi: 10.1016/j.porgcoat.2013.10.006.

[272] P. Chen, Y. Wang, J. Li, H. Wang, and L. Zhang, "Adhesion and erosion properties of epoxy resin composite coatings reinforced with fly ash cenospheres and short glass fibers," *Prog. Org. Coatings*, vol. 125, no. July, pp. 489–499, 2018, doi: 10.1016/j.porgcoat.2018.09.029.

[273] R. Morrell and A. J. Gant, "Edge chipping of hard materials," *Int. J. Refract. Met. Hard Mater.*, vol. 19, no. 4–6, pp. 293–301, 2001, doi: 10.1016/S0263-4368(01)00030-0.

[274] T. A. Rodil, "Edge effect on abrasive wear mechanisms and wear resistance in WC-6wt .% Co hardmetals," pp. 1–40, 2006.

[275] N. J. Delollis and O. Montoya, "Mode of failure in structural adhesive bonds," *J. Appl. Polym. Sci.*, vol. 11, no. 6, pp. 983–989, 1967, doi: 10.1002/app.1967.070110617.

[276] F. Askari, E. Ghasemi, B. Ramezanzadeh, and M. Mahdavian, "Mechanistic approach for evaluation of the corrosion inhibition of potassium zinc phosphate pigment on the steel surface: Application of surface analysis and electrochemical techniques," *Dye. Pigment.*, vol. 109, pp. 189–199, 2014, doi: 10.1016/j.dyepig.2014.05.024.

[277] M. Ganjaee Sari, M. Shamshiri, and B. Ramezanzadeh, "Fabricating an epoxy composite coating with enhanced corrosion resistance through impregnation of functionalized graphene oxide-co-montmorillonite Nanoplatelet," *Corros. Sci.*, vol. 129, no. September, pp. 38–53, 2017, doi: 10.1016/j.corsci.2017.09.024.

[278] T. V. Nguyen, Tuan Anh, Nguyen, Huyen, Nguyen and X. Thai, Hoang, Shi, "Effect of nanoparticles on the thermal and mechanical properties of epoxy coatings," *J. Nanosci. Nanotechnol.*, vol. 16, no. 9, pp. 9874–9881, 2016, doi: 10.1166/jnn.2016.12162.

[279] L. Zhai, G. Ling, J. Li, and Y. Wang, "The effect of nanoparticles on

the adhesion of epoxy adhesive," *Mater. Lett.*, vol. 60, no. 25–26, pp. 3031–3033, 2006, doi: 10.1016/j.matlet.2006.02.038.

[280] A. Nassar, M. Salem, I. El-Batanony, and E. Nassar, "Improving wear resistance of epoxy/SiC composite using a modified apparatus," *Polym. Polym. Compos.*, vol. 29, no. 9_suppl, pp. S389–S399, 2021, doi: 10.1177/09673911211002731.

[281] Z. Liu, L. Pandelaers, P. T. Jones, B. Blanpain, and M. Guo, " Effect of Al 2 O 3 and SiO 2 Addition on the Viscosity of BOF Slag ," *Adv. Molten Slags, Fluxes, Salts*, no. 1, pp. 439–446, 2016, doi: 10.1002/9781119333197.ch46.

[282] M. M. Sakka, Z. Antar, K. Elleuch, and J. F. Feller, "Tribological response of an epoxy matrix filled with graphite and/or carbon nanotubes," *Friction*, vol. 5, no. 2, pp. 171–182, 2017, doi: 10.1007/s40544-017-0144-z.

[283] S. Abdou, A. Elkaseer, H. Kouta, and J. Abu Qudeiri, "Wear behaviour of grey cast iron with the presence of copper addition," *Adv. Mech. Eng.*, vol. 10, no. 10, pp. 1–8, 2018, doi: 10.1177/1687814018804741.

[284] A. Nassar, M. Younis, M. Ismail, and E. Nassar, "Improved Wear-Resistant Performance of Epoxy Resin Composites Using Ceramic Particles," *Polymers (Basel).*, vol. 14, no. 2, 2022, doi: 10.3390/polym14020333.

[285] R. Jamshidi, A. Heidarpour, H. Aghamohammadi, and R. Eslami-Farsani, "Improvement in the mechanical and tribological behavior of epoxy matrix with the inclusion of synthesized Ti3AlC2 MAX particles," *J. Compos. Mater.*, vol. 53, no. 26–27, pp. 3819–3827, 2019, doi: 10.1177/0021998319848140.

Appendix

Appendix A Tables of Samples properties values

Table 4.9: Glass transition temperature value of different toughening agents /epoxy blends			
Sample number	Toughening agent	Samples Composition	**T_g (°C)**
1	No toughening agent	EP	**83.76**
2	(EO-PPO-EO) TBCP	3% TBCP/EP	**60.89**
3	=	6% TBCP/EP	**58.95**
4	=	9% TBCP/EP	**56.54**
5	=	12% TBCP/EP	**53.10**
6	120 Quickmaster (polyol)	3% PU/EP	**69.69**
7	=	6% PU/EP	**66.01**
8	=	9% PU/EP	**65.00**
9	=	12% PU/EP	**65.69**
10	Liquid silicon rubber	3% LSR/EP	**68.55**
11	=	6% LSR/EP	**67.91**
12	=	9% LSR/EP	**63.85**
13	=	12% LSR/EP	**62.70**

14	Liquid polyvinyl chloride	3% PVC/EP	**73.41**
15	=	6% PVC/EP	**69.97**
16	=	9% PVC/EP	**69.71**
17	=	12% PVC/EP	**69.39**
18	Polysulphide polymer	3% PSR/EP	**68.72**
19	=	6% PSR/EP	**65.73**
20	=	9% PSR/EP	**63.63**
21	=	12% PSR/EP	**60.92**

Table 4.10: Tensile properties of different toughening agents/epoxy blends

Sample number	**Blends**	**Tensile strength (MP_a)**	**Tensile modulus (GP_a)**	**Elongation at break (%)**
1	Unmodified epoxy	17	0.28	12.8
	TBCP/EP			
2	+ 3wt% TBCP	34	0.44	12.5
3	+ 6wt% TBCP	34	0.41	12.8
4	+ 9wt% TBCP	32	0.42	9
5	+ 12wt% TBCP	30	0.40	8.8
	PU/EP			
6	+ 3wt% PU	17.7	0.21	16.3
7	+ 6wt% PU	14.3	0.21	16.7

8	+ 9wt% PU	13.3	0.18	17.1
9	+ 12wt% PU	12	0.17	17.9
		LSR/EP		
10	+ 3wt% LSR	19	0.27	12.4
11	+ 6wt% LSR	19	0.28	10.3
12	+ 9wt% LSR	18.3	0.28	9.3
13	+ 12wt% LSR	18	0.25	9.4
		PVC/EP		
14	+ 3wt% PVC	10.3	0.14	14.2
15	+ 6wt% PVC	10	0.12	18.4
16	+ 9wt% PVC	10.3	0.12	16.7
17	+ 12wt% PVC	10	0.13	17.7
		PSR/EP		
18	+ 3wt% PSR	11	0.14	14.9
19	+ 6wt% PSR	11.3	0.14	15.1
20	+ 9wt% PSR	10	0.14	14.5
21	+ 12wt% PSR	7.3	0.11	14.8

Table 4.11: Fracture toughness and impact strength properties of all toughening agents/epoxy blends

Sample number	Blends	Fracture toughness ($MP_a .m^{1/2}$)	Impact strength (Kj/m^2)
1	Unmodified epoxy	1.2	5.3

TBCP/EP			
2	+ 3wt% TBCP	2.6	13
3	+ 6wt% TBCP	2.7	10.7
4	+ 9wt% TBCP	2.8	9.6
5	+ 12wt% TBCP	2.7	8
PU/EP			
6	+ 3wt% PU	3	9.1
7	+ 6wt% PU	2.2	9
8	+ 9wt% PU	2.3	9.5
9	+ 12wt% PU	2.2	5.4
LSR/EP			
10	+ 3wt% LSR	2.9	10.9
11	+ 6wt% LSR	3.7	12.9
12	+ 9wt% LSR	3.5	9.1
13	+ 12wt% LSR	2.7	7.9
PVC/EP			
14	+ 3wt% PVC	2.6	10.9
15	+ 6wt% PVC	2.1	11.9
16	+ 9wt% PVC	2.4	12.9
17	+ 12wt% PVC	2	13.1
PSR/EP			
18	+ 3wt% PSR	2.6	5.8
19	+ 6wt% PSR	2.9	5.7
20	+ 9wt% PSR	2.9	8.3
21	+ 12wt% PSR	2.7	5.3

Table 4.12: Hardness value of all toughening agents/epoxy blends		
Sample number	Blends	Hardness Shore D
1	Unmodified epoxy	65.6
	TBCP/EP	
2	+ 3wt% TBCP	68.9
3	+ 6wt% TBCP	66.7
4	+ 9wt% TBCP	66.6
5	+ 12wt% TBCP	67.6
	PU/EP	
6	+ 3wt% PU	63.4
7	+ 6wt% PU	64
8	+ 9wt% PU	62.3
9	+ 12wt% PU	60.6
	LSR/EP	
10	+ 3wt% LSR	64.7
11	+ 6wt% LSR	64.6
12	+ 9wt% LSR	64.3
13	+ 12wt% LSR	62.7
	PVC/EP	
14	+ 3wt% PVC	61.4
15	+ 6wt% PVC	59.8
16	+ 9wt% PVC	54.7
17	+ 12wt% PVC	58

	PSR/EP	
18	+ 3wt% PSR	66.9
19	+ 6wt% PSR	67.2
20	+ 9wt% PSR	66.6
21	+ 12wt% PSR	62.8

Table 4.13: Pull-off strength values of all toughening agents/epoxy blends

Sample number	Blends	Pull off strength (MPa)
1	Unmodified epoxy	1.6
	TBCP/EP	
2	+ 3wt% TBCP	2.3
3	+ 6wt% TBCP	2
4	+ 9wt% TBCP	1.9
5	+ 12wt% TBCP	2.3
	PU/EP	
6	+ 3wt% PU	3
7	+ 6wt% PU	2.9
8	+ 9wt% PU	2.7
9	+ 12wt% PU	1.9
	LSR/EP	
10	+ 3wt% LSR	1.6
11	+ 6wt% LSR	2
12	+ 9wt% LSR	1.4

13	+ 12wt% LSR	1
	PVC/EP	
14	+ 3wt% PVC	2.1
15	+ 6wt% PVC	2.2
16	+ 9wt% PVC	1.6
17	+ 12wt% PVC	2
	PSR/EP	
18	+ 3wt% PSR	1.3
19	+ 6wt% PSR	1.1
20	+ 9wt% PSR	1.1
21	+ 12wt% PSR	1.2

Table 4.14: T_g values for two epoxy nanocomposites

Sample number	Matrix nanocomposite	Samples composition	**T_g (°C)**
1	Neat epoxy	EP	**83.76**
2	Neat epoxy	1% WC/ EP	**90.22**
3	=	2% WC/EP	**93.36**
4	=	3% WC/EP	**94.86**
5	Epoxy/3% wt TBCP	1% WC/TBCP/EP	**89.64**
6	=	2% WC/TBCP/EP	**94.76**
7	=	3% WC/TBCP/EP	**98.83**

Table 4.15: Tensile properties value for two epoxy nanocomposites					
Sample number	**Matrix nanocomposite**	**Samples composition**	**Tensile strength (MPa)**	**Tensile modulus (GPa)**	**Elongation at break (%)**
1	Neat epoxy	EP	17	0.28	12.8
2	Neat epoxy	1% WC/ EP	25	0.35	12.9
3	=	2% WC/EP	26.3	0.41	11.8
4	=	3% WC/EP	23	0.37	11.5
5	Epoxy/3% wt TBCP	1% WC/TBCP/EP	27	0.39	13
6	=	2% WC/TBCP/EP	26.3	0.41	14.3
7	=	3% WC/TBCP/EP	26	0.41	12.8

Table 4.16: Mechanical properties of two epoxy nanocomposite					
Sample number	Matrix nanocomposite	Samples composition	Fracture toughness MPa.√m	Impact strength (Kj/m^2)	Hardness Shore D
1	Neat epoxy	EP	1.2	5.3	65.6
2	Neat epoxy	1% WC/ EP	4.1	5.9	66
3	=	2% WC/EP	5.4	6.5	66.4
4	=	3% WC/EP	3.9	6.9	67.05
5	Epoxy/3% wt TBCP	1% WC/TBCP/EP	3.7	11	68.6
6	=	2% WC/TBCP/EP	4.2	10.5	67.3
7	=	3% WC/TBCP/EP	3.7	8.7	68.7

Table 4.17: Pull off the strength of two epoxy nanocomposites			
Sample number	Matrix nanocomposite	Samples composition	Pull off strength (MPa)
1	Neat epoxy	EP	1.6
2	Neat epoxy	1% WC/ EP	1.8
3	=	2% WC/EP	2
4	=	3% WC/EP	1.4
5	Epoxy/3% wt TBCP	1% WC/TBCP/EP	1.8
6	=	2% WC/TBCP/EP	2.2
7	=	3% WC/TBCP/EP	1.4

Table 4.18: Wear rate values of two epoxy nanocomposites		
Sample number	Samples composition	**Wear rate (g/mm)**
0	**EP**	**6.8085E-09**
1	**1% WC/ EP**	**3.4043E-09**
2	**2% WC/EP**	**2.5532E-09**
3	**3% WC/EP**	**2.5531E-09**
4	**1% WC/3%TBCP/EP**	**2.9787E-09**
5	**2% WC/3%TBCP/EP**	**2.5532E-09**
6	**3% WC/3%TBCP/EP**	**1.7021E-09**

الخلاصة:

تُستخدم مادة الإيبوكسي في العديد من التطبيقات الصناعية ، ولكن بسبب هشاشيتها المتاصلة فإنها تحد من استخدامها ومع خواصها الترايبولوجية الضعيفة كمقاومة البلى ، مما يقلل من استخدام الإيبوكسي كطلاءات مقاومة للبلى كاستخدامها لطلاء انابيب النفط والغاز.

في الجزء الأول من هذه الدراسة ، تم استخدام خمسة عوامل تمتين مختلفة لتعزيز متانة الايبوكسي النقي. وهي (تراي بلوك كوبوليمر ، بوليوريثان بولي إيثر بوليول ، مطاط السيليكون السائل ، مادة لاصقة من البولي فينيل كلوريد السائل ، وبوليمر بولي سلفايد), jستخدم مع المصلد (إيزوفورون داي امين). تم الحصول على سلسلة من خلطات الايبوكسي مع اختلافات في محتوى التحميل بنسبة ٣ و ٦ و ٩ و ١٢٪ بالوزن. وتم دراسة خصائص الشد ، ومقاومة متانة الكسر ، ومقاومة الصدمة ، والصلادة ،ومقامة الالتصاق. تمت دراسة الخصائص الهيكلية والفيزيائية عن طريق الماسح المجهري الإلكتروني، والتحليل الطيفي للأشعة تحت الحمراء لتحويل فوريه ، ومسعرالمسح التفاضلي

بناءً على نتائج الاختبارات ، كان أفضل مزيج لعامل تقوية / ايبوكسي هو (إيبوكسي + ٣٪ تراي بلوك كوبوليمر) وتم اختياره لتحضير الجزء الثاني من مركبات الإيبوكسي النانوية المقواة بنسبة مختلفة من دقائق كاربيد التنجستن النانوية مع محتوى تحميل للدقائق (١ و ٢ و ٣) نسبة وزنية على التوالي ، مرة مع ارضية إيبوكسي فقط ومرة أخرى بالارضية المتكونة من مزيج (إيبوكسي + ٣٪ تراي بلوك كوبوليمر).

أظهرت النتائج أن نتائج FTIR أثبتت عدم وجود تفاعل كيميائي ، وأن هناك تفاعل فيزيائي فقط بين عوامل التقوية وارضية الايبوكسي. أوضحت النتائج أنه من خلال زيادة النسبة المئوية لاضافة تراي بلوك كوبوليمر، تم تحسين مقاومة الشد وخصائص معامل المرونة وكانت النسبة الأفضل عند ٣٪ تراي بلوك كوبوليمر. وصل معدل التحسن عند هذه النسبة المئوية إلى [١٠٠٪ ، ٥٧٪] ، وتبين أن مادة تراي بلوك كوبوليمر تمنح خصائص كسر أفضل وقوة صدم جيدة للايبوكسي عند مستوى تحميل منخفض دون فقدان الخصائص الميكانيكية الأخرى.

علاوة على ذلك ، تم تعديل أنظمة الايبوكسي باستخدام بولي يوريثان بوليول ، بولي فينيل كلورايد ، وبوليمر بولي سلفايد . تم وصف الخلائط الناتجة على نطاق واسع من حيث النوعية والكمية للكشف عن تأثير كل عامل تقوية على خصائص الايبوكسي. وقد تبين أن كل عوامل التمتين هذه تمنح

خواص متانة كسر أفضل للايبوكسي عند مستوى تحميل منخفض مع فقدان بعض خصائص الشد الميكانيكية الأخرى.

في حالة الايبوكسي المعدل بعامل تمتين مطاط السليكون ، عند زيادة النسبة المئوية لاضافة مطاط السليكون ، تم تحسين مقاومة الشد ومقاومة الالتصاق وكانت النسبة الأفضل عند ٦% مطاط سليكون. وبلغ معدل التحسين لتلك الخواص عند هذه النسبة [١٢٪ ، و ٢٥٪].

أوضحت النتائج أنه من خلال زيادة النسبة المئوية لاضافة دقائق كاربيد التنكستن للمادة المركبة النانوية المتكونة من ارضية الايبوكسي / ودقائق كاربيد التنكستن ، تم تحسين الخواص الميكانيكية وكانت النسبة الأفضل عند ٢% لاضافة دقائق كاربيد التنكستن. يصل معدل التحسن عند هذه النسبة المئوية إلى قوة الشد ومعامل المرونة [٥٥٪ ، ٤٦٪] ، متانة الكسر [٣٥٠٪] ، مقاومة الالتصاق [٢٥٪] ومقاومة البلى [٦٣٪]. اما بالنسبة الى المادة المركبة النانوية المكونه من ارضية (مزيج من الايبوكسي + عامل التمتين تراي بلوك كوبوليمر بنسبة ٣%) مع الدقائق النانويه لكاربيد التنكستن ، تم تحسين الخواص الميكانيكية وكانت النسبة الأفضل عند ٢% دقائق كاربيد التنكستن. بلغ معدل التحسن عند هذه النسبة المئوية لمعامل المرونة [٤٦٪] ، ومتانة الكسر [٢٥٠٪] ، ومقامة الالتصاق [٣٨٪] ومقاومة البلى [٦٣٪].

جمهورية العراق

وزارة التعليم العالي والبحث العلمي

جامعة بابل

كلية هندسة المواد

قسم هندسة البوليمرات والصناعات البتروكيمياوية

(تحضير وتوصيف خلائط بوليمرية نانوية متراكبة)

اطروحة مقدمة الى

عمادة كلية هندسة المواد / جامعة بابل وهي جزء من متطلبات نيل

درجة الدكتوراه فلسفة في هندسة المواد /البوليمر

من قبل

زينب عبد الرحيم عبد الحسن ناصر

بكالوريوس هندسة المواد/ لامعدنية ٢٠١١

ماجستير هندسة البوليمرات ٢٠١٤

بإشراف :

أ.د. ذو الفقار كريم مزعل

أ.د. محمد عبد الحمزة الكرعاوي

١٤٤٤ هـ

٢٠٢٢م